Use of Energy and Other Monitored Data to Calibrate a Whole Building Energy Model

David Reddy

A thesis submitted in partial fulfillment of the requirements for the degree of

Master of Science in Mechanical Engineering

University of Washington

2013

Committee:

Ashley Emery

Keith Elder

Dean Heerwagen

Program Authorized to Offer Degree:

Mechanical Engineering

University of Washington

Abstract

Use of Energy and Other Monitored Data to Calibrate a Whole Building Energy Model

David Reddy

Chair of the Supervisory Committee:
Professor Ashley Emery
Mechanical Engineering

This thesis documents an approach to utilize energy and other measured data to improve the calibration of a whole building energy model. Each chapter documents important steps of the process, and provides building energy analysts with insight on how to use this information to improve modeling assumptions, and hence energy model predictions. Important components of the study included creation of a custom, annual simulation weather file, designing and implementing an electrical sub-metering system, and disaggregating electrical energy use by model zone and energy end-use. Data and information were aggregated to create a DOE-2.2 whole building energy model, and the incremental improvement in model calibration was demonstrated as input assumptions were refined. The results of this study show accurate description of dynamic model inputs, particularly inputs that describe occupant's manipulation of building systems, was the most influential factor affecting energy model calibration.

Table of Contents

Table of Figures

Table of Tables

Acknowledgements

The author wishes to acknowledge and thank the committee members and ME graduate adviser, Maria, for their guidance, feedback, encouragement, and perhaps most importantly their patience throughout the process of completing this thesis. Furthermore, this study would not have been possible without Benjamin Lynch, who generously allowed free access to his new building. Many thanks to Aric Naue and Eric Anderson for sharing their time and electrical engineering knowledge, as well as Luke Hovee, for your help gathering data and supporting this work all while starting a new company with me. I also have enormous gratitude for the steadfast support of my family and friends, particularly my brother Daniel for being my on-call equipment catalog; and my mother, who without her encouragement, love, and sacrifice, I am certain I would not be in a position to achieve this goal. Lastly, to Lisa; without your love and support, I could not have seen this through.

1 Introduction

Residential and commercial buildings account for roughly 40% of United States primary annual energy consumption and carbon dioxide emissions (Department of Energy 2011). At the same time, the building sector also represents a large reservoir of untapped energy savings, attainable through use of the efficient technologies, materials, and design practices.

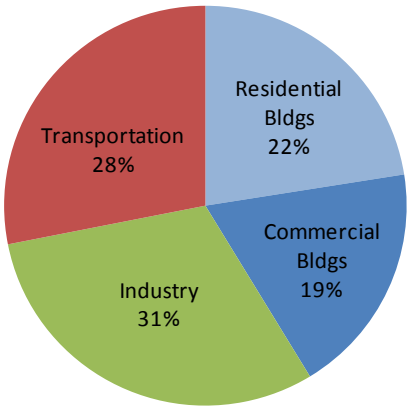

Figure 1 - U.S. primary annual energy end-use fractions by segment

In recent years, whole building energy simulation has been utilized more and more by the building industry for the following, principal purposes:

- Quantify the magnitude of building energy end-uses so targeted efficiency strategies can be developed.
- Estimate the energy consumption and cost impacts of various efficiency measures, which stakeholders can use to make informed investment decisions.
- Develop performance ratings of buildings for energy code compliance or green building performance standards, such as Leadership in Energy and Environmental Design (LEED®), which in turn, have progressively driven industry-wide focus on reducing building energy use.

Given these important applications, accurate energy model predictions are not only critical to the building industry, but also to the world if building energy efficiency is to fulfill its role in curtailing demand on global energy resources and greenhouse gas emissions.

Energy modeling is primarily used during the design phase of new building development and existing building retrofit, but in most cases, little emphasis is placed on verifying model predictions or the actual impacts of energy efficiency measures. Studies comparing design phase model predictions to actual building performance have indicated that on a project-specific basis, there is poor correlation between predicted and actual building energy performance (Turner and Frankel 2008, Newsham et al 2009). On a whole, it appears that energy modeling is likely an important tool for designing more efficient. However, the discrepancy between design phase predictions and actual building performance suggests an opportunity to improve this process.

A principal motivation for this work is rooted in the idea that expanding the use of energy model calibration is an effective way to improve the energy modeling process. Model calibration is the process of tuning simulation inputs so that the predicted energy use matches the observed energy performance. Calibration of an existing building model and using the model to identify and verify the impacts of energy efficiency retrofits is one common application of this process. For new construction projects, calibration of design phase models to actual performance is performed infrequently. In either case, the process is often expensive and time-consuming, making calibration of models after construction a low priority for many projects. Yet, forgoing model validation establishes an open loop design process, where modelers may never fully understand the impact or relevance of critical model assumptions, and designers and owners are uncertain that energy efficiency strategies met expectations. Calibration has the potential to "close the loop" and provide direct feedback to the industry on modeling assumptions and the effectiveness of design decisions.

This thesis documents an approach for using energy and other monitored data to calibrate an energy model, while providing building energy analysts with practical insight into each step of the process.

The principal objectives of this thesis were:

1) Develop a building survey and monitoring plan to characterize inputs for a calibrated, whole building energy model of an existing building.
2) Assemble components for and install a cost-effective data acquisition system to monitor building energy use and thermal conditions.
3) Create a custom, annual simulation weather file from readily available weather observations, and complete a basic comparison of weather variables (including global horizontal solar radiation) to local measurements and a commercially available weather file source.
4) Develop and implement a process for disaggregating branch circuit electrical sub-metering data by building zone/energy end-use for use in energy models.
5) Assemble survey, weather, and building sub-metering data to calibrate a whole building energy model using the eQUEST/DOE-2.2 simulation software.
6) Demonstrate the step-wise impact of improving energy model assumptions on model calibration and end-use energy predictions.

2 Background and Literature Review

2.1 Motivations for this Research

Like any modeling exercise, validation is a crucial step in determining that model parameters and algorithms accurately mimic the system modeled. Significant public and private funding, as well as over forty years of research have been invested in creating building energy simulation (BES) programs that can accurately represent building performance. Even with this firm foundation, these programs are still evolving to improve and expand simulation capabilities, as well as to provide features that facilitate their use in the mainstream design process. The LEED Energy and Atmosphere Prerequisite 1 (US Green Building Council 2012) and California Title 24 Performance Approach (California Energy Commission 2008) are two established examples of integrating energy modeling into the design and code compliance process. Both rating methods require creating well-developed, whole building energy models. Yet despite the greater penetration of energy simulation to optimize and appraise building performance, very little emphasis and effort is placed on validating the predictions modeling practitioners make with design phase models. In nearly all cases, the validity of the model results is left to the judgment of the analysts who develop and the reviewers who approve the results of these simulations, even when the industry is aware the difference between predicted and actual building performance can be large (Diamond et al 2006, Turner and Frankel 2008).

Energy model calibration offers a potential solution to this problem. Model calibration is the process of tuning simulation inputs such that the predicted energy use matches the observed energy performance. Although calibration can only be performed after a building is operational, the process offers the following significant benefits to the design process and building owners:

- Provide better insight on actual audit and driving inputs, thus creating a feedback loop for modelers (and the industry as a whole) to improve future design predictions.
- Illustrate to project stakeholders the real impacts energy efficiency strategies, so lessons are learned and applied to future projects.
- Identify building equipment or control faults early so corrective action can be implemented, saving operational costs and unnecessary impacts on the environment.

2.2 Factors Influencing Energy Model Calibration

Whole building energy simulation requires a detailed physical and thermodynamic description of building parameters. Sophisticated computer algorithms are used to calculate energy and other performance characteristics at discrete time steps (typically 60 minutes or less) over the course of a longer period of environmental conditions (typically a calendar year). This study is premised on the idea that the factors contributing to the differences between energy model predictions and the actual building performance can be classified into three principal categories[1]:

1. Definition of Audit Inputs: In this context, audit inputs describe the as-built, static description of the building that could be ascertained from design information (as-built drawings, equipment submittals, commissioning reports, etc.) or a detailed building survey. Examples of audit inputs include building wall constructions, glazing performance, installed lighting power, and mechanical system set. Audit inputs are often the primary inputs for BES tools, which are then characterized by schedules or performance curves that describe the performance of systems at part-load or off-design conditions.
2. Description of Driving Inputs: The driving inputs of a building encompass phenomena that cannot be predicted by the creator of an energy model or a

[1] The concept of "audit" and "driving" inputs are similar to the concepts described by Subbarao (1988), though here used in the context of whole building energy simulation tools like DOE-2 or EnergyPlus.

simulation tool. Examples of driving inputs are weather, air movement through the building envelope, but perhaps most importantly, the effects of occupants on building operation. Some driving inputs are readily measurable ex-post or in-situ, such as the electrical energy used by lights, however, others, such as air infiltration, are very difficult to measure even with ideal testing circumstances and sophisticated equipment.

3. Simulation Tool and User Capabilities: The commonly used BES programs, such as DOE-2 and EnergyPlus, have varying levels of ability to model the thermodynamics of buildings. The algorithms BES tools use are being continually refined, and as new technologies are introduced to the market, new algorithms are developed. However, differences between the simulated and actual systems are inevitable. Finally, regardless of BES tool capabilities, accuracy is also limited by the experience of the analyst performing the simulations. Each tool has unique intricacies, methods, and potentially software bugs, which typically require thousands of training hours to grasp.

Though all three categories are believed important, this thesis only attempts to provide insight on gathering and improving the definition of audit and driving inputs. The algorithms of simulation programs can be evaluated using highly calibrated models (Haberl and Cho 2004, Sullivan and Winkelmann 1998), and at least one researcher has spoken to the ability of novice energy simulators to calibrate an energy model (Wasilowski and ReinHart 2009). However, investigating the influence of the third category was not a principal objective of this work.

2.3 Calibration Procedures

One of the impediments to more widespread energy model calibration is the lack of well-developed methods and software tools to facilitate this process. By many accounts, calibration is currently considered an art form that relies on the experience and judgment of

the modeler to "turn the knobs" on various audit and driving inputs until the simulation correlates with the observed energy performance (Reddy 2006). Resolution is often limited by the fact that only monthly, or now in many cases, hourly or fifteen minute interval total building energy use is known. If sub-metering information is available, the quantity of information can be vast, and therefore complex and time-consuming to integrate into the modeling process. There are numerous published case studies documenting model calibration exercises (Reddy 2006), and there are industry guidelines for quantifying the calibration of models (ASHRAE 2002). However, there is a dearth of publications that outline explicit details on processing and aggregating important background information, such as weather and sub-metering data, which are often important for creating calibrated simulations. In recent years, researchers and practitioners have identified this barrier and offered practical guidance on gathering data and calibrating models (Raftery et al 2011, Hubler et al 2010); adding to this body of knowledge is one goal of this thesis.

2.4 Calibration Data

Another obstacle to model calibration is the resolution and availability of data needed to evaluate model predictions. These data typically include energy, weather, and other model information, such as occupancy and building space temperature. Ideally, the resolution on this information is available at the same time interval as the BES program. Each data category, described below, can be both difficult to obtain and challenging to integrate into calibrated simulations.

2.4.1 Utility Interval Data

Monthly energy consumption information is readily available for most buildings, though from the perspective of the energy analyst, even obtaining this information can be time consuming and imperfect. Unless the building owner/manager has retained complete utility bill records, the information must be obtained directly from the utility provider. This

requires the building owner to sign information waivers, in some cases for multiple accounts and different utilities. Once obtained from the utilities, utility measurements must be aggregated and put into a format that can be compared to energy model output. In almost all cases, the utility billing periods do not match the calendar month intervals most modeling programs tabulate results by, so either model output must be aggregated by billing period, or utility data must be adjusted to calendar month intervals using weighted daily average (Hubler 2010) or regression-based methods (ASHRAE 2002).

In recent years, the use of automatic meter read (AMR) technology has led to greater availability of hourly or 15-minute interval utility energy consumption. AMR meters transmit consumption and demand information to the utility through a wireless network. However, metered utility information is not always made available to customers or energy analysts who need these data. In the case of this study, owner authorization was obtained and special on-line account access was set-up by Puget Sound Energy, the local electric utility. Hourly or sub-hourly utility information provides greater resolution on the model calibration, and when combined with short-term end-use monitoring, has been used to generate occupancy and end-use energy profiles (Mazzuchi 1992). However, before assuming AMR information is suitable for calibration purposes, interval data should be inspected for gaps and other anomalies. Despite the greater use of AMR electric meters, interval reporting of natural gas and district heating/cooling energy flow is less common, so installing sub-metering equipment is often the only way to obtain higher resolution energy data for model calibration exercises.

2.4.2 Sub-Metering Data

Energy sub-metering is typically the highest resolution information available for model calibration. Electrical sub-metering requires sensors be placed on the various feeders and branches of the building electrical distribution system, which are then tied into a local data

acquisition system. Due to the costs of these additional sensors and related equipment, these systems are typically only found in large or high performance buildings. The number of sensors required to monitor the major end-uses (i.e. lighting, receptacle, heating, ventilating, and air conditioning (HVAC), etc.) can be significant if building electrical and other energy distribution systems are not aggregated by these end-uses. This is common for existing buildings where sub-metering was not a considered during the initial design or subsequent alterations/additions. Even modern buildings designed with a sophisticated energy monitoring systems (EMS) suffer from monitoring data not being organized by energy end-use (Raftery et al 2011 (2)). Ultimately, understanding the flow of energy to each end-use is critical for valid conclusions on calibration and subsequent estimation of energy conservation measure (ECM) impacts. For example, if a lighting retrofit is considered, the cost-effectiveness of the measure is highly dependent on the baseline lighting load and hours of use. In addition, end-use loads, such as lighting and receptacle energy are often a principal driving factor of HVAC energy use. As such, inaccurate estimation of these loads can have a ripple effect on the overall energy model calibration.

With these considerations in mind, a principal focus of this study was to implement an energy sub-metering system to provide a higher-level of calibration data. In the case of this study, electricity is the only primary energy source used at the building site. This simplified the effort of sub-metering energy use, yet the cost of the metering system was also a significant constraint. For this reason, current metering equipment was chosen as opposed to true power metering. According to one source, design and installation of permanent, true root mean square (RMS) power metering equipment costs roughly $3,000-$5,000 per channel, compared to $800-$1,000 per channel for current metering equipment (Pacific Gas and Electric Company 2010). The additional cost for power metering is driven in part by the need for more sophisticated data acquisition equipment. These systems must be capable of acquiring both current and voltage simultaneously, and perform signal

analysis to determine the ratio of real power to the apparent power, or the "power factor" (PF) of the alternating current (AC) circuit. Real power is the quantity measured by utilities and the value predicted by building energy simulations. A resistive load, such as an electric resistance heating element, has a PF ratio of 1. On the other hand, an inductive or non-linear load, typical of an AC motor or transformer used in many appliances, induces an offset in the phase-angle between current and voltage, thereby exhibiting higher apparent power demand (thus current draw) for the given true power measurement. To translate measurements of current to true power, spot or short-term measurement of true power and power factor (using a power meter) can be used to calibrate current measurement to true power (Pacific Gas and Electric Company 2010). Despite the lower costs of long-term current monitoring, published energy model calibration studies do not appear to use this less-costly method for characterizing dynamic model inputs. To evaluate this method, exclusive use of current monitoring, combined with spot measurements of power, was used in this study.

2.4.3 Energy Use Disaggregation

Building energy models contain a description of the various spaces in the building, as well as the energy end-uses. A complication of using sub-metering information is that the energy conduits can serve more than one location in the building and/or energy end-use. Internal loads influence HVAC system energy consumption, so inaccurate appropriation of energy to building spaces can lead to model error. Additionally, mischaracterizing the energy used by end-uses compromises accurate estimation of energy conservation measures (ECMs) that target a specific end-use. Both considerations make it difficult to calibrate an energy model, and even if a model calibrates well to building energy data, the model behavior may not be valid under a different set of driving conditions. For this reason, methods to disaggregate electrical data by both building space and energy end-use were investigated in this study.

Techniques to identify and disaggregate building energy use have evolved over the past twenty years. "Nonintrusive load monitoring" (NILM) was pioneered in the context of disaggregating the electrical loads of residential buildings by monitoring power at the main utility meter and correlating the step change in both real and reactive power to the on-off switching of a specific household appliance (Hart 1992). The principal motivation of this approach was to improve utility-scale understanding of household electric demands, while minimizing the cost and intrusiveness of installing sub-metering systems in homes. Subsequent to Hart's original work, the algorithms and applications continued to evolve, and were further extended to disaggregating more complex loads in commercial buildings (Norford and Leeb 1996). In both cases, direct sensing of time-series electrical power, detecting on/off events, and classifying the events by comparison to a database of known electrical end-uses was required. Another approach, developed specifically in the context of calibrating DOE-2 energy models, relies on using an energy model to first estimate the whole-build end-use load fractions, and then use the correlation between the simulated energy end-uses and hourly outside air temperature to predict disaggregated energy use over an actual calibration period (Akbari 1995). This topic appears to be experiencing a renaissance, using less expensive sensors and more sophisticated computer algorithms to identify the digital "signatures" of electrical appliances as well as disaggregation of water and natural gas flows (Froelich et al 2011).

The researchers referenced above cite the applications and benefits of accurately disaggregating building energy flows by end-use as an important first step to identifying efficiency strategies. However, few researchers address the task of also identifying the location of energy consumption, which can be important since energy loads, such as lights, people, and electrical equipment influences the energy consumption of building HVAC equipment. With this in mind, this study included development of a method to disaggregate building sub-meter data, and assign it to both an energy end-use and model zone. The

methods used in this study follow the same basic approach of original NILM methods, that is, analyzing time-series electrical current data measured on a specific circuit, detecting switching events, and classifying the events based on the previously identified electrical end-uses. Though thought to be important factor, the sensitivity of model calibration to the location of loads and HVAC systems was not directly investigated in this study.

2.4.4 Weather Data

The energy use of most buildings is dependent on environmental conditions. In the United States, design phase predictions often stem from using typical meteorological year (TMY) weather files in simulations. The most current TMY data set, TMY3, distributed by the National Renewable Energy Lab (NREL), assembles solar and other weather observations for years 1991-2010 into a single, annual data file for use in hourly simulations (Wilcox 2008). However, for calibration purposes, it is usually important to obtain actual hourly data for the calibration period.

The U.S. Department of Energy (DOE) Energy Efficiency and Renewable Energy website (Weather Data for Simulation 2013) provides an excellent summary of currently available sources for actual hourly weather information. The sources for actual data have expanded since beginning this research, and it is now possible to obtain a site-specific weather file, including solar radiation data, in various BES program formats for as little as $40 USD/location/year (Weather and Climate Data 2013). However, this research was initiated prior to these weather data services being available, and thus, a principal goal of this study was to obtain actual hourly weather observations from the National Climatic Data Center (NCDC) and create a custom binary weather file using the DOE-2 Weather Processor program (Buhl 199).

Solar radiation is typically the most difficult weather parameter to measure. Weather stations equipped with solar radiation sensors are not common, and therefore building

calibration studies often rely on some combination of TMY3 solar data and other weather measurements (dry bulb temperature, humidity, wind speed, etc.) from the closest weather station (Raftery et al 2011, Hubler et al 2010). One method for calculating global horizontal solar radiation from traditionally available weather information is the empirical "Zhang-Huang" model (Qingyuan 2002). This model is currently used by the EnergyPlus Weather Converter program to calculate solar values if they are missing from user input (Department of Energy 2012). Despite the relative simplicity of the model and availability of the necessary weather variables, no literature was found describing its use in creating custom weather files for calibrated BES. Therefore, one component of this study was to apply and evaluate the Zhang-Huang solar model in this context. Validation of the model was not a principal goal of this work; however, a comparison of the model results to measured global horizontal solar radiation is presented.

2.5 Literature Review Summary

This study contributes to the current body of work by:

- Providing a detailed overview of the equipment and other practical considerations involved in acquiring building energy, temperature, and solar radiation.
- Outlining steps for creating a custom annual weather file from publically available NCDC weather data, including a method for tailoring the Zhang-Huang solar model to local conditions using readily available weather information.
- Describing a detailed approach to gathering electrical sub-metering data and using energy use disaggregation to develop inputs for a building energy model.
- Illustrating the use of detailed audit and metering data to guide the calibration process, as opposed to methods based on multiple model iterations and parameter optimization routines.

3 Building Survey and Monitoring Plan

3.1 Building Description

3.1.1 Overview

The study building, shown in Figure 2, is a 6,410 ft^2 commercial building built in 2008 and located Bellingham, Washington. It was purchased in late 2009 by a close friend of the author, and used as an office/distribution center for a small online retail business. The owner generously provided liberal access to survey the facility, install data monitoring equipment, and measure building energy and temperature data throughout 2010.

Figure 2 - Exterior photo of building site, viewed from the NW

3.1.2 Space Plan

Figure 3 shows the building space plan. The metal building shell is divided into two areas: office/bathrooms with an unconditioned attic space above, and an open warehouse. Pictures of the building interior, taken from the numbered positions identified in Figure 3, are shown in Figure 4 through Figure 7.

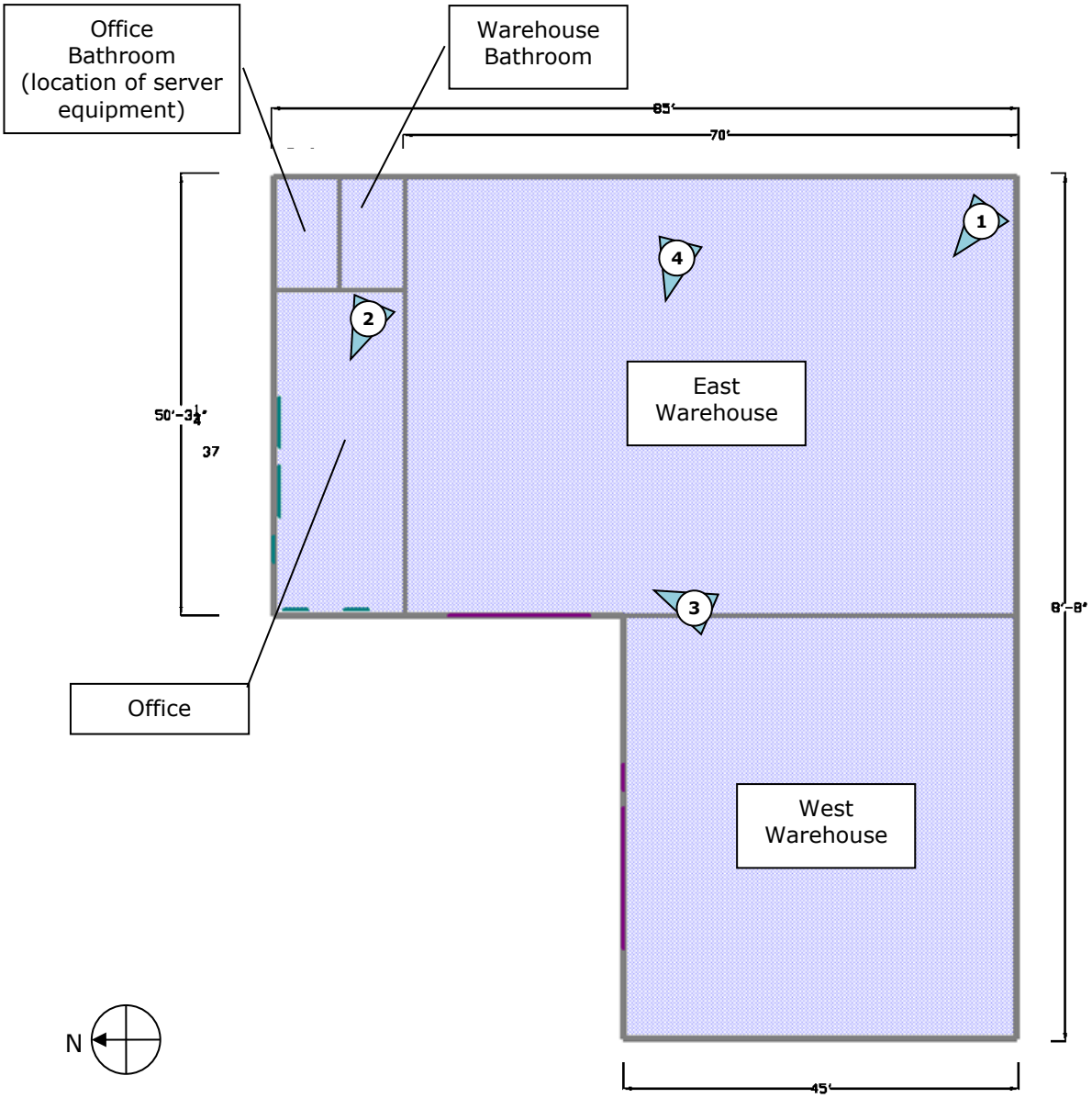

Figure 3 - Building space plan

Figure 4 - Interior photo (1) of E & W warehouse, prior to occupancy

Figure 5 - Interior photo (2) of the office, prior to occupancy

Figure 6 - Interior photo (3) of E warehouse, prior to occupancy

Figure 7 - Interior photo (4) of E warehouse, after to occupancy

3.1.3 Description

The building is divided into 5,660 ft^2 of warehouse space, and 750 ft^2 of office/bathrooms. The warehouse is an open space with shelving for products, and an approximately 250 ft^2 "packing area" centrally located area with benches, used by personnel to pack and ship products each day. Typical weekday occupancy includes 5-7 employees, with 2-3 people working in the warehouse, and 3-4 people in the office. Typical operating hours are from 8am to 6pm Monday thru Friday; closed Saturday, Sunday, and holidays.

The metal framed/clad building was built to meet minimum 2006 Washington State Energy Code (WSEC) requirements. Linear fluorescent lighting fixtures with T-8 lamps and electronic ballasts are used throughout the building, with an overall installed lighting power density (LPD) of 0.43 W/ft^2. Only two exterior lighting fixtures are installed, one at the front door to the office, and one for warehouse parking lot, both controlled by integral photosensors.

Exterior walls are typically composed of 8 inch or deeper metal studs framed between structural steel posts. By cutting an inspection hole, the framed wall cavities were found to contain 5.5 inch fiberglass insulation batts, with an estimated thermal resistance value of 21 $hr\text{-}ft^2\text{-}°F/Btu$ (R-21). The balance of the cavity was open air space. Additional inspection to determine if insulation is supported against the inner wallboard with wire supports was not possible. The office/bathrooms have a dropped ceiling height of 10ft and 9ft respectively, with R-30 fiberglass insulation in wood ceiling framing. The metal warehouse roof is insulated with R-9 fiberglass insulation, and the open ceiling height varies from 15 to 17 ft. The office includes 87 ft^2 of vinyl, double-paned windows and doors. The warehouse has two large, insulated panel garage doors that open to the parking area. Based on information provided by the building manager, the warehouse garage doors are opened n most mild/hot temperature days to allow light and fresh air enter the space. On cooler

days, the east warehouse garage door was opened 2-4 times per day while delivery trucks delivered or picked up packages.

The main office is served by two, 2.4 kW wall heaters controlled by a 7-day programmable wall thermostat. Each bathroom includes one 4 ft (1 kW) baseboard heater with integral thermostatic control. The warehouse was unheated at the time of purchase, but in late 2010, an electric radiant panel heater was installed over the main shipping/packing area, as shown in Figure 7. The building has no mechanical cooling, although the owner is interested in methods to reduce the warehouse and office temperatures on hottest summer days without using air conditioning.

The only plumbing fixtures are two faucets in each bathroom. Domestic hot water is supplied by a six gallon electric storage water heater located in the unconditioned attic space above the office/bathrooms.

The main electric service is provided by Puget Sound Energy (PSE) and the electrical meter is automatic meter reading (AMR) compatible. The electrical service enters the building through the main electrical panel, located in the northwest corner of the east warehouse bay (see Figure 6). The building currently does not have natural gas service.

Overall, the simple building configuration, combination of heated and unheated space, and unhindered access to the building made it an ideal candidate for a small-scale building analysis study.

3.2 Building Survey

The study began with a survey of the structure to identify the static inputs of the building energy model. The following characteristics were surveyed:

3.2.1 Building Geometry/Envelope

a. Building orientation and dimensions obtained from permit plans and verified with field inspections.
b. Description of opaque surfaces (walls, floor, roof), window, and door components. Descriptions taken from permit plans and verified with field inspections.
c. Building operation schedules based on observations and occupant feedback.

3.2.2 HVAC

a. Identify building thermal zones based on thermostat control or other thermal/usage characteristics.
b. Record HVAC equipment type, capacity, and controls.

3.2.3 Lighting

a. Lighting zones determined according to controls and electrical branch circuits.
b. Lighting fixture power based on inspection and default assumptions of lamp/ballast performance.

3.2.4 Receptacle Equipment

a. Receptacle zones identified according to electrical branch circuits.
b. Record of equipment type by building space, though due to availability of sub-metering data, this information was not used to develop model inputs.

3.2.5 Service Hot Water Heating

a. Hot water heating equipment performance (capacity, thermostat setpoint, efficiency, etc.) and location.
b. Hot water fixtures and location.

From the survey, an "as-built" description of the facility was defined; survey forms are included as an electronic supplementary file. The audit description is summarized in Table 1 below, and is the basis of static inputs for the calibrated energy model.

Table 1 - Summary of building survey information

Component	Description/Performance
Opaque Envelope	
Above-grade Walls	Warehouse: Metal siding with 8-10" deep metal stud framing. 2" (R-10 assumed) or 5.5" (R-21 assumed) insulation observed at varying locations, airspace for rest of cavity depth. 2-3 layers of 5/8" gypsum wall board (GWB) observed for fire rating. Office: Metal siding with 10" deep metal stud framing, 5.5" wood stud wall with 5.5" (R-21 assumed) framed inside of steel structure and 1 layer of 5/8" GWB.
Roof/Ceilings	Main steel structure: Metal building roof with single layer, R-10 (assumed) insulation. Conditioned office/bathroom ceiling: 9.25" wood framing with R-30 insulation above drop ceiling.
Slab-on-Grade	No perimeter slab insulation noted on construction plans for observed at exterior.
Fenestration	
Windows	Mix of fixed/operable units in office. Vinyl frames with double-glazing. Assumed LowE coating and air fill.
Glazed Doors	Quantity (1) single leaf glazed door at office entry. Vinyl frame with double-glazing. Assumed LowE coating and air fill.
Opaque Doors	Quantity (2) metal, un-insulated single-leaf doors (one interior door between office and unconditioned warehouse) Quantity (2) metal, section roll-up doors to each warehouse bay. Doors have insulated foam panels and one panel with un-insulated glazing.
Interior Lighting	
Lighting Types	T-8 linear fluorescent fixtures with electronic ballasts. Office/bathroom lighting recessed into drop ceiling. Warehouse suspended high-bay.
Lighting Power Densities	Office/Bathroom = 1.13 W/ft^2 Warehouse = 0.34 W/ft^2
Exterior Lighting	
Lighting Types	Front door: Compact fluorescent lamp (CFL) w/ photosensor control Parking lot: High intensity discharge (HID) lamp w/ photosensor control
Lighting Power	Total: 0.3kW
HVAC	
Office	Quantity (2) 2.4 kW electric resistance wall heaters with fans. Wired to 7 day programmable thermostat. Program at start of study: M-F 7:30am to 6pm = 68 °F All other hours = 58 °F
Bathrooms	Quantity (1) 1.5 kW electric resistance baseboard heater with built-in thermostat. Thermostat set to lowest setting at start of study.
Exhaust Fans	80 cfm (assumed) exhaust fan in each restroom, wired on same circuit as restroom lights.
Plumbing	
Fixtures	Lavatory faucet each restroom (quantity 2)
SHW Heater	Bradford White, 6 gallon 1500 W (120V) electric water heater Setpoint = 135 °F

3.3 Data Acquisition System

Many new and existing buildings typically have no central building control system or metering infrastructure. The only energy metering is often the main utility meters that serve the building, which do not provide good resolution on where or for what end-use energy is used for. To gather information used to generate a calibrated building energy model, a data acquisition (DAQ) system was designed and sensors installed to record electrical, temperature, and solar radiation measurements.

3.3.1 Data Logger

The data logger is the heart of the DAQ system, as it is necessary component for reading and storing sensor data. Data loggers are available with a wide range of options, and vary widely in price and capabilities. For this project, the Dataq DI-710-EH-PGH (Figure 8) was chosen for the following reasons:

- Analog Voltage Measurement: All of the sensors used in this study can be configured to output an analog, direct current (DC) voltage signal. The 710 data logger is designed for voltage measurements.
- Number of Channels: The 710 unit uses a single, 14bit analog-to-digital convertor and an analog multiplexer to read 16 single-ended input channels. This type of equipment offers a reasonable compromise between accuracy, number of channels, and cost.
- Ethernet Port Connection: Memory capacity is a significant concern when logging many channels over a long period of time. For this reason, the logger was configured with an Ethernet output and connected to a personal computer (PC) while logging data. The Ethernet connection provides the flexibility of having the logger installed on a local network, and therefore does not need to be located in the same location as the PC.

3.3.2 Current Transducers

Current transducers were used in this study to meter electrical energy. True RMS power metering requires simultaneous measurement and analysis of current and voltage signals, which dramatically increases the cost of the DAQ system (Pacific Gas and Electric 2010). The high cost is a barrier for metering true RMS power, both for this study, and for building owners who consider installing energy monitoring systems. As described in Chapter 2, using current as a proxy for power is not a novel idea, however, application and better understanding of this approach was a principal goal of this study.

In this case, Veris H923 split-core current transducers were used to meter current (see Figure 8). This sensor was chosen for the following reasons:

- Voltage Output: Many current transducers output an AC voltage or current signal, which would not be compatible with the data logger selected for this project. The Veris sensor outputs a 0-10 Volts DC (VDC) signal, so no additional signal conditioning was needed.
- Self-powered: These sensors require no external power supply, simplifying wiring and power supply requirements.
- Adjustable Current Range: The sensor range is adjustable for 20-100-150 amp circuits, allowing the measurement sensitivity to be tailored to branch or feeder circuit applications.
- Split-core: Facilitates installing the sensor without interrupting building operations.

(a) (b)

Figure 8 - Dataq DI-710 data logger (a) and Veris H923 (b) current sensor

3.3.3 Temperature Sensors

Space temperature is one of the variables compared to building energy model outputs and used to guide the calibration process. Many different types of temperature sensors are available. For this study, the Veris TS-P was used for interior, and the Veris TO-P was used for exterior temperature measurements (see Figure 9). These sensors contain an integrated circuit (IC) chip, designed to output a 0-5 VDC voltage or 4-20 mA current signal that is proportional to temperature. These sensors were chosen for the following reasons:

- Voltage Output: These sensors can be directly connected to the data logger without additional signal conditioning.
- Low-profile Design: These sensors are designed for commercial building applications, with inconspicuous interior (a) or weather-tight exterior (b) housings.

(a) (b)

Figure 9 - Interior (a) and exterior (b) temperature sensors

3.3.4 Solar Radiation Sensor

Solar radiation has a substantial impact on building heating and cooling loads, particularly buildings with large areas of glazed fenestration. In the case of this project, the lightweight building construction type and large unconditioned spaces were expected to be influenced by solar radiation (both direct radiation and influence on local air temperatures). For this project, the Davis Instruments Vantage Pro2 Global Horizontal Radiation pyranometer was used. This sensor uses a silicon photodiode to convert incident solar radiation to a 0-3 VDC signal. It was chosen for the following reasons:

- Voltage Output: This sensor can be directly connected to the data logger without additional signal conditioning, and read at the same voltage gain as other sensors connected to the logger.
- Low-profile/cost: Compared to a thermopile pyranometer, such as an Eppley PSP, the Davis sensor is small and can be mounted on lightweight platform. Also, at $160, it is significantly less expensive.

Figure 10 shows the Davis solar radiation sensor installed on the roof of the building.

Figure 10 - Solar radiation sensor installed on the roof

3.3.5 Other DAQ Components

In addition to the data logger and sensors, the following other components were purchased and assembled into the overall DAQ system:

1. Laptop PC Computer: A Dell Inspiron laptop computer was dedicated to controlling and storing data acquired by the Dataq logger.
2. Power Analyzer: A Fluke 41 Power Analyzer was loaned from an associate to make spot measurements of true RMS voltage and power, which was used to correlate current measured by the DAQ system to real power.
3. AC and DC Power Supplies: The Veris temperature and Davis solar radiation sensors require an external DC voltage supply, both at different input levels. A six outlet AC power strip was used to provide power to all the DAQ system components, which was plugged into a dedicated receptacle installed for this study at the main electrical panel.
4. 4-port Ethernet Switch: The laptop PC was connected to both the data logger and the buildings internal network via an Ethernet switch. This allowed remote access and control of the DAQ system.
5. Fused and Un-fused Terminal Blocks: Fused terminal blocks provided protection of the data logger from electrical surge, and in general, terminal blocks allowed for clean, organized connections of the many DAQ components.
6. Custom Enclosure: The computer, data logger, and other peripherals were located in the corner of the open warehouse area. To protect the system damage, a custom wood enclosure was built and positioned on a small stand below the electrical panel for easy access.
7. Low-voltage Wiring: All of the sensors are individually connected to the data logger via low voltage wiring. Current sensors are in close proximity (<10 ft) to the data logger, however, temperature sensors were positioned in various rooms of the

facility and the radiation sensor is located on the roof. Connecting all components to the logger required over 600 ft of 2 or 3-conductor, shielded, 18 AWG low voltage wiring.

Figure 11 shows the custom DAQ enclosure, laptop computer, and power analyzer in-situ during initial set-up. The data logger and other DAQ components are housed in the space below the laptop computer; Figure 12 shows the layout of components within the custom enclosure.

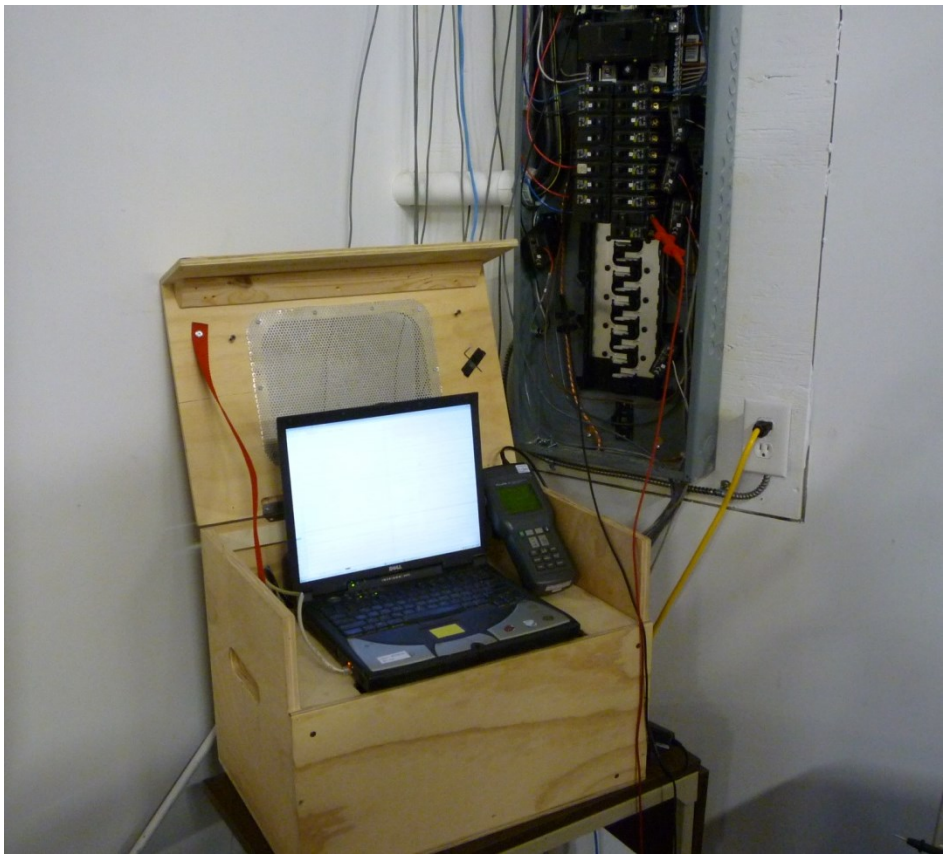

Figure 11 - DAQ system enclosure situated at the main electrical panel during setup

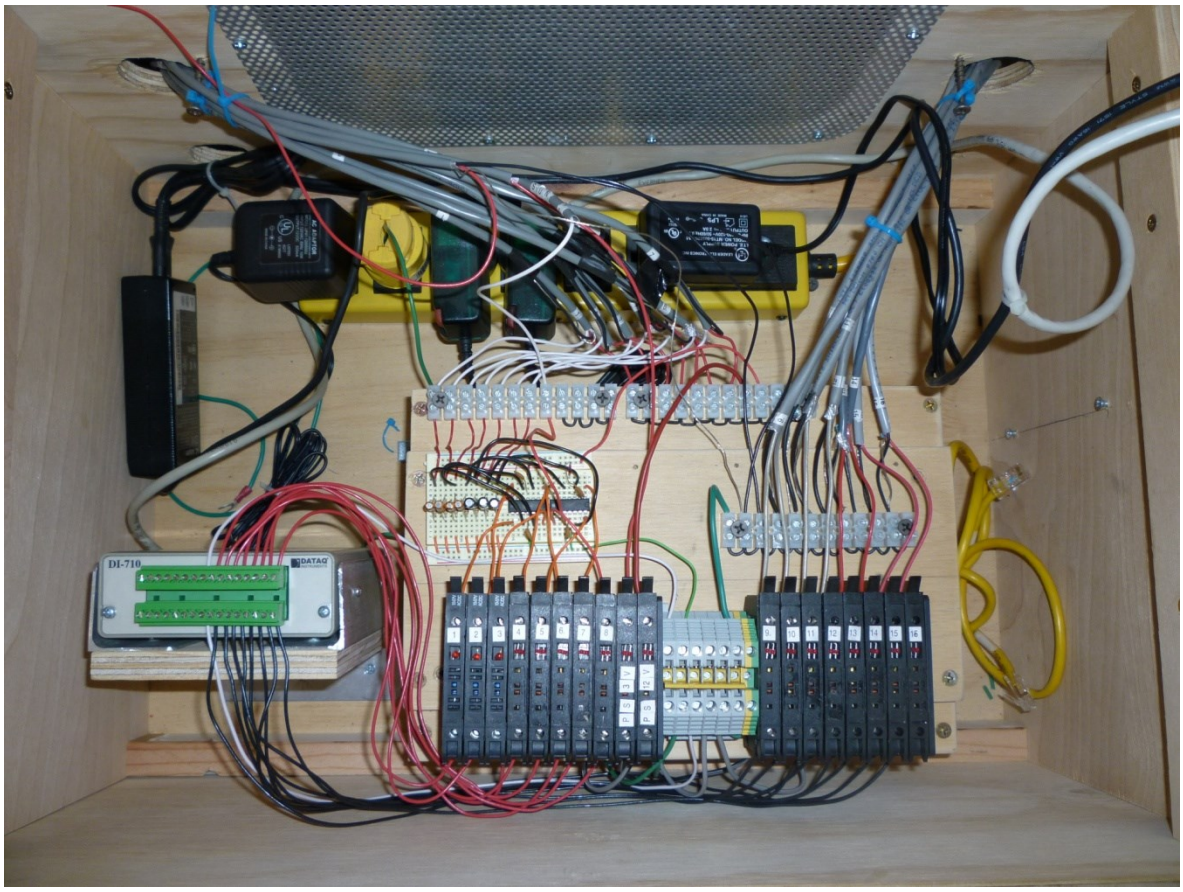

Figure 12 - Layout of DAQ components within the custom enclosure

3.3.6 DAQ System Components and Costs

Table 2 summarizes all of the components purchased for use in this study. Some components were not purchased, rather salvaged or loaned for this project. Equipment was paid for out-of-pocket, so the final configuration and quantities of sensors was a balance of available budget, data logger channels, and metering needs.

Table 2 - Summary of DAQ and metering system components and costs

Item	Item	Mfr/Model	Qty	Unit Cost	Total Cost
1	Data Logger	Dataq 710-EH	1	$ 599.00	$ 599.00
2	Current Transducers	Veris H923	8	$ 108.00	$ 864.00
3	Internal Temperature Sensor	Veris TS-P	6	$ 45.00	$ 270.00
4	External Temperature Sensor	Veris TO-P	1	$ 45.00	$ 45.00
5	Solar Radiation Sensor	Davis 06450	1	$ 160.00	$ 160.00
6	Laptop PC	Dell Inspiron	1	$ -	$ -
7	Portable Power Analyzer	Fluke 41	1	$ -	$ -
8	Power supplies	n/a	2	$ 20.00	$ 40.00
9	Ethernet Switch	D-Link	1	$ -	$ -
10	Fuse blocks	n/a	18	$ 3.50	$ 63.00
11	3-cond Sensor Wire	n/a	600	$ 0.20	$ 120.00
12	2-cond Sensor Wire	n/a	64	$ 0.12	$ 7.68
13	Misc supplies/tools	n/a	-	$ -	$ 100.00
				TOTAL	**$ 2,268.68**

3.4 Metering Plan

3.4.1 Main Electrical Meter

The main electrical meter is automatic meter read (AMR) compatible, meaning it is capable of transmitting interval electrical data to the utility. After the building was occupied in Feb 2010, a request for access to 15-minute interval meter data was submitted to Puget Sound Energy (PSE). Though not normally provided unless the building is involved in the utility's energy efficiency programs, special access was granted for this study, and values were downloaded monthly via the utility's web portal, www.energyintervalservice.com.

After downloading the first 2-3 months of utility data, it was clear there were intermittent gaps in interval readings. Gaps were typically only a few hours, but in some cases , a day or two in length. In addition, gaps in data were inserted at daylight savings time transitions, which required manual adjustment of the interval timestamps to line up with the continuous hourly reports produced by the energy model. Once adjusted, only the hours with complete interval data were used to determine calibration of the energy model.

3.4.2 Electrical Sub-Metering

The hub of the building's electrical systems is a new, 200 amp, two-phase electrical service panel, typical of small retail/office buildings. Reliable electrical power/lighting plans were not available, and only basic circuit labeling information was listed on the inside of the electric panel door. This is not uncommon for many systems, and therefore, a combination of switching circuits ON/OFF and observing the amplitude of measured electrical current was used to identify and confirm which zones and end-uses were served by each branch circuit. Table 3 summarizes the building circuits, as they appear on the left and right buses of the main panel; an 'X' indicates which circuits were metered during the monitoring period.

Table 3 - List of building electrical circuits

Circuit	Breaker	Building Location	End-use	Metered
LEFT BUS				
1	20A	E Warehouse Wall	Receptacles	
3	20A	S&W Warehouse Walls	Receptacles	
5	30A	Office	Space Heating	X(1)
7	30A			
9	20A	E Warehouse, Electrical Panel	Receptacles	
11	20A	Dedicated Data	Receptacles	X
13	20A	Warehouse Packing Area	Receptacles	X
15	20A	Warehouse Packing Area	Space Heating	
RIGHT BUS				
2	20A	W Warehouse	Int. Lights	
4	20A	E Warehouse	Int. Lights, Ext. Lights, Receptacles	X
6	20A	Attic over office/bathrooms	DHW	X
8	20A	Office and Bathrooms	Int. Lights, Ext. Lights, Exhaust Fans	X
10	20A	N Office Wall	Receptacles	X
12	20A	S&W Office Walls	Receptacles	X
14	20A	N Warehouse Wall	Receptacles	X(2)
16	20A	Bathroom	Receptacles	
18	20A	Office and Warehouse Bathrooms	Space Heating	
20	20A			

1) Metered for during late spring 2010
2) Metered during summer 2010

For this study, eight current transducers were available for metering branch circuits. The final sub-metering plan, indicated in Table 3, allowed for metering the majority of the building's electrical use during the monitoring period. Table 4 provides a brief description of non-metered circuits, and how neglecting them was accounted for or potentially affected the energy model calibration exercise.

Table 4 - Description of non-metered electrical circuits

Circuit	Building Location	End-use	Impact
1	East Warehouse Wall	Receptacles	Warehouse plug loads are primarily limited to packing area (circuit #13) and the north wall (circuit #14), which are metered in this study. The remaining two un-metered warehouse receptacle circuits were observed unused in the beginning of the monitoring period. Later in 2010, the refrigerator was moved to the E side of the warehouse (circuit #1). However, even though not metered, the energy use of this appliance will still be accounted for in average day profiles, described further in Chapter 5.
3	South & West Warehouse Walls	Receptacles	
7	Office	Space Heating	Only one of the two circuits serving the two-phase electric resistance office heaters was metered; the second, un-metered circuit was confirmed to have the same current draw when the heater was operated. Therefore, the current for the single metered circuit was multiplied by two to obtain total heater current draw.
9	East Warehouse, Electrical Panel	Receptacles	This receptacle was installed to provide power to the DAQ system, drawing a small continuous load of 0.3 Amps. This results in 0.9kWh/day of unmetered electricity, or roughly 1.7% of daily consumption during non-heating periods. This constant load will be accounted as a separate input for the final calibrated energy model.
15	Warehouse Packing Area Heater	Space Heating	The panel heater was installed in mid-2010, after the study had begun. However, utility interval data suggests this heater is used during the winter. It is controlled by a 60min timer operated intermittently by employees, so it is difficult to predict energy consumption in the energy model. An estimate will be made for final calibration runs; however, not metering this circuit was expected to undermine model calibration during the fall and winter months.
2	West Warehouse	Interior Lights	The west portion of the warehouse was intermittently occupied and lights were observed unused, and therefore excluded from the metering. However, utility interval data suggests these lights were periodically ON. Therefore, not metering this circuit is expected to undermine model calibration during fall and winter months.

Circuit	Building Location	End-use	Impact
16	Bathroom	Receptacles	No appliances were observed to be connected to these receptacles, so this circuit was not metered. Not metering this circuit is not expected to have a significant impact on model calibration.
18/20	Office and Warehouse Bathrooms	Space Heating	The company's computer server was located in the office bathroom (see Figure 14) was assumed to generate enough heat to maintain the temperature in the bathroom. The warehouse bathroom heater was not observed to be ON during the summer and fall of 2010, however, it may have been enabled in the winter months to mitigate freezing pipes. Therefore, not metering this circuit is expected to undermine model calibration during fall and winter months.

3.4.3 Temperature Metering

Temperature sensors were installed throughout the facility. They were located to obtain measurements that could be compared to modeled zone temperatures, while at the same time not interfering with building operations or substantially altering the aesthetic appearance of rooms. The locations and heights of the sensors are shown in Figure 13. The limitations on sensor locations meant they were located in the drop ceiling of the office and restroom spaces, as shown in Figure 14. Warehouse sensors were attached to a central column at different elevations, or hanging from the roof, as shown in Figure 15. The location of the outdoor air and solar radiation sensors was limited by the distance that PVC conduit could be routed from the door opening adjacent to the DAQ system, as shown in Figure 16.

The outdoor air temperature sensor was located within a PVC pipe to shield the temperature probe from the effects of solar radiation. It was also located in the corner of the building below a gutter, which was thought to provide additional shading. However, in late afternoon of summer days, the sun was observed to radiate the temperature sensor, resulting in the measured air temperature to spike by 5-10°F. A custom, polished

aluminum radiation shield was manufactured for the sensor (see Figure 17); however, this did not entirely mitigate temperature spikes. It was concluded that shielding did not solve the problem due to sun heating the metal walls and asphalt parking lot below, resulting in warm air current rising up into the location of the sensor. These observations reinforce the importance of both shielding from the sun, and locating it in open-air currents.

3.4.4 Solar Radiation Metering

The solar radiation sensor was located on the highest point of the building roof at the location shown in Figure 13. It was oriented horizontal to the ground using the sensor's built-in bubble level. No obstructions to the sky from surrounding buildings or terrain were identified. Throughout the study, temperature and solar radiation were measured simultaneously with sub-metered electrical circuits.

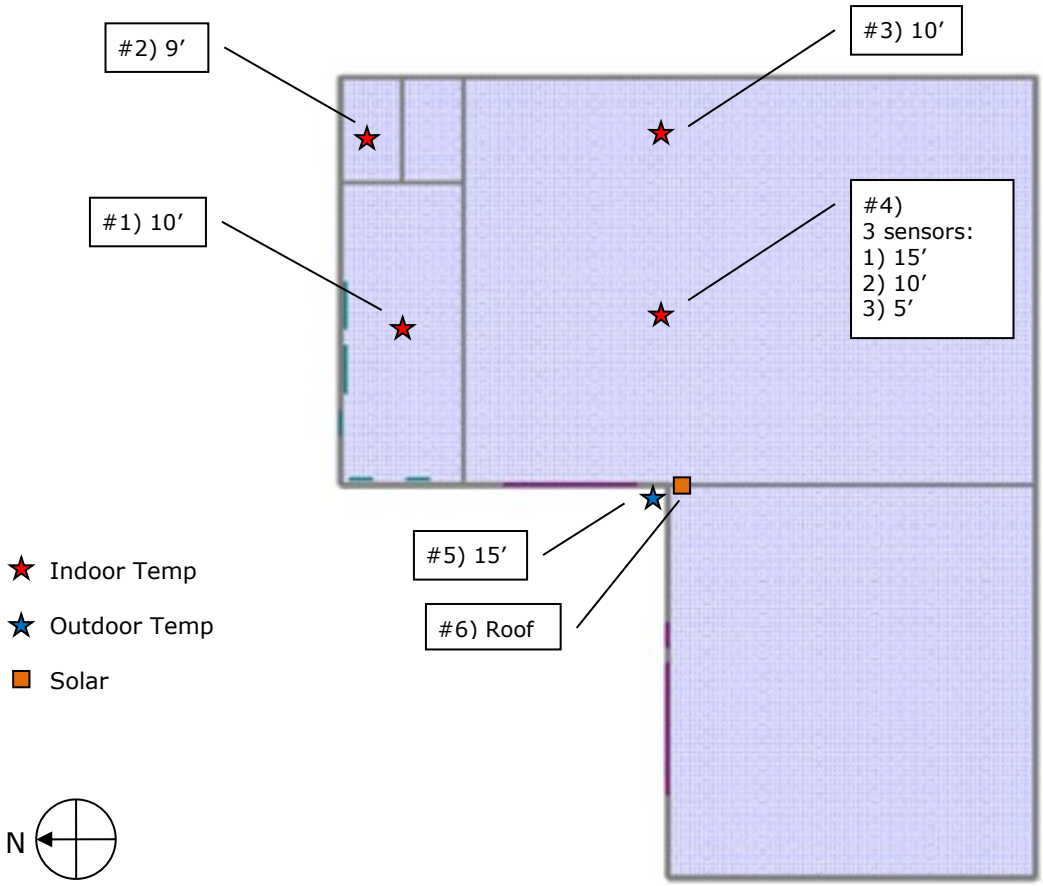

Figure 13 - Plan view of temperature and solar sensor locations

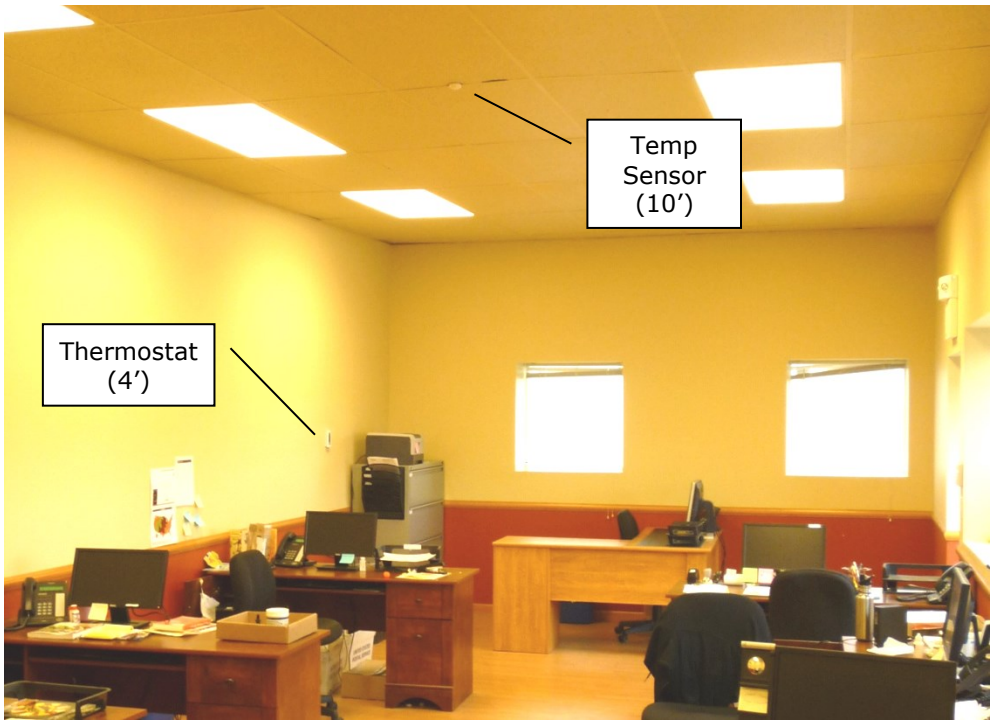

(a)

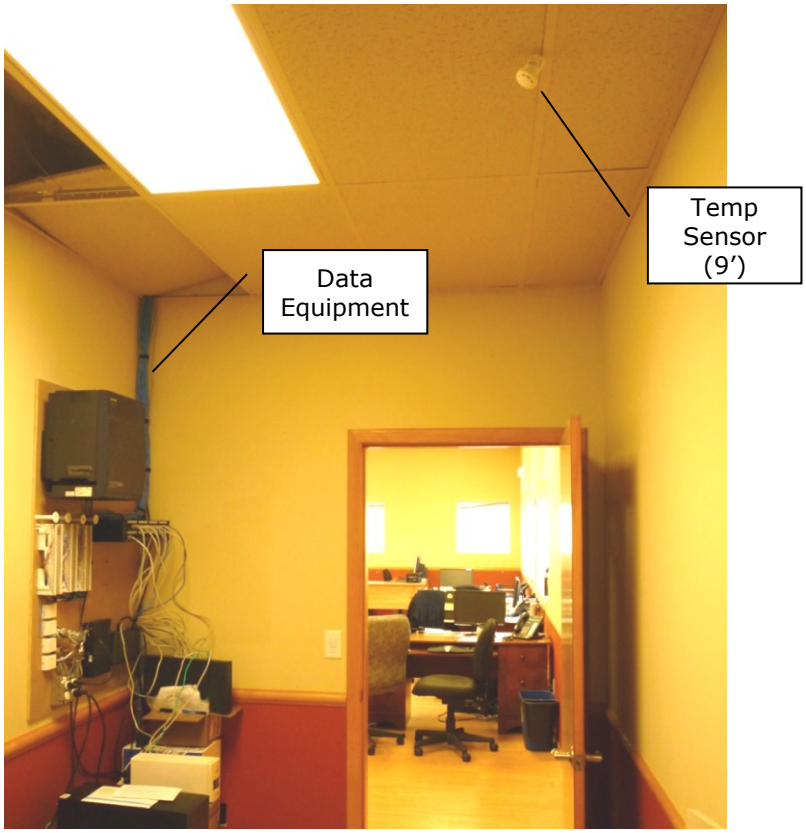

(b)

Figure 14 - Office and server/bathroom temperature sensor locations

Figure 15 - Warehouse temperature sensor locations

Figure 16 - Outdoor air temperature and solar radiation sensor location

Figure 17 - Close-up of custom outdoor air temperature shield

3.4.5 Temperature Sensor Thermal Capacitance

Upon receiving the Veris TS-P temperature sensors, a brief experiment was conducted to evaluate the accuracy and sensitivity of the sensor. The experiment consisted of simultaneously measuring the temperature readings of a calibrated thermocouple (Physitemp PT-6, Type T, 5' length) and the Veris TS-P sensor (see Figure 18) while subjecting them to changing free air temperature environments. In this case, the change in environmental temperature was created by moving the sensors from the ambient temperature of a basement room (T_{room} ~15°C) to a chest freezer ($T_{freezer}$ ~-15°C). The TS-P sensor voltage output was measured using a digital multi-meter (DMM, Fluke model 179) and converted to temperature, while the thermocouple was monitored using a digital thermocouple reader (Omega HH23). Readings of temperature were taken manually every 30-60 seconds.

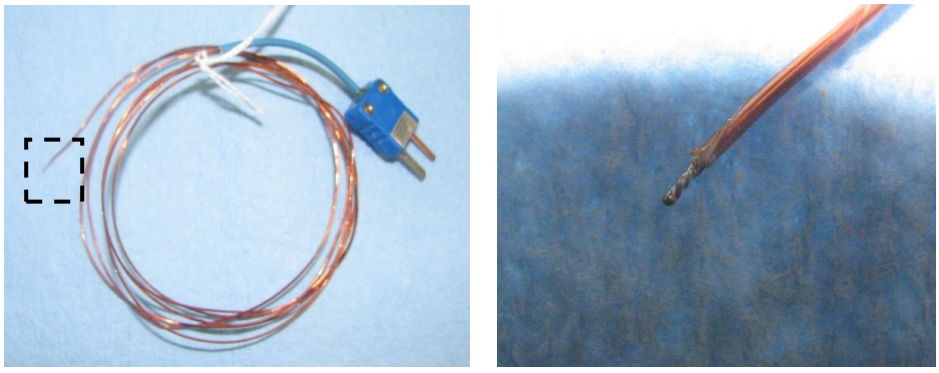

(a)

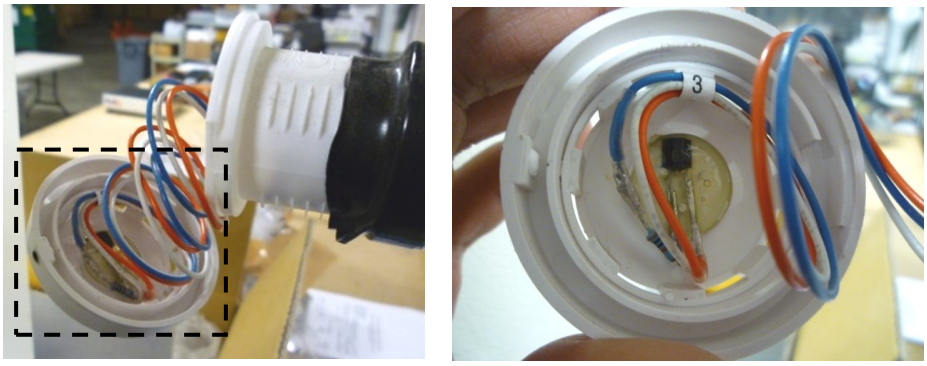

(b)

Figure 18 - Pictures of thermocouple (a) and TS-P (b) temperature sensors.

Figure 19 plots the measured temperatures for the devices during the experiment. Compared to the thermocouple, the TS-P sensor does not react as quickly to the abrupt change in environmental temperature. Within the first 30 seconds, the thermocouple achieves approximately 60% of the change in temperature, while the TS-P device takes nearly 10 times as long to reach this same temperature. This is likely explained by the fact that the TS-P IC chip is potted in epoxy, which is in turn bonded to a plastic housing. In contrast, the thermocouple is comprised of two metal wires (copper-constantan), welded at one end with a very thin polymer (Kapton) sheath surrounding the wires.

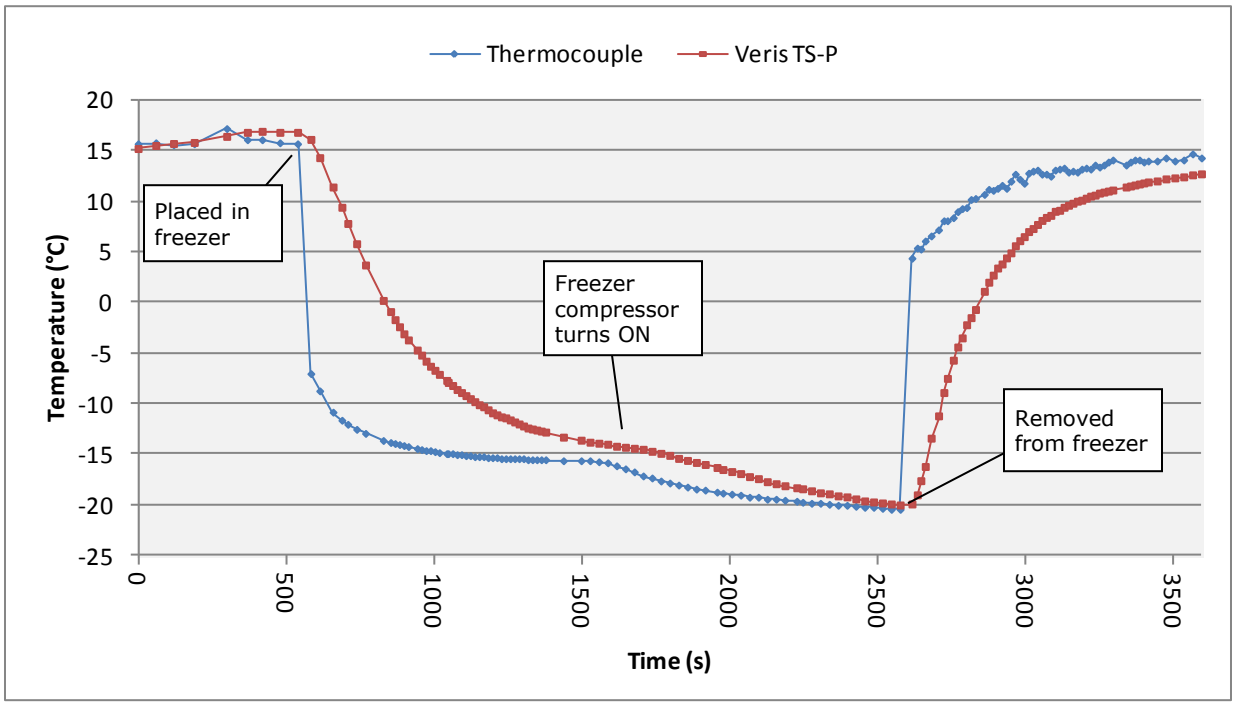

Figure 19 - Temperature vs. time data for sensor testing experiment

Evaluating the transient temperature performance of these sensors in the context of a lumped capacitance model, a time constant (τ) for the sensor, or the time it takes to reach 63.2% of the final environmental temperature, was estimated. The time constant can be determined from the slope (m) of the curve $\ln[\Delta T(t)/\Delta T(0)]$, where $\Delta T(0)$ is the temperature difference between the initial and final steady-state temperatures of the

experiment. Equations (1) through (5) show the derivation of the thermal time constant from temperature vs. time data, while Figure 20 plots the heating and cooling data for both sensors.

$$T(t) = T_{env} + (T(0) - T_{env})e^{-t/\tau} \quad (1)$$

$$\Delta T(t) = T(t) - T_{env} \quad (2)$$

$$\Delta T(t) = \Delta T(0)e^{-t/\tau} \quad (3)$$

$$\ln\left[\frac{\Delta T(t)}{\Delta T(0)}\right] = -\frac{1}{\tau}t = mt \quad (4)$$

$$\tau = -\frac{1}{m} \quad (5)$$

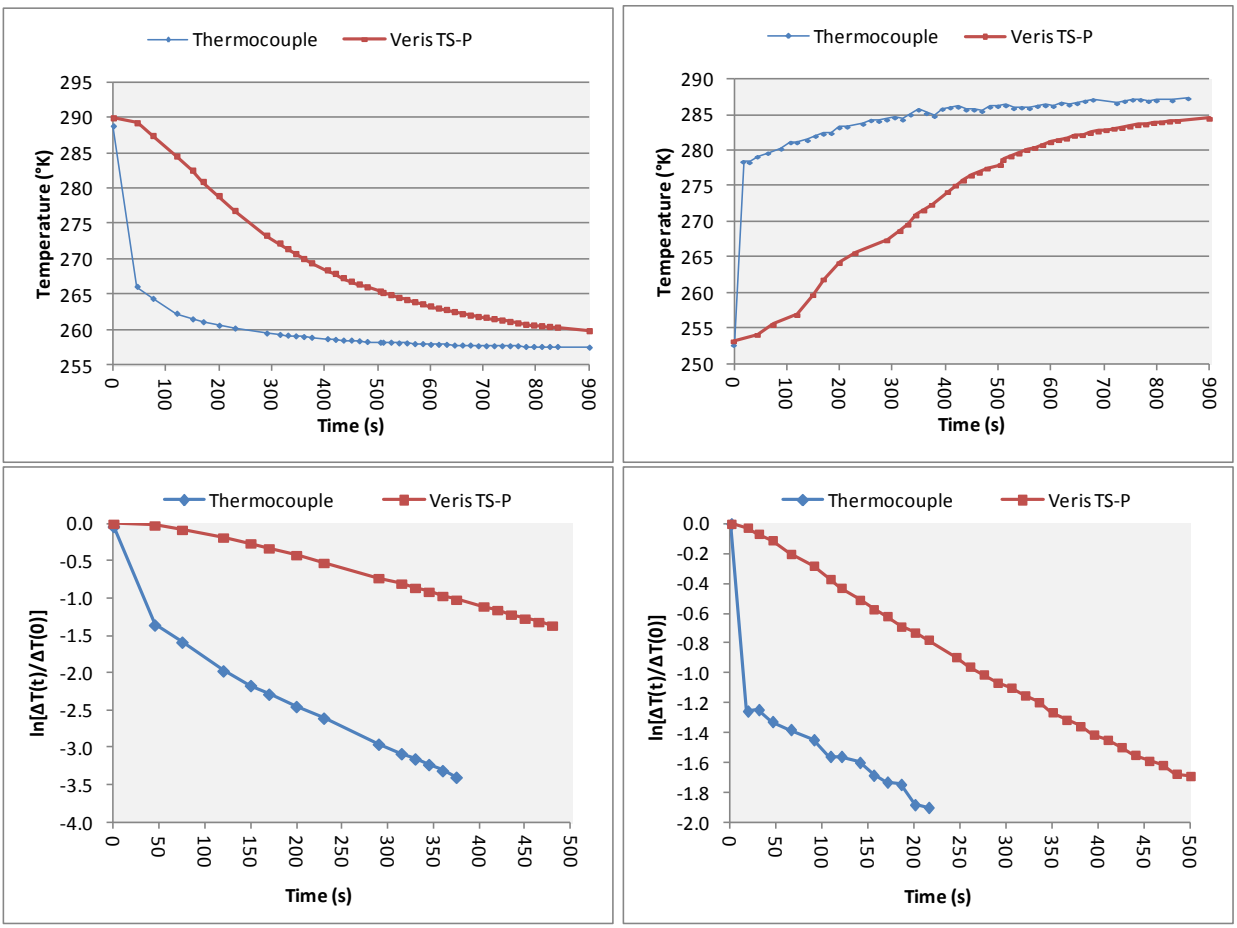

(a) Cooling (b) Heating

Figure 20 - Temperature performance of thermocouple and Veris TS-P sensor

This experiment demonstrates the relatively high thermal capacitance of the Veris temperature sensor results in a slow reaction to changing air temperature. At the same time, despite a quick initial reaction to temperature change, the thermal capacity of the thermocouple's polymer sheath and long wire leads are believed to prolong the time needed to report the final environmental temperature. In the case of heating, the thermocouple's time constant was observed to be approximately 5-10 seconds. For both heating and cooling, the time constant of the Veris sensor was approximately 5 minutes. This is clearly less than the 60 minute time step used by many energy modeling programs, yet the thermal capacitance of temperature sensors, particularly ones used in building applications, should be considered when trying to accurately monitor fluctuating room temperatures.

3.4.6 Sensor and Data Logger Impedance

After installing the Veris TS-P temperature sensors, each sensor's reported temperature was compared to the temperature measured using the calibrated Type T thermocouple described above. For each sensor, there was an approximate 2.5°C difference between the thermocouple and DAQ temperature measurement. The difference was well outside the expected deviation of both sensors, and therefore an investigation of the discrepancy was initiated.

As described earlier, the temperature sensor outputs a voltage signal that is read by the data logger. The sensor has an internal resistance of ~10kΩ, and is designed to output a 10mV/°C signal. The output of the sensor is theoretically 0 mV at absolute zero, but in more practical terms, 2.982 VDC corresponds to 25°C, not including any calibration offset defined by the manufacturer.

The first check was to verify the voltage output of each TS-P sensor using another voltage measurement device; again in this case the Fluke DMM. When measured with the DMM, the sensor output voltage, converted to temperature, correlated well with the thermocouple

measurement. The next thought was a malfunctioning data logger or some other component in the DAQ system was influencing the measured voltage output. Wiring connections were tested, the data logger and temperature calibration certificates were reviewed, and the voltage drops of wiring estimated; all checks resulted in no explanations for this temperature discrepancy.

Describing the situation to a colleague who specializes in electrical engineering, he suggested comparing the data loggers input impedance with the impedance of the temperature sensors measured. An ideal voltage measurement device has infinite input impedance, meaning it draws zero current from the circuit under test, and thus the measured potential closely reflects the actual potential across the external component. Practically speaking, the input impedance of voltage metering devices are finite, with most DMMs commonly having an input impedance of 10MΩ. Using a 10MΩ input impedance device to measure the voltage potential across an external, 10kΩ component (the rated resistance of Veris TS-P sensors), 0.1% of the voltage will be dropped through the external component and 99.9% of the potential will be measured by the meter. In this case, the expected minimum offset of the measured temperature at 25°C is expected to be ~0.25°C. Comparatively, the rated internal impedance of the Dataq 710 data logger is 1MΩ, an order of magnitude less than the DMM, resulting in only 99.0% of the potential drop across the sensor being measured, thus explaining the 2.5°C difference in temperature measured by the DMM and Dataq logger at typical room temperatures.

To evaluate the relationship between internal and external impedance, an experiment was performed to compare the Dataq and DMM voltage measurements across shunts of varying resistances. Figure 21 compares the difference in measured potential between the Dataq and DMM device, showing a very clear relationship between sensor impedance and the voltage offset. Based on these observations, a preliminary decision was made to wire the

sensor for current output (1µA/°C), and measure the potential across a lower impedance (1kΩ) shunt placed in series with the sensor, resulting a 1mV/°C signal output.

Veris Temperature Sensor (TS) Correlation (Current Output)
1 µA/degC
Voltage Measurement Instruments
Fluke DMM 179, 10MΩ Impedence, ±0.09% + 2 of reading (Calibrated)
Dataq 710-EH, 1MΩ Impedence, ±0.05% of full scale range ± 0.05mV

Resistor (Ohms)	ΔmV/degC	Dataq Gain Level (±V)	ΔV, DMM-Dataq (mV)
150	0.2	1.25	
978	1.0	1.25	0.5
2199	2.2	1.25	0.9
4620	4.6	2.50	4.3
10000	10.0	5.00	24.0
14530	14.5	5.00	52.3
21700	21.7	10.00	120.0

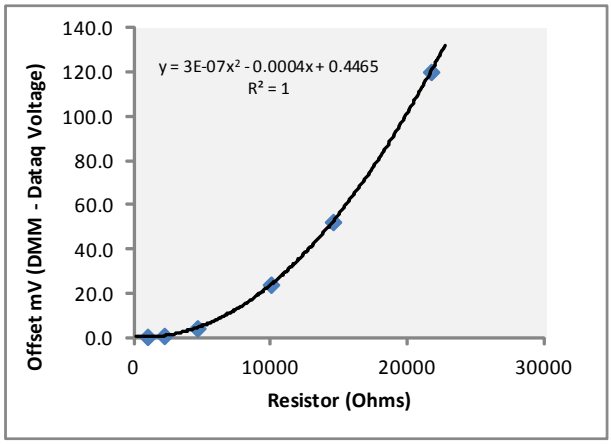

Figure 21 - Comparison of DMM and Dataq voltage measurements for various resistors

The lower external resistance reduces the offset, however, also lowers the signal voltage. This introduces yet another contribution to measurement error, that is, the limited resolution of the logger's analog-to-digital (A/D) convertor, which converts the analog potential measurement into a signal read by the computer. The Dataq 710 uses a 14bit A/D converter, meaning the maximum resolution is a $1/2^{14}$ change in the full-scale gain level. For example, on the ±1.25V full-scale gain setting, the maximum A/D resolution is 0.122mV (±1.25V = 2.5V / 2^{14}). If the signal output is 1mV/°C, a 0.15°C (0.27°F) change in sensor temperature must occur for the data logger to register the change. At the same time, the rated accuracy of the A/D convertor, as a percentage of full-scale output, does not change.

On the ±1.25V gain level, the rated accuracy of the Data logger is ±0.05% of full-scale ±0.05mV, or 1.3°C (2.34°F).

Ultimately, a hardware-based solution was used to mitigate the offset/sensitivity situation encountered. The input impedance of the DAQ was increased by placing a unity gain buffer circuit, also known as a voltage follower, between the sensor and the DAQ. The voltage follower circuit was created using a JFET operational amplifier (op amp, Radio Shack LM324), wired into the system as shown in Figure 22.

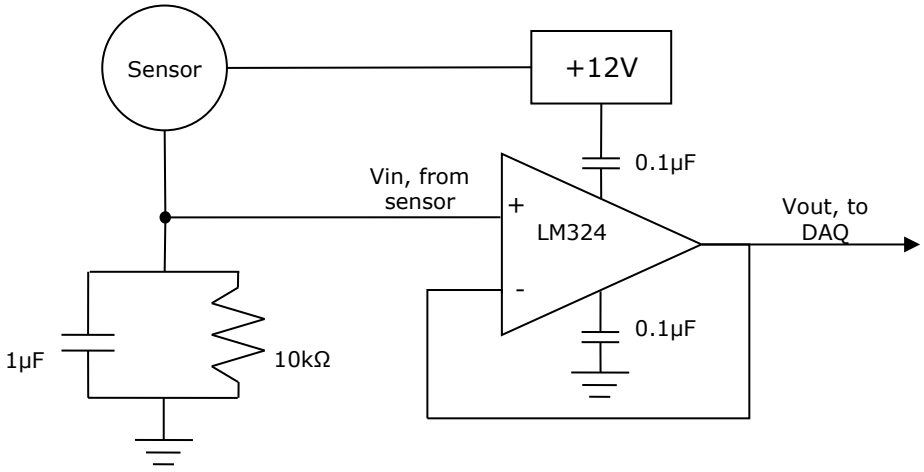

Figure 22 - Unity gain buffer circuit

The buffer circuit effectively transfers the voltage potential across a resistor in the sensor circuit to the DAQ circuit without any change in the magnitude of the voltage, while reducing the input impedance of the circuit. Figure 23 shows a picture of the buffer circuit, as implemented into the DAQ system. In addition to adding a unity gain buffer to each temperature sensor circuit, a low-pass filter was installed to help filter high-frequency noise that may be inducted into the sensor circuit. After implementing this modification, the DAQ

temperature sensor measurements were again compared to the thermocouple, and as shown in Figure **24**, a good correlation was observed.

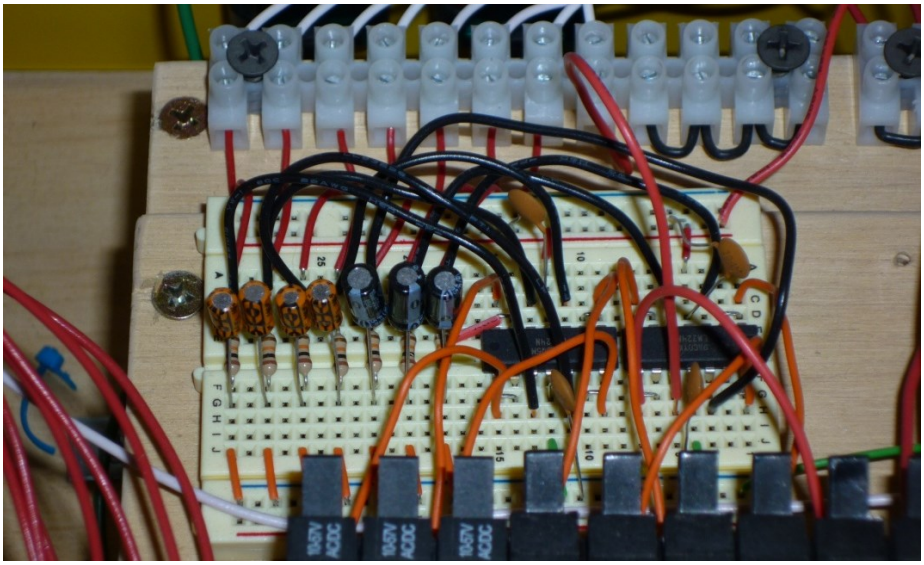

Figure 23 - Buffer circuits implemented in DAQ system

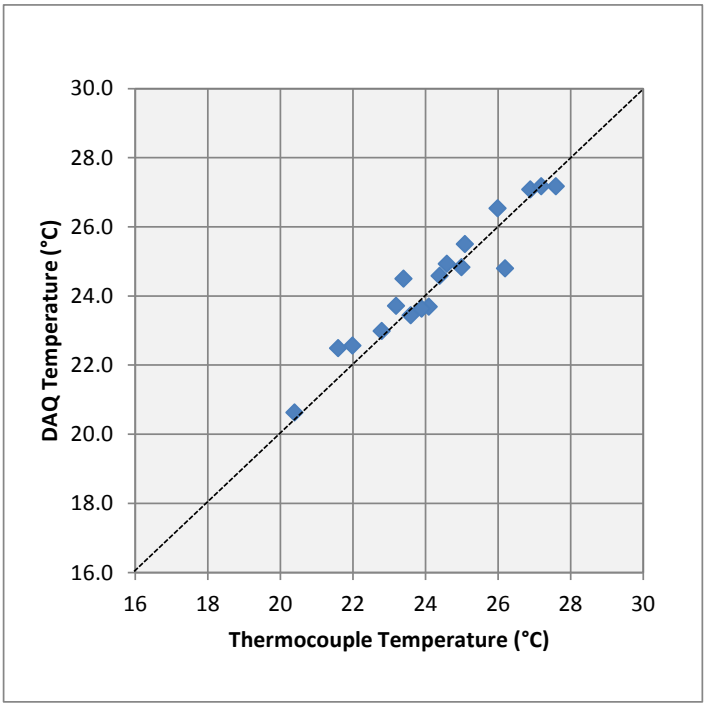

Figure 24 **- Comparison of DAQ and thermocouple temperature measurements, after implementing buffer circuit**

4 Weather Data

Building energy use is typically sensitive to environmental conditions. The HVAC heating load in most climates is proportional to outdoor air temperature, while peak cooling loads are often driven by solar heat gain. The lighting load, particularly in the northern latitudes, varies depending on the length of day and available daylight illumination. Energy modeling is typically performed using TMY weather data files, which are available for hundreds of weather stations across the United States. These weather files are acceptable for design phase estimates of building energy use and ECM impacts, however, model calibration studies typically necessitate accounting for actual meteorological conditions.

As mentioned in Chapter 2, it is now possible to purchase actual year weather files for BES programs for as little as $40/year. However, at the time of starting this project, these services were not available, and therefore, a Matlab program was developed to process weather observations for the closest weather station (Bellingham International Airport, KBLI) and create a custom annual weather file for this calibration exercise. Solar radiation is not measured at this weather station, so it was estimated from cloud cover and other available weather information using an existing solar model customized for the specific site location. In mid-2012, a weather file was provided at no cost by Weather Analytics, and used as a comparison to the outcome of this project. After first outlining the procedure used to develop a custom weather file, a brief summary comparison, as well as comparison of to the commercially available weather files and site-measured variables is described.

4.1 Weather File Processor

The process of creating a weather file spans from obtaining the raw weather data, to converting weather data into a format that can be read by the simulation program. The fundamental weather variables needed for the DOE-2 program and most BES software include:

a) Dry bulb temperature
b) Dew point or wet bulb temperature
c) Wind speed
d) Wind direction
e) Atmospheric pressure
f) Humidity ratio or relative humidity
g) Cloud cover (used to estimate solar radiation variables if solar is not available)
h) Solar radiation (global and direct normal)

These variables, with the exception of solar radiation, are typically available for local government weather stations from the National Climatic Data Center (NCDC). Many processing steps lie between the raw weather data and the software weather file compatible with the BES program, which is likely why this step of calibrating an energy model can take a significant amount of time. The basic steps used in this study were:

1. Identify and download weather data for the closest NCDC station with hourly observations.
2. Clean data, i.e. remove extraneous data points and fill gaps in data streams.
3. Calculate solar radiation data.
4. Organize all data into a format compatible with the BES software.

4.1.1 NCDC Integrated Surface Data

The NCDC integrated surface database (ISD) is comprised of over 11,000 active stations worldwide, with observations as far back as 1901 (National Climatic Data Center 2013). These stations are typically located near international, national, or regional airports, and most include hourly observations of parameters a-g listed above. In recent years, as the cost of small scale weather observation stations has fallen, a network of non-NCDC stations has grown. The Weather Underground (Historical Weather 2013) is a web resource offering access to both NCDC and private/non-NCDC stations, including download of hourly historical weather data in comma-delimited files. However, the NCDC ISD service includes some level of automated quality control, and therefore, increased confidence the observations are valid.

As summarized in Table 5, the closest suitable NCDC station for this project was located six miles away. ISD data is delivered via email from NCDC servers as a comma-delimited file with a key to the various columns of observations. The standard format is designed to contain hundreds of possible observed or calculated variables, though for most sites, only the principal observations listed above are populated with real values. Access to archived ISD information is now available at no cost, though at the time of starting this project, it was only available for purchase if procured outside of government networks (including the University of Washington). Figure 25 provides a satellite view of the Bellingham area, illustrating the proximity of the building site to the NCDC station.

Table 5 - Project site and NCDC weather station location

Project Address	1708 Kentucky St, Bellingham, WA 98226
Latitude	48.76° N
Longitude	122.45° W
NCDC Station	Bellingham International Airport (KBLI)
Latitude	48.79° N
Longitude	122.54° W
Distance from project	6 miles
TMY3 Station	Same as NCDC Station

Figure 25 - Satellite view of local region showing proximity of project location to local NCDC weather station

4.1.2 Cleaning Weather Data

In most cases, ISD data includes at least one observation of each variable for each hour. However, in the case of the data file obtained for this project, there were two main issues to address:

1. More than one recorded observation in a single hour
2. One or more missing hourly variables.

4.1.2.1 Removing Extraneous Points

For the KBLI weather station site, the most consistent hourly observation was time stamped at the 53rd minute of each hour. However, in some hours, there were more observations, though typically no more than two or three. The Matlab routine evaluated the timestamp of each observation and selected the observation closest to the end of a whole hour; using that value to describe the condition for the previous hour. For example, if the observation timestamp was 0053, corresponding to 00:53 (24hr notation), that record was used to represent the hourly temperature for the 00:00 to 01:00 energy modeling interval. During this process, if there was no observation for an hour, an empty timestamp was inserted into the data file for the gap filling routine to recognize in the next major step of the process. Finally, all timestamps were converted to local standard time (LST), as ISD time records are defined at Greenwich Mean Time (GMT), while the simulation program assumes weather values are LST.

4.1.2.2 Gap Filling

Inevitably, archived weather station data may be missing some hourly values. Therefore, a gap filling routine is usually necessary to provide a complete data set. Table 6 summarizes the NCDC variables used in creating the DOE-2 weather file, including the number of missing hourly values for each parameter. For this project, the gap filling routine used by the DOE EnergyPlus weather data service was used (Long 2006):

If the missing period is less than 6 hours, points are filled linearly as shown in Equation (6). If the missing period is greater than 6 hours but less than 48 hours, points are filled using a combination of the previous valid day (d) values, offset by surrounding values, as shown in Equation (7). If the missing period is greater than 48 hours, the values are not filled by the Matlab routine; this condition did not exist in 2010, the calibration year for this study.

$$f(t_n) = f(t_1) + \left(\frac{f(t_2) - f(t_1)}{t_2 - t_1}\right) n \quad (6)$$

$$f(t_n) = f(t_{n-d}) + \left(f(t_1) - f(t_{1-d})\right) + \left(\frac{\left(f(t_2) - f(t_{2-d})\right) - \left(f(t_1) - f(t_{1-d})\right)}{t_2 - t_1 + 1}\right) n \quad (7)$$

where:
$f(t_n)$ = the time step to fill
$f(t_1)$ and $f(t_2)$ = the values around the missing time step
d = the offset back to the previous valid day

Table 6 - NCDC weather variables used to create custom annual weather file (8760 total hours)

Observation	Units	Missing Hourly Values
Dry Bulb Temperature	°F	46
Dew Point	°C	55
Wind Speed	meters/second	47
Wind Direction	Deg CW from North	2550
Atmospheric Pressure	Millibars	78
Cloud Cover	Tenths	55
Relative Humidity	%	55

4.1.3 Calculation of Solar Radiation

Solar radiation is typically the most difficult information to gather for an actual calibration period. Only select sites across the United States measure the necessary solar radiation variables, global horizontal and direct normal (or diffuse) radiation, and these data are not always readily available. If a measurement site is in close proximity (<50miles) to the building site, varying cloud conditions can still contribute to a significant difference between locations. Analysts creating a custom weather file without access to local solar radiation information have two basic options:

a) Use hourly TMY solar radiation data for the closest TMY weather site.

b) Calculate solar radiation data using available weather observations and a model.

This author chose to experiment with the latter method, as for most building simulations, the coincidence of solar and other conditions can have a large impact on the building loads, and hence, energy consumption. Unless otherwise indicated, definition of solar variables and equations in the following sections are taken from Duffie and Beckman (2006)

4.1.3.1 Global Horizontal Radiation

Global horizontal radiation (G, W/m^2) is the total amount of solar flux (beam and diffuse) received on a horizontal surface. Terrestrial G_{Horz} is readily measured using a pyranometer mounted with a clear view of the sky. In this report, the amount of radiation incident on surface for a given hour (I or I_{horz}), is also expressed with the units of W/m2, but assumed to be the average instantaneous flux over the course of the entire hour. In this procedure, global horizontal radiation is calculated first, and then other components, hourly beam (I_b) and diffuse (I_d) radiation, are estimated using additional correlations. An exhaustive evaluation of solar models was outside the scope of this project; however, two different models are described in the EnergyPlus Weather Converter Program and Engineering Reference manual for use in annual building simulations (Department of Energy 2012):

ASHRAE Clear Sky Model: The original ASHRAE Clear Sky model was recently updated, and is the recommended model for estimating design solar radiation values under uniform atmospheric conditions. As such, it is not intended for estimating solar radiation under the varying or complete cloud conditions that commonly occur in the Pacific Northwest.

Zhang-Huang (ZH) Model: An empirical model initially developed to calculate hourly solar radiation values for Chinese TMY files; see Equation (8). The model is described to be suitable for other sites, though at the time of starting this project, only model regression coefficients for locations in China were available.

$$I = \frac{[I_{sc}\sin(h)\,(c_0 + c_1 CC + c_0 CC^2 + c_3(T_n - T_{n-3}) + c_4\varphi + c_5 V_w) + d]}{k} \quad (8)$$

where:
I = estimated hourly global horizontal solar radiation, W/m2
I_{sc} = solar constant, 1355 W/m2[2]
h = solar altitude angle, i.e., the angle between the horizontal and the line to the sun[3]
CC = cloud cover, based on observer's judgment
φ = relative humidity, %
T_n, T_{n-3} = dry-bulb temperature at hours n (current) and n-3, respectively
V_w = wind speed, m/s

4.1.3.2 ZH Model Validation

To gain confidence in using the ZH model for this study, a basic validation exercise was completed using TMY3 weather data. The variables in the TMY3 file for the Bellingham Airport (KBLI) were used as inputs to the ZH model, and the calculated hourly global horizontal radiation was compared to the "true" value contained in the TMY3 file.

Figure 26 provides a comparison of the monthly average hourly solar radiation for this initial evaluation. The ZH model parameters developed for locations in China consistently over-estimated the hourly solar radiation for this Pacific Northwest site. In an attempt to improve the ZH model formulation for this study, new coefficients/constants were developed using the KBLI TMY3 data as true model inputs/outputs. Multiple fits were developed using Matlab's *nlinfit* function and varying the model parameters. In generating new coefficients, only daytime hourly solar radiation values (I_{horz} >0) were used.

[2] This is the solar constant reported for the initial formulation of this model, which is less than the currently accepted value of 1367 W/m^2. See Chapter 1.2 of Duffie and Beckman for historical background on this value.
[3] In this study, the solar altitude used to calculate hourly values of global and other radiation components was defined at the midpoint of each hourly period.

The combination that yielded the smallest difference between the ZH model and the true TMY3 monthly and annual hourly average profiles was found by relaxing parameters c_1, c_2, c_3, and k (see Table 7). The parameters affected by these coefficients intuitively matches expectations for this local climate, where solar radiation is strongly dependent on cloud cover, and solar conditions have a strong impact on ambient temperature. Figure 27 again illustrates the monthly average hourly solar radiation profiles with the new ZH model coefficients. The revised model correlates well with actual values in most months, however, the peak daily radiation in the months of April, May, June, and to a lesser degree, July, is under-estimated.

Table 7 - Summary of original and revised ZH model parameters

Parameter	Description	Original ZH model parameters	Revised ZH model parameters
c0	Linear constant	0.5598	0.5598
c1	CC (cloud cover)	0.4982	-0.3571
c2	CC^2	-0.6762	-0.0802
c3	T_n-T_{n-3}	0.02842	0.0136
c4	φ (relative humidity)	-0.00317	-0.00317
c5	V_w (wind speed)	0.014	0.014
d	Additive constant	-17.853	-17.853
k	Divisor constant	0.843	0.8404

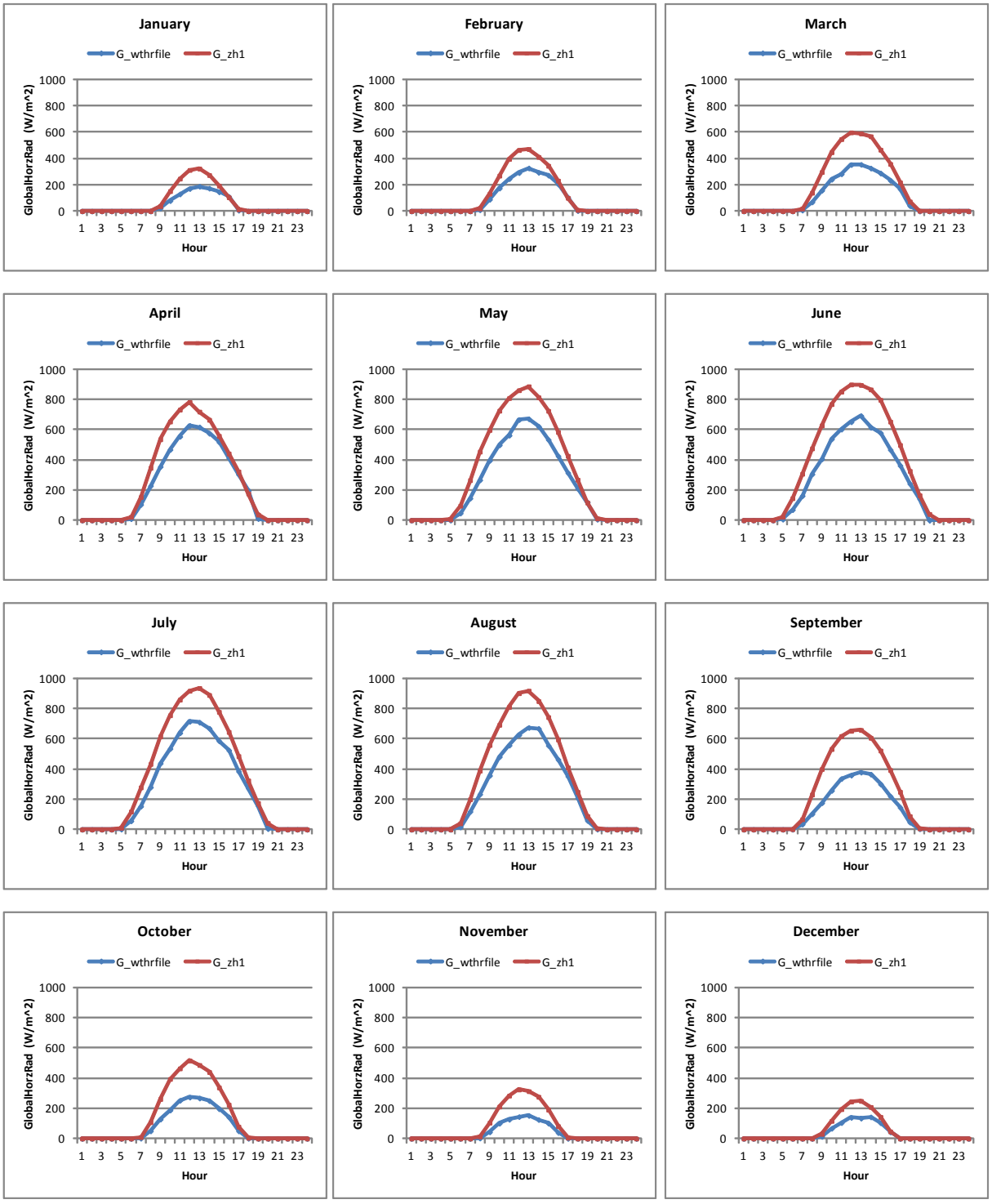

Figure 26 - Monthly average hourly global radiation profiles using original ZH model parameters (developed for China locations)

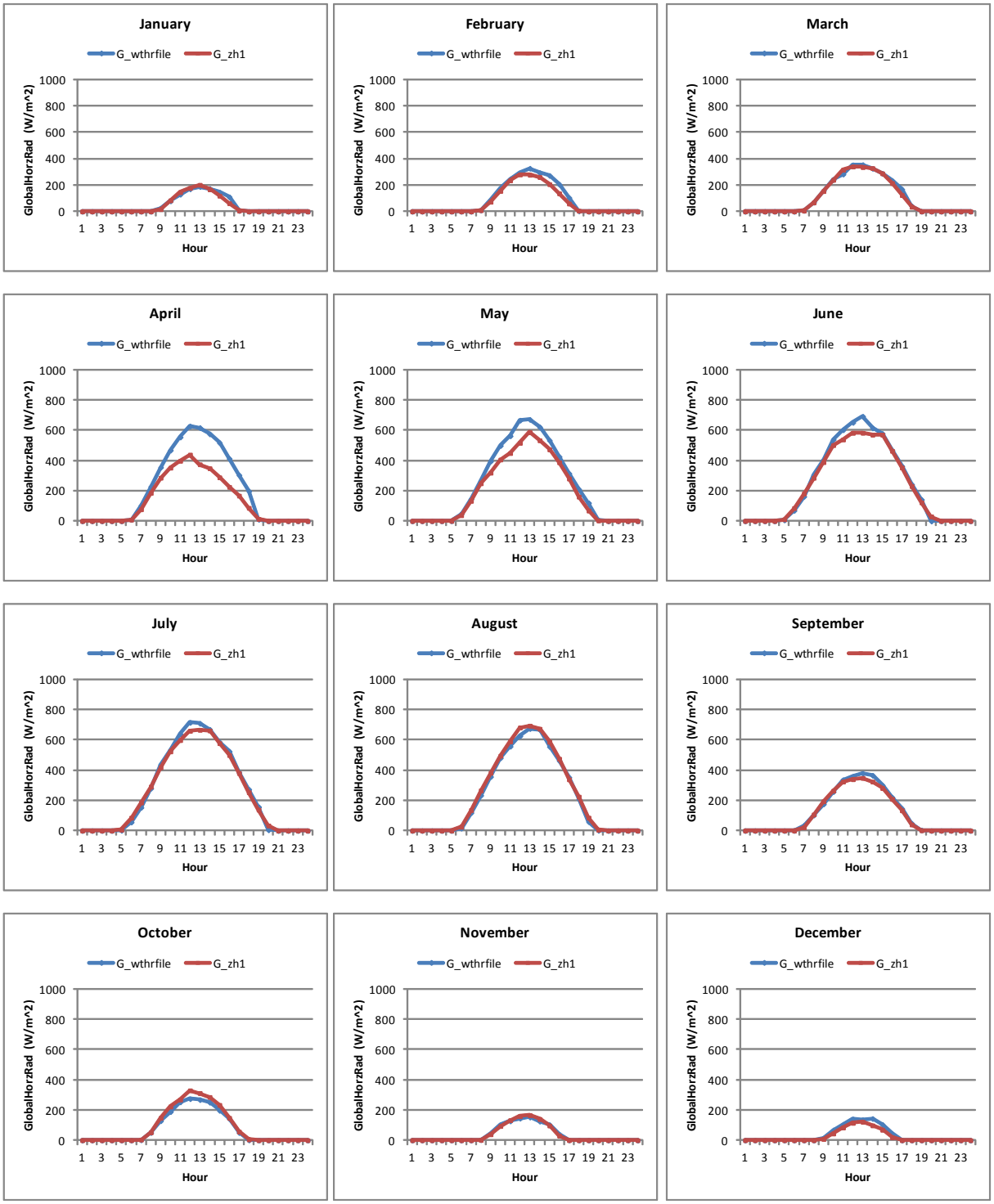

Figure 27 - Monthly average hourly global radiation profiles using revised ZH model parameters (developed for KBLI location)

A brief inspection and comparison of the hourly TMY3 cloud cover and I_{horz} values showed numerous times when the values in the TMY3 file did not correlate well. Figure 28 compares the hourly TMY3 I_{Horz}, Max I_{Horz} (see Equation (9)) and the cloud cover values for five days in April. This plot illustrates how TMY3 solar radiation and cloud cover values are not always consistent with each other. It is not known if the inconsistency is due to the subjective nature of cloud cover measurement, or an artifact of how the TMY3 data sets were developed. However, it is believed this is one contributor to the proposed solar model error and to be kept in mind when applying this model in other applications.

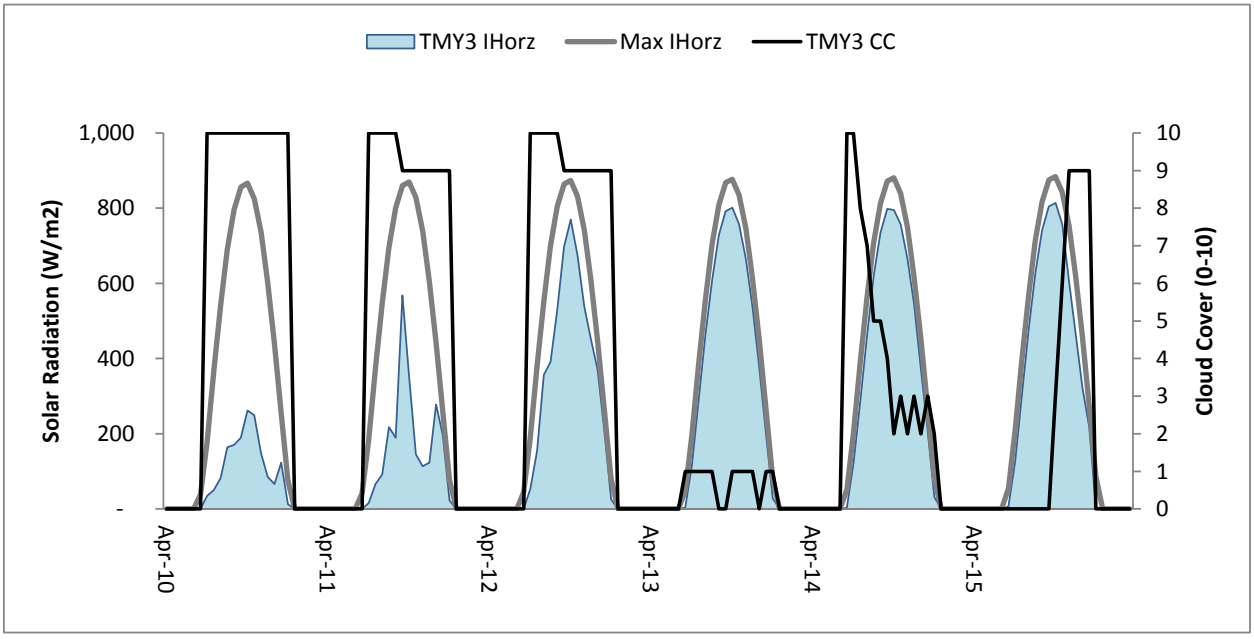

Figure 28 - Example comparison of TMY3 solar radiation and cloud cover data

$$Max\ I_{Horz} = I_{sc} \sin(h) \tag{9}$$

where:
Max I_{Horz} = Maximum hourly global horizontal solar radiation, W/m^2
I_{sc} = solar constant
h = solar altitude angle

A detailed optimization and parameter sensitivity study that might have facilitated a better model formulation was outside the scope of this project. However, the revised model coefficients fit the TMY3 data better than the original model values, and therefore, were used in this study to estimate hourly global horizontal radiation from the available ISD weather variables.

4.1.3.3 Beam and Diffuse Solar Radiation

With annual hourly global horizontal radiation calculated using the modified ZH model, the other important solar components, beam and diffuse, can be calculated. Global horizontal radiation is the sum of the beam and diffuse components (Equation (10)), and if two of the components are known, the other is readily available. A common approach is to first determine the diffuse component using an empirically determined relationship between the hourly clearness index, k_T (Equation (12)) and the ratio of diffuse to total horizontal radiation (I_d/I). More than one empirical correlation for this relationship exists; all derived from separate databases of measured diffuse and global solar radiation. However, a correlation developed with Seattle, Washington measurements of solar radiation, indicated here as UW-BESTR model and described in Equation (12), was found to fit local measurements better than other published correlations (Piguet 1987); thus utilized for this project. With the diffuse component calculated, the beam component is converted to direct normal radiation, the value needed for the weather file processor, using Equation (13). Calculation of all hourly solar radiation variables, such as I_0, requires evaluating the multiple angles that describe the position of the sun with respect to the building site for each hour, of each day, in a year.

$$I = I_b + I_d \tag{10}$$

$$k_T = \frac{I}{I_0} \tag{11}$$

$$\begin{aligned} I_d &= I\left[1 - \left(0.032{k_T}^{0.2696} exp(4.8036 k_T)\right)\right] \quad \text{for kT<0.72} \\ I_d &= 0.1I \quad \text{for kT≥0.72} \end{aligned} \tag{12}$$

$$I_{dn} = \frac{I_b}{\cos\theta_z} \tag{13}$$

where:
I = global horizontal solar radiation, W/m2
I_b = beam solar radiation, W/m2
I_d = diffuse solar radiation, W/m2
k_T = clearness index
I_0 = extraterrestrial solar radiation on a horizontal surface, W/m2.
I_{dn} = direct normal solar radiation
θ_z = zenith angle, evaluated at the middle of hour.

4.1.4 Creation of Weather File

With the NCDC data cleaned, gaps filled, and hourly solar radiation calculated, values are processed into the format used by the simulation program. Unlike other programs that utilize weather data in an ASCII format, the DOE-2 program requires the weather data to be compiled into a binary (.bin) file format. This processing step is completed using the DOE-2 Weather Processor utility (Buhl 199); however, before it can be "packed" into the binary file, weather data must be organized into a format recognized by the processor. The utility supports a few different formats, however, the columnar TMY2 file structure (Marion 1995) is the recommended structure if global and direct normal solar radiation variables are defined. The TMY2 format is also compatible with weather file visualization tools, such as DView (2013), a free and capable tool weather visualization program.

4.2 Comparison of Weather Data to Other Sources

After compiling a weather file, a prudent measure is to compare the output to other sources and make sure the values are acceptable. In this project, the file created for this thesis was compared to two other sources:

1. An actual meteorological year (AMY) weather data file obtained from Weather Analytics for the site location.
2. Outdoor dry bulb temperature and global horizontal radiation measured at the building site using the equipment described in Chapter 3**Error! Reference source not found.**.

First, the weather file created for this thesis was compared to source #1, since the information can be evaluated over the course of the entire year. Second, the weather file values were compared to available measured solar radiation and temperature observations.

4.2.1 Comparison to Weather Analytics Data

Late in the course of this project, a custom weather file from Weather Analytics (WxA) was obtained. Mentioned previously, the DView program was used to graphically compare the weather variables. The following variables are believed to have the largest impact on the modeled space temperatures and therefore building heating energy demands, as well as to demonstrate the validity of the solar modeling algorithms:

a. Dry bulb temperature (Figure 29)
b. Wind Speed (Figure 30)
c. Global Horizontal Radiation (Figure 31)
d. Diffuse Radiation (Figure 32)
e. Direct Normal Radiation (Figure 33)

The WxA data are shown in green, while the data compiled for this thesis (360ZH1) are shown in orange.

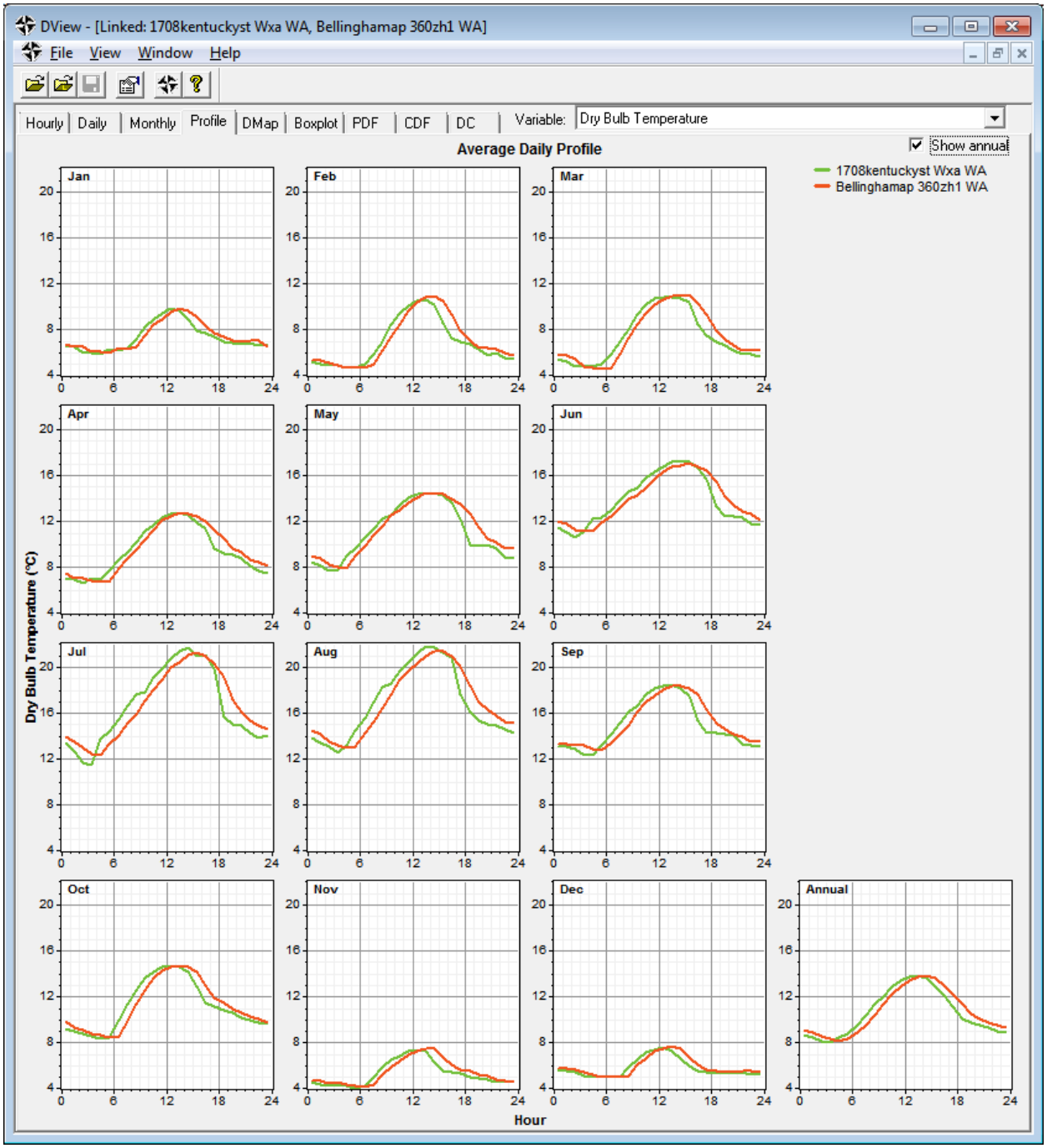

Figure 29 - WxA/360 monthly weather comparison, dry bulb temperature

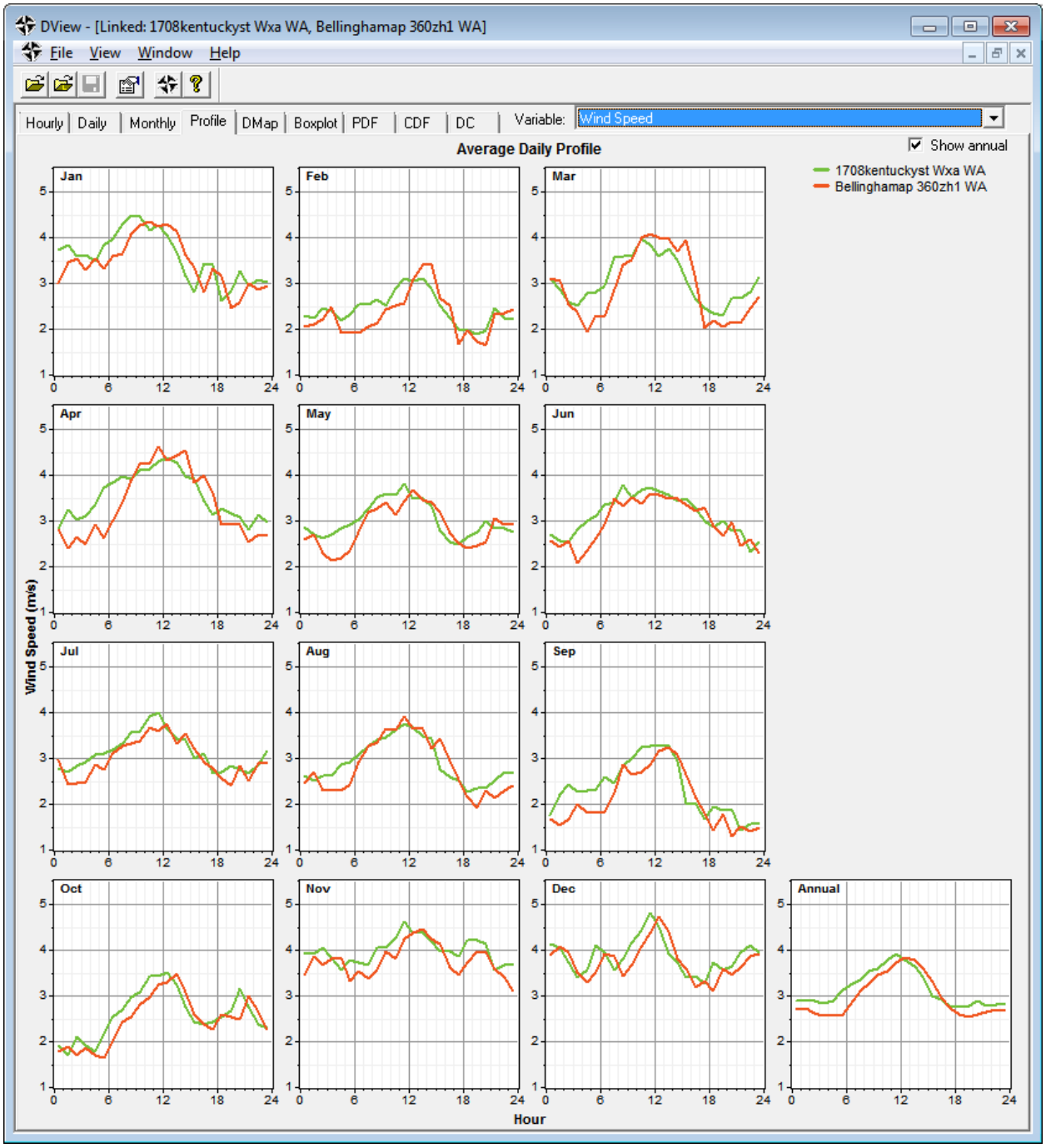

Figure 30 - WxA/360 monthly weather comparison, wind speed

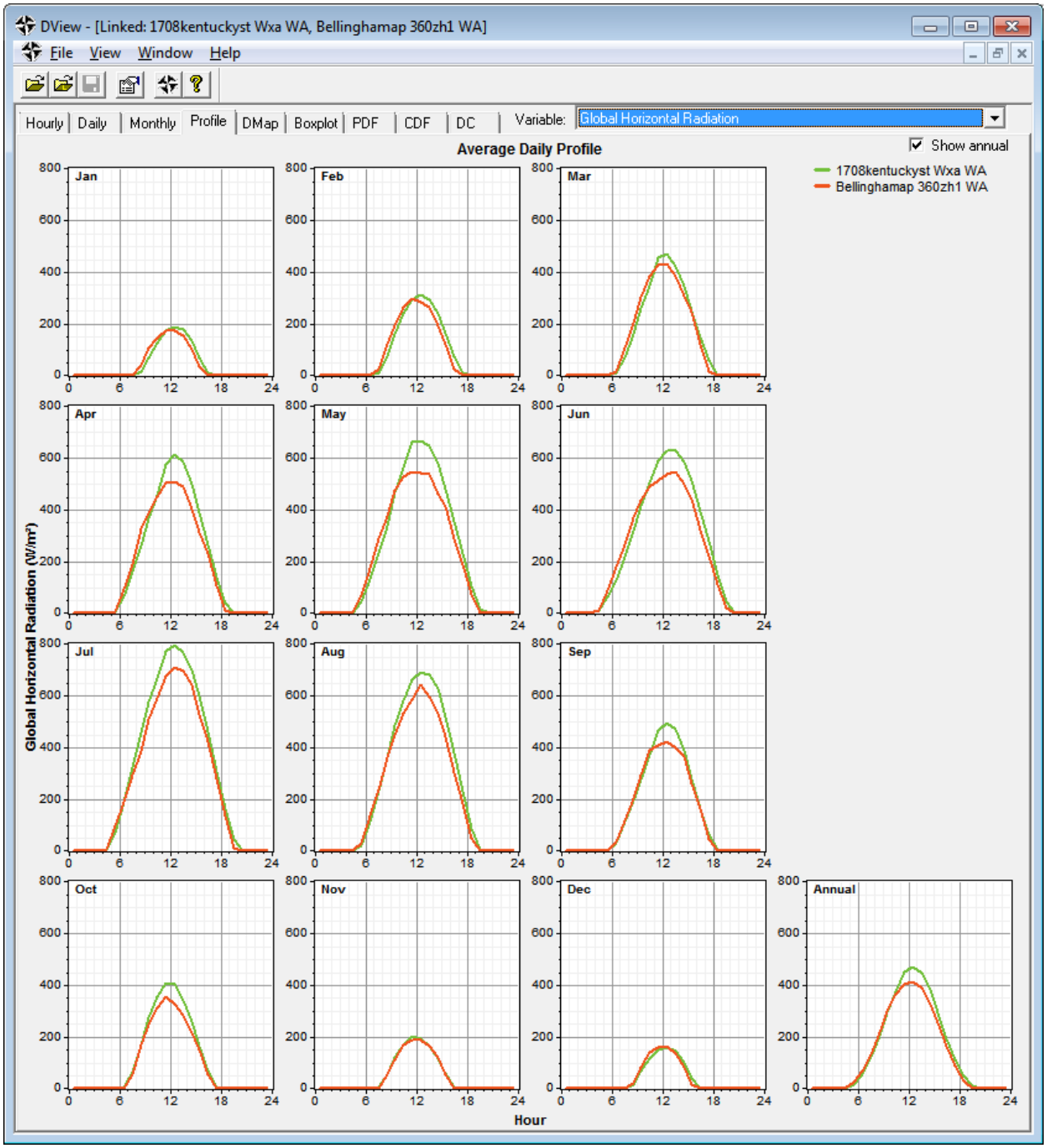

Figure 31 - WxA/360 monthly weather comparison, global horizontal radiation

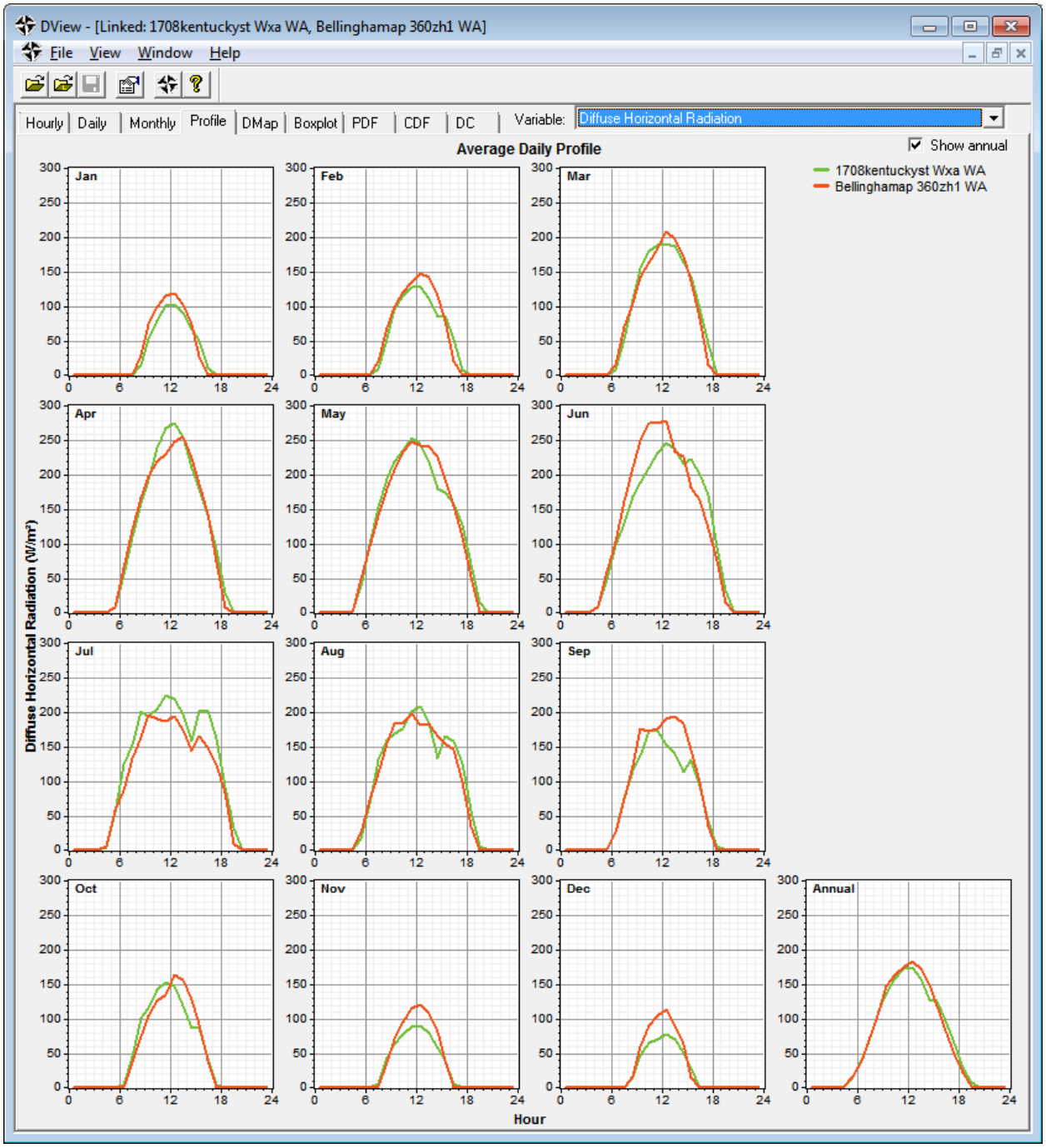

Figure 32 - WxA/360 monthly weather comparison, diffuse horizontal solar radiation

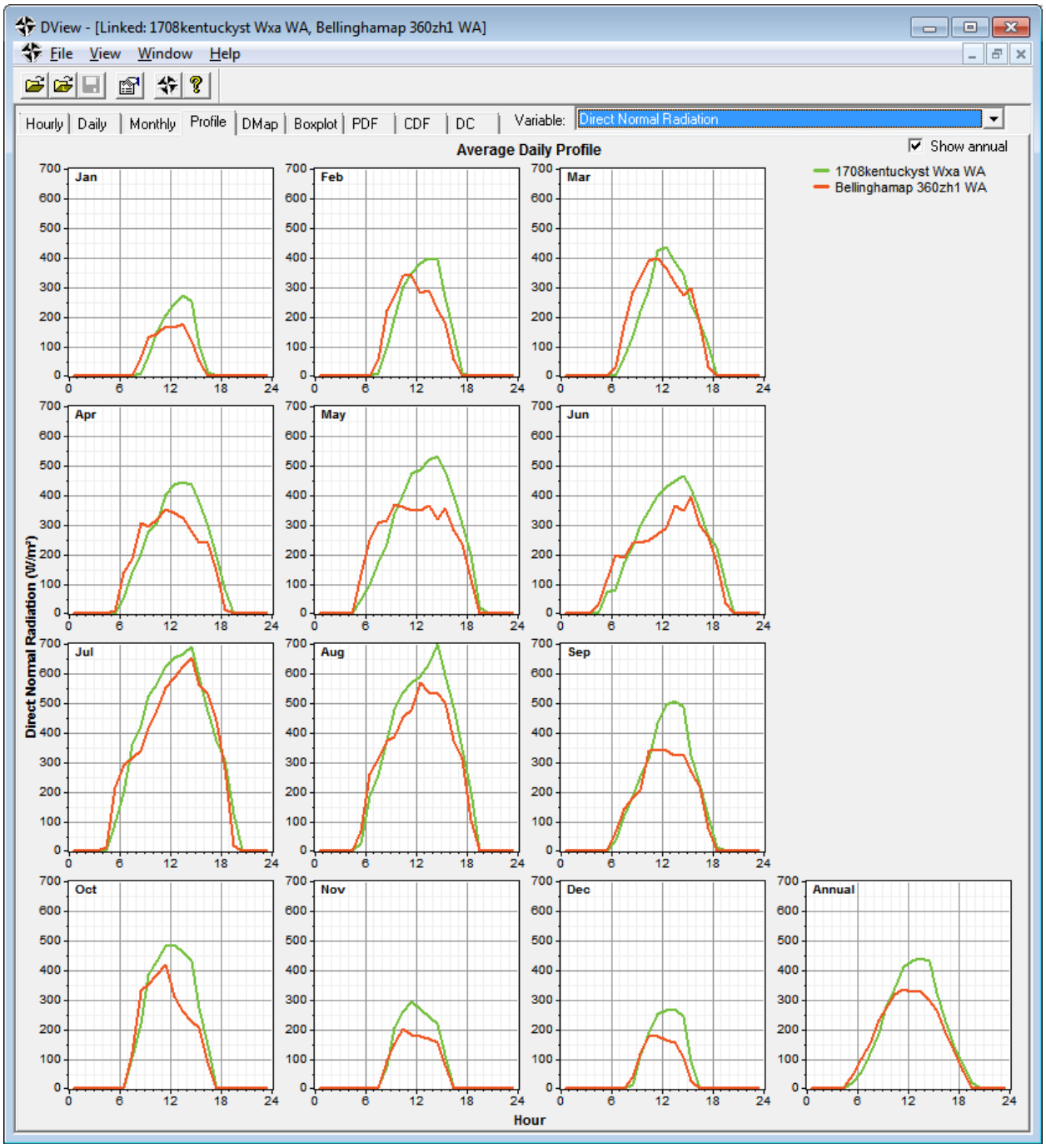

Figure 33 - WxA/360 monthly weather comparison, direct normal solar radiation

The first thing to be noted is the temperature and wind speed correlate well in magnitude and variation throughout the day, with the exception of a distinct one-hour offset between the profiles. An investigation and comparison with other sources of historical data indicates hourly KBLI weather station records are typically defined at the 53rd minute of each hour. By cross-referencing these readings, it appears that the WxA temperature, wind speed, and other surface observations are listed assuming that the reading reported at XX:53 is for the previous hour, whereas in this study, the XX:53 weather reading was assumed for the current hour. Table 8 below illustrates the difference in weather observation times for the first day in 2010.

Table 8 - Comparison of temperature observations for 1/1/2010

Time of KBLI Observation (PST)	Time period for simulation	KBLI Temperature (°C)	360 ZH1 Temperature (°C)	WxA Temperature (°C)
0:53	0:00 - 1:00	3.3	3	3.3
1:53	1:00 - 2:00	3.3	3	3.4
2:53	2:00 - 3:00	3.3	3	3.4
3:53	3:00 - 4:00	3.3	3	3.4
4:53	4:00 - 5:00	3.3	3	4
5:53	5:00 - 6:00	3.9	4	11
6:53	6:00 - 7:00	11.1	11	10.5
7:53	7:00 - 8:00	10.6	11	10.5
8:53	8:00 - 9:00	10.6	11	11
9:53	9:00 - 10:00	11.1	11	11
10:53	10:00 - 11:00	11.1	11	11
11:53	11:00 - 12:00	11.1	11	11
12:53	12:00 - 13:00	11.1	11	10.5
13:53	13:00 - 14:00	10.6	11	9.9
14:53	14:00 - 15:00	10	10	9.9
15:53	15:00 - 16:00	10	10	9.3
16:53	16:00 - 17:00	9.4	9	8.8
17:53	17:00 - 18:00	8.9	9	8.8
18:53	18:00 - 19:00	8.9	9	8.2
19:53	19:00 - 20:00	8.3	8	8.2
20:53	20:00 - 21:00	8.3	8	8.2
21:53	21:00 - 22:00	8.3	8	8.2
22:53	22:00 - 23:00	8.3	8	8.2
23:53	23:00 - 0:00	8.3	8	8.2

Subsequent to these findings, Weather Analytics was contacted in an effort to determine the cause for this discrepancy. They indicated their principal source for surface observation data are not from NCDC, but rather via the Meteorological Assimilation Data Ingest System (2013), or MADIS; the following is a brief description from the web homepage:

> *MADIS subscribers have access to an integrated, reliable, and easy-to-use database containing the real-time and saved real-time observational datasets described below. Also available are real-time gridded surface analyses that assimilate all of the MADIS surface datasets (including the highly-dense integrated mesonet data). The grids are produced by the Rapid Update Cycle (RUC) Surface Assimilation System (RSAS), which incorporates a 15-km grid stretching from Alaska in the north to Central America in the south, and also covers significant oceanic areas. The RSAS grids are valid at the top of each hour, and are updated every 15 minutes.*

The energy model results using the WxA weather file are described in Chapter 6.4.1, but further investigation into the effect of a one hour offset in weather file surface measurements on model calibration was not in the scope of this study. However, depending on the modeling/building applications, the temporal impacts of weather variables may be an important consideration for modelers. WxA solar radiation data streams do not appear to have this offset, though WxA's algorithm for calculating solar radiation was not examined in this review.

Based on the comparison to the WxA weather file, the following concluding remarks can be made:

- The magnitude of important surface observation values are in line with those described in the WxA weather file.

- The 360ZH1 peak daily global horizontal solar radiation, and correspondingly, the direct normal radiation, is less than the values predicted by WxA, particularly in the middle half of the year.
- The 360ZH1 model predicts higher solar radiation in the morning, and conversely lower solar radiation in the afternoon.
- The diffuse components correlate well, though the 360ZH1 model consistently predicting higher diffuse radiation in the middle the day.

4.2.2 Comparison to Measured Data

As described in Chapter 3, building interior and outdoor air dry bulb (OADB) temperatures and global solar radiation (I_{horz}) were measured in this study. For all monitoring periods, OADB and I_{horz} were measured. In addition, I_{horz} was measured simultaneously using the Davis silicon photodiode sensor and an Eppley PSP 180° pyranometer for a 12 day period in September 2010 (9/22 - 10/4). Both solar sensors were located at approximately the same height and location on the building rooftop, as shown in Figure 34. Figure 16 in Chapter 3.4.3 demonstrates the spatial relationship between the solar sensors and the OADB sensor.

Figure 34 - Photo of installed Davis and Eppley global solar radiation sensors

4.2.2.1 Solar Radiation Comparison

The Eppley meter, though lacking recent calibration status, was considered in this study as the measured "standard" for solar radiation. To mitigate any measurement bias induced by the DAQ system, sensor outputs were acquired by a separate logger with higher sensitivity (16bit Datataker 80). Figure 35 plots the measured I_{horz} using the Davis sensor (y-axis) with respect to the Eppley sensor (x-axis). There is excellent correlation between the two measurements, and thus, the Davis sensor was assumed to be a reliable benchmark for measured I_{horz}.

Figure 36 plots the WxA and 360ZH1 modeled solar radiation with respect to the Eppley measurements; both models provide reasonable correlations. For this 12 day period, the 360ZH1 appears to fit the local solar conditions better, though for many hours of low irradiance, the 360ZH1 model over-predicts I_{horz}; an observation also noted when comparing to the WxA model.

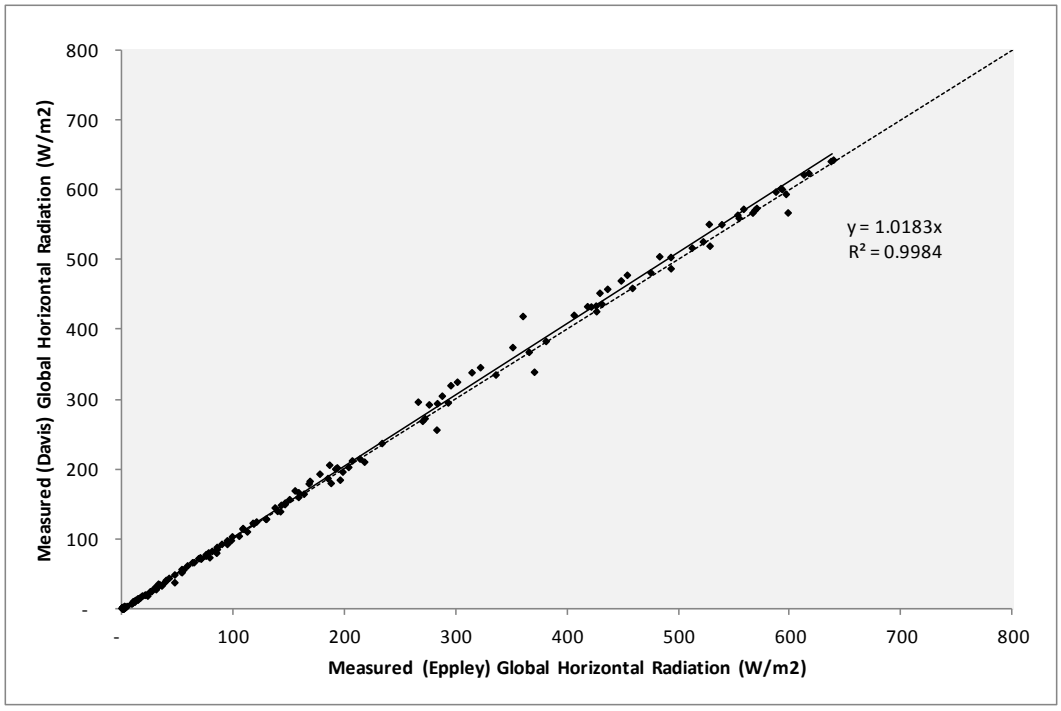

Figure 35 - Scatter plot of measured Eppley vs. measured Davis sensor Ihorz for a 12 day period in September 2010

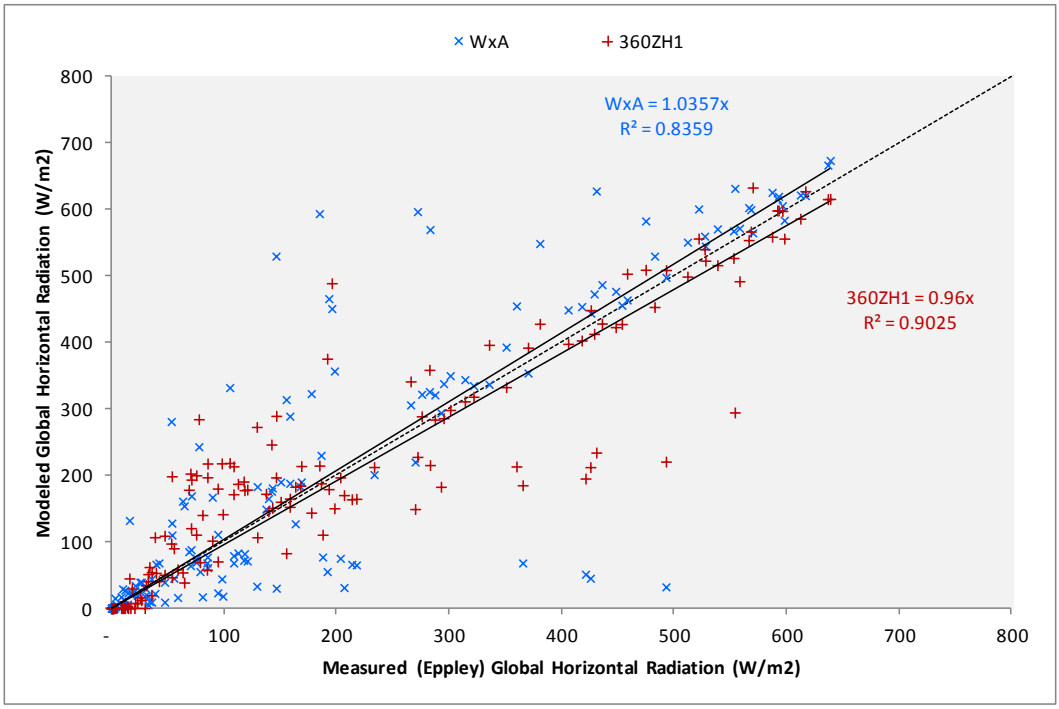

Figure 36 - Scatter plot of measured vs. modeled I_{horz} for 12 days in September 2010

With the Davis sensor "validated" as an acceptable I_{horz} measurement device, the evaluation of the WxA and 360ZH1 models could be expanded to the additional days when only Davis sensor measurements were available. The larger data set consisted of approximately 138 days throughout the months of June and December of 2010. Figure 37 illustrates the greater scatter between the measured and modeled data sets, and indicates the 360ZH1 model generally under-predicts I_{horz} except at low levels of radiation, though with a slightly tighter distribution to the measured value. Figure 38 includes two daily profiles: one for a relatively clear day, and one for a partly cloudy day. The scatter plots and review of the daily profiles yield the following observations:

- The 360ZH1 model over-predicts morning but under-predicts peak and afternoon I_{horz} on clear days.

- The WxA daily profile is a better indicator on clear days, with a slight tendency to over-predict the peak and afternoon I_{horz}.
- The 360ZH1 model better represents I_{horz} when cloud cover is variable, though this conclusion is tentative without further quantitative measurement and analysis.

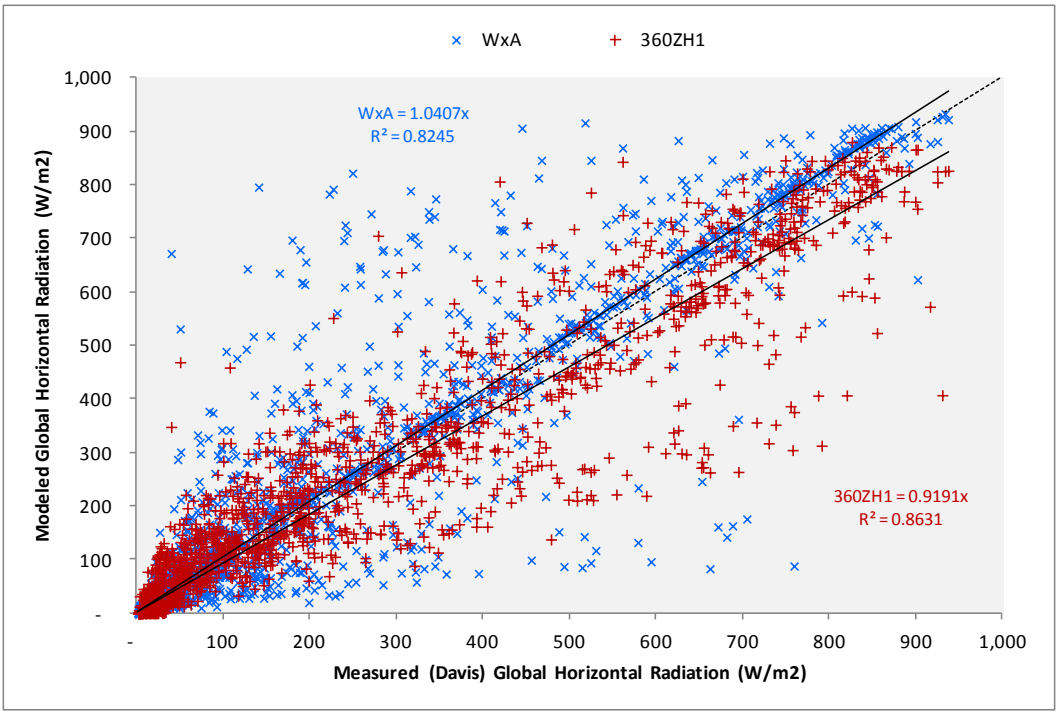

Figure 37 - Scatter plot of measured vs. modeled I_{horz} for 138 days throughout June-Dec 2010

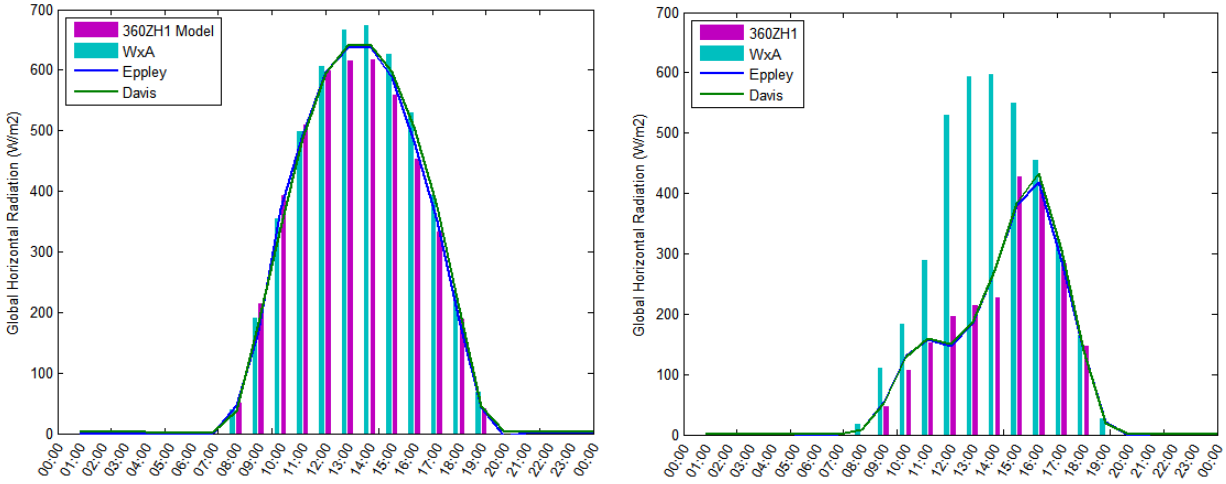

Figure 38 - Two daily profiles of measured and modeled I_{horz} from September 2010

4.2.2.2 Temperature Comparison

The 360ZH1 weather file values are determined from surface observations at the local airport, approximately six miles away from the building site. Building site temperature measurements were recorded every second and averaged for each hour compared. Figure 39 shows the temperature and solar conditions for three relatively clear days in August 2010. In addition to the OADB measurements, the average hourly temperature was measured at the center of the East Warehouse space (location #4 in Figure 13); solar radiation is shown for reference.

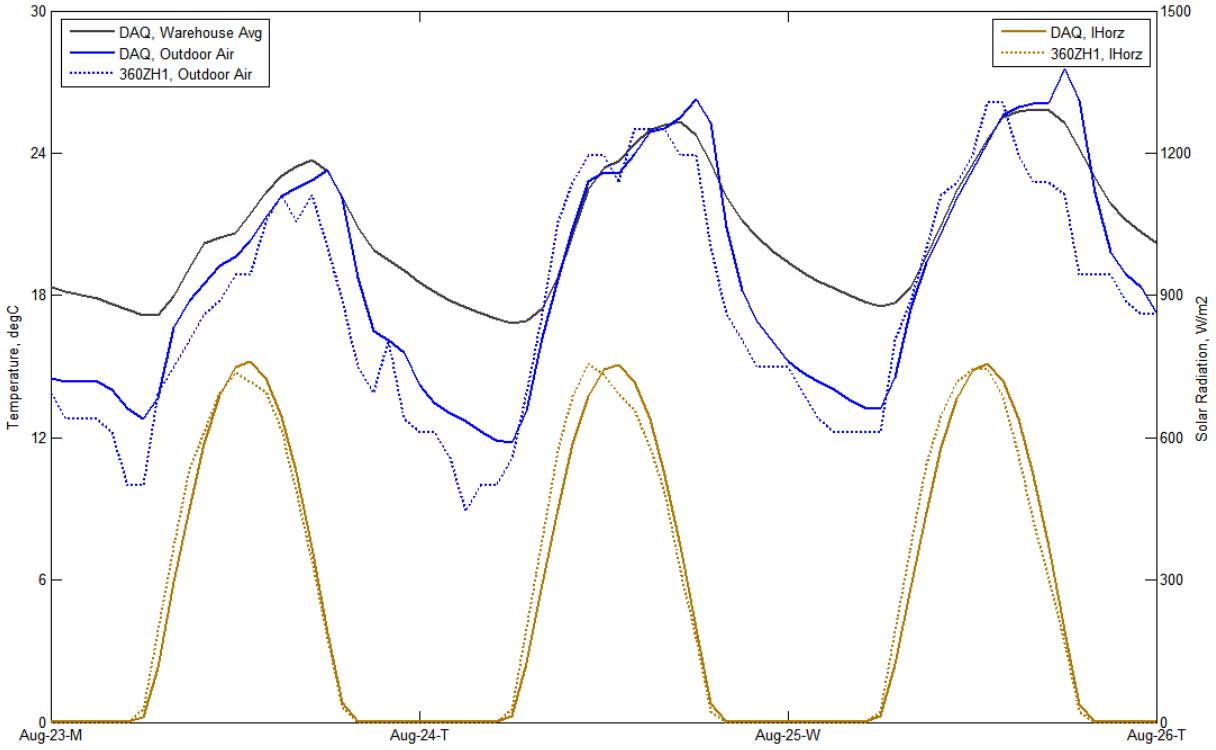

Figure 39 - Daily OADB and Ihorz measurements for Apr 23-26, 2010

One noted observation is a late afternoon peak in DAQ measured OADB. The spike is the assumed result of sun striking the side of the building where the OADB sensor is located (see Figure 40). For most hours of the day, the sensor is shaded by the study building

itself, and in late hours of the day, by an adjacent building. However, for approximately 1-2 hours in summer evenings, the sun is far enough north to directly strike the location of the temperature outdoor air temperature sensor. Despite attempts to add a radiation shield, the problem was not alleviated during the summer months of the year (from early June to mid Sept). As shown, the sensor is mounted at the inside corner of two building walls and above the building's asphalt parking lot. In this location, it is believed the ambient air is heated by the warm surrounding building and ground surfaces, and is carried upward by buoyancy into the sensor location.

Figure 40 - Photo of building OADB sensor in direct sun, observed for short periods of each afternoon evening.

These considerations make the site measurement of OADB dubious during many hours of the day, especially under high solar conditions. A comparison of the DAQ measurements to the NCDC values during the colder, cloudier months of October, November, and December (see Figure 41), indicates a distinct 1-2°C upward offset in temperature.

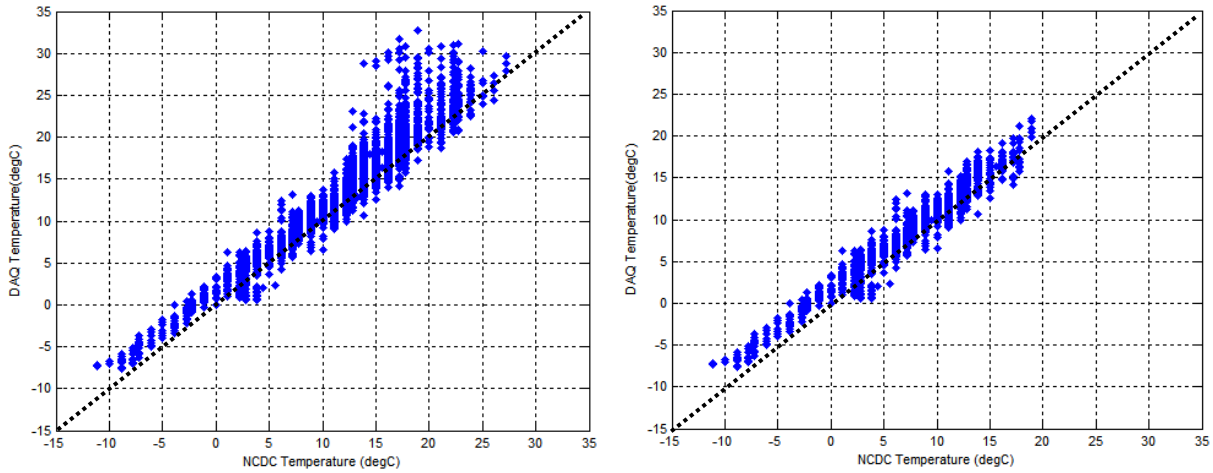

(a) (b)

Figure 41 - Scatter plot of NCDC vs. DAQ measured outdoor air temperatures for (a) entire period and (b) months of Oct-Dec

The comparison of temperature data yields the following insights:

- It is important to locate outdoor air temperature sensors where they will not be influenced by solar radiation. Shielding of a sensor, provided it is located in free airflow, may be acceptable, but convective and radiant effects due to surrounding features should be considered.
- The site measured temperature, even during cooler, cloudier months was observed to be regularly 1-2°C higher than the local airport temperature. This could be explained by the location of the air temperature sensor, or systemic measurement error in either sensor. However, the airport location is closer to the ocean waters of Bellingham Bay with fewer obstructions to wind, while the building's local terrain is an industrial/commercial area, predominantly covered by warehouses and car dealerships with asphalt parking lots and concrete streets. This suggests that despite being less than 2-3 miles from Bellingham Bay, this industrial area does experience some heat island effect.

5 Data Processing

Installing and commissioning a building energy energy/temperature monitoring system is another critical step to developing a well-calibrated building energy model (BEM). However, once this system is installed and acquiring information, the amount of information, often vast in quantity, must be processed into a format compatible with the whole building energy modeling program being used. Temperature, solar, and natural gas sub-metering information are examples of measurements that can often be directly translated to or compared to the outputs of a calibrated model. Sub-metered electrical circuit data streams, on the other hand, are often more complex, as a single circuit can provide energy for a number of building zones or end-uses. As the number of metered electrical circuits, thermal zones, and end-uses increases, the task of processing metered electrical data can quickly become unmanageable with standard engineering tools, such as spreadsheets, especially if the modeler wishes to disaggregate the energy consumption of single circuits serving one or more zone or end-use. For this reason, this thesis chapter primarily focuses on processing electrical sub-meter data into energy model inputs; followed by a brief discussion of processing of the measured temperature/solar radiation data, and utility interval data.

5.1 Program Initialization

Upon a call to the data processing program, high-level analysis parameters are defined. These include:

- File path and file names of the raw DAQ data files (comma-delimited (CSV) format) to be processed.
- The name of channel attribute file (CAF) that describes each DAQ channel and relevant processing parameters (see Figure 42).
- Global variable definitions, including number and names of model zones (m) and end-uses (n).

- The analysis year, so timestamps can be assigned and metered information can be processed according to day type (weekday, weekend, etc)
- Various flags to switch certain portions of the analysis routine on or off. For example, once the source CAFs are read, the processed Matlab variables are saved to disk for future use and that particular routine does not need to be repeated.

Chnl	Read Flag	Chnl Description	Units	Interval Method	Filter Method	Filter Window	Filter Criteria	Trigger Method	Trigger Frequency	Trigger Criteria	Trigger Range	QA Check Frequency	QA Criteria	QA Tolerance	Items File	Correction Factor Type	Correction Factor
1	1	WH Center Column @ 15ft	degC	1	0	0	0	0	0	0	0	0	0	0	none	0	0
2	1	WH Center Column @ 10ft	degC	1	0	0	0	0	0	0	0	0	0	0	none	0	0
3	1	WH Center Column @ 5ft	degC	1	0	0	0	0	0	0	0	0	0	0	none	0	0
4	1	East Wall @ 10ft	degC	1	0	0	0	0	0	0	0	0	0	0	none	0	0
5	1	Main Office Bath @ 9ft	degC	1	0	0	0	0	0	0	0	0	0	0	none	0	0
6	1	Main Office @ 10ft	degC	1	0	0	0	0	0	0	0	0	0	0	none	0	0
7	1	Outdoor Air	degC	1	0	0	0	0	0	0	0	0	0	0	none	0	0
8	1	Solar Ghorz	W/m2	1	0	0	0	0	0	0	0	0	0	0	none	0	0
9	1	DHW Heater	Amps	1	0	0	0	0	0	0	0	0	0	0	IAF_09.csv	1	1.092
10	1	Office and Bath Lts	Amps	1	3	20	0.1	3	2	0.1	2	6	0.05	0.085	IAF_10.csv	1	1.035
11	1	Office Heat	Amps	1	0	0	0	0	0	0	0	0	0	0	IAF_11.csv	1	1.995
12	1	WH Lts	Amps	1	3	30	0.5	3	5	0.5	1	6	0.05	0.5	IAF_12.csv	1	1.02911
13	1	Packing Area Plugs	Amps	1	0	0	0	0	0	0	0	0	0	0	IAF_13.csv	1	1.14912
14	1	Dedicated Data Plugs	Amps	1	0	0	0	0	0	0	0	0	0	0	IAF_14.csv	1	0.9301
15	1	Ofc North N Plugs	Amps	1	0	0	0	0	0	0	0	0	0	0	IAF_15.csv	1	0.9491
16	1	Ofc S&W Plugs	Amps	1	0	0	0	0	0	0	0	0	0	0	IAF_16.csv	1	1.15479

Figure 42 - Channel attribute file (CAF) syntax

5.1.1 Annual Data Arrays

The data processing program is currently structured to read, process, and store data for each hour of individual days for a single calendar year. This follows the convention of the whole building energy modeling program, eQUEST, used for this study. That is, schedules that define variation of the hourly internal and external loads of the energy model are categorized by the days of a given week throughout a single calendar year.

After reading the CAF files, a cell arrays are initialized to store data for each day of the analysis year. The cell array is used to store the following information:

1. Date of year
2. Day type: Integer 1-8 corresponding to days of week, Sun-Sat, 8 = Holiday)

3. Metered Data Flag: Integer 0-1, indicating whether there exists metered data for the day.
4. Arrays for storing daily interval channel data (all channels)
5. Arrays for storing the daily interval current data for each model zone and its defined electrical end-uses.

Once created, the cell array is stored as a separate file, and therefore, only needs to be initialized once for each year that data are logged. From that point forward, the annual array file is opened and the file is overwritten or appended each time the program is run. This strategy eliminates the need to re-process all data each time the program is run, and maintains one database used to create energy model inputs, described in later steps.

5.1.2 Calculating Interval Data

One of the principal goals of this software routine is to convert metered DAQ information into formats compatible with the energy modeling program. In the case of branch circuits, electrical current data are logged in discrete, short intervals, shorter than what is simulated by BEM programs. Higher logging frequency facilitates both a) integration of total power and other DAQ measured information over longer intervals, and b) observation of electrical items being switched ON/OFF, even if only for a short time period.

For each DAQ channel, the discrete measurements will be used to calculate the total or average value over 60 minute intervals, beginning at the start of each clock hour, which correlates with the time intervals used by the BEM software used in this study. The discrete values are converted to an interval value for a longer period using a simplification of the midpoint (a.k.a. rectangle) rule, illustrated in Figure 43, and described in Equation (14). This calculation reduces to the average of all values measured over the course of one hour.

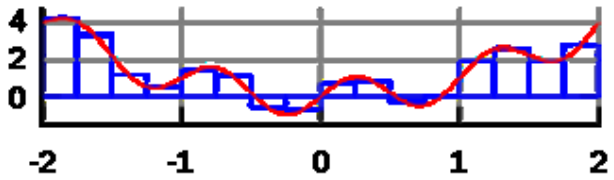

Figure 43 - Illustration of the midpoint rule

$$\mathrm{I}_{\mathrm{hour}} = \int_{a}^{b} I(t) \approx (b-a) \times I\left(\frac{a+b}{2}\right) \approx \frac{1}{N}\sum_{i=1}^{N} \mathrm{I}_i \times \Delta t \qquad (14)$$

where:
I_i = instantaneous current measured with current sensor (Amps)
N = number of current samples in the given interval period. For a one hour interval, sampled at a regular frequency *f* (seconds), N = 3600/*f*
Δt = time period of interval (1hr)
I_{hour} = interval current measurement (Amp-hr)

5.2 Processing Sub-Metered Electrical Data

For this project, Matlab software routines were developed to convert metered electrical current data into formats compatible with the DOE-2.2 energy model. These routines were expanded from simple read/process/write operations, to disaggregating and allocating electrical energy consumed on each circuit to building zones and/or energy end-uses. This additional processing step may or may not be required for electrical distribution systems that are well organized by building area and energy end-use. However, for small or existing buildings, it is common for single branch circuits to serve multiple end-uses or model zones. Additionally, the methods identified here could potentially be used to monitor feeder circuits in larger electrical distribution systems, upstream of subpanels, and allocate electrical energy using the same principals.

5.2.1 Zones and End-uses Served by Branch Circuits

In the context of a calibrated BEM, the electrical branch circuits can typically be divided into one of three categories:

1. A circuit that provides electricity for a single energy end-use of a zone or appliance. For example, a circuit that provides lighting for a single model zone, or a dedicated circuit for an electric storage water heater.
2. A circuit that serves a single energy end-use in multiple zones. For example, a lighting circuit that serves general lighting in more than one model zone.
3. A circuit that serves a multiple energy end-uses in multiple zones. For example, a lighting circuit with general interior lighting and exterior lighting fixtures.

Category 1 requires no processing of current data, as it is always clear what model zone or end-use the energy use should be assigned to it. Category 2 requires disaggregation of electric use by model zone, which can be performed if changes in electrical current can be correlated to the individual zones. Alternatively, the energy use can be uniformly

distributed to model zones based on audit information, such as allocating lighting energy based on the fraction of installed lighting power in each space. Category 3 requires disaggregation to both different zones and different end-uses. Here again, knowledge of electric use for specific items served by the branch circuit is needed, but is complicated by the fact that changes in current draw are correlated to both model zones and end-uses. If this information is not available or difficult to identify reliably, energy use can also be distributed based on audit information. Table 9 lists the branch circuits monitored in this study, with the end-uses/zones served and how each falls into the three branch circuit categories listed above.

Table 9 - Metered branch circuits and model zones/end-uses served

Circuit #	Daq Ch#	Branch Circuit Category	Zones	End-uses
4	12	3	E Warehouse	Interior lighting, exterior lighting, receptacle
7	11[1,2]	1	Office	Space heating
6	9	1	Attic space over office/bathrooms	Domestic water heating
8	10	3	Office, warehouse and office bathrooms	Interior lighting, exterior lighting, exhaust fans
10	15	1	Office (north wall)	Receptacles
11	14	1	Server room (Office bathroom)	Receptacles
12	16	1	Office (south & west wall)	Receptacles
13	11[1]	1	E Warehouse (packing area)	Receptacles
14	13	1	E Warehouse (north wall)	Receptacles

1. Circuits monitored for separate monitoring periods using the same DAQ channel.
2. Circuit is one phase of 2-phase heater.

5.2.1.1 Electrical Consuming Items

At this point, it is helpful to introduce the concept of an electrical consuming item (N). An electrical item corresponds individual devices or combinations of devices and can be

assigned to a particular model zone and energy end-use. To illustrate this concept, Figure 44 shows a typical metered weekday current profile for Circuit #8, the office lighting circuit. For this particular circuit, there are four items (N=4), described in Table 10.

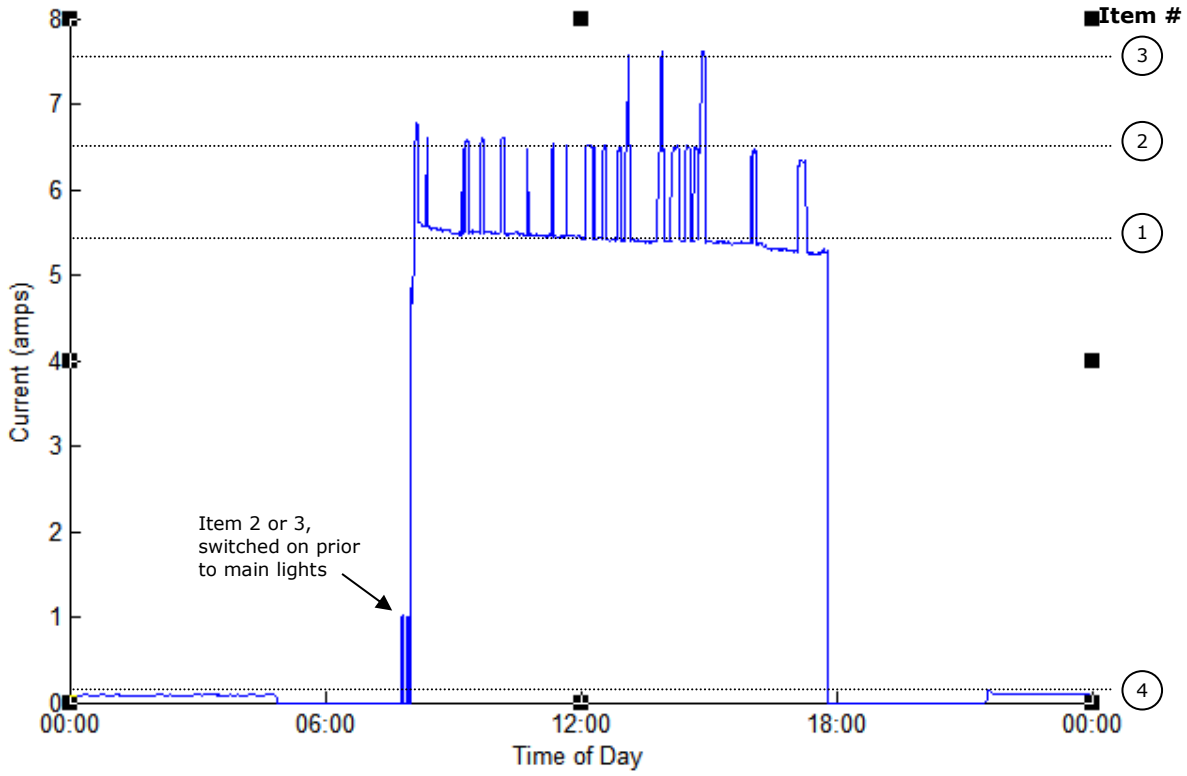

Figure 44 - Typical weekday metered current profile for Circuit #8 (Office Lights)

Table 10 - Electrical consuming items for Circuit #8

Item #	Description	Additional details
1	Office Lights	General lighting, 6 – 2ft x 4ft lighting fixtures with T-8 lamps mounted in drop ceiling
2	Office Bathroom Lights+Fan	General lighting, 1 - 2ft x 4ft lighting fixture with T-8 lamps mounted in drop ceiling. Switched ON/OFF via wall-mount occupancy sensor, along with exhaust fan.
3	WH Bathroom Lights+Fan	General lighting, 1 - 2ft x 4ft lighting fixture with T-8 lamps mounted in drop ceiling. Switched ON/OFF via wall-mount occupancy sensor, along with exhaust fan. Same light/fan combination as office bath.
4	Front Exterior Light	Fixture with CFL mounted over exterior entry to office. Controlled by photocell.

Each item is switched ON/OFF at various times of the day, which results in stepped changes in the current amplitude. For comparison, Figure 45 illustrates current data for Circuit #6, which is dedicated to the 120V storage hot water heater that supplies domestic hot water for the two building bathrooms. In this case, the heater is shown to cycle ON/OFF throughout the day. However, all of the branch circuit electrical energy is for domestic hot water (DHW) heating. Therefore, there is only one electrical consuming item (N=1), and all of the energy metered on this circuit can be allocated to this one model end-use.

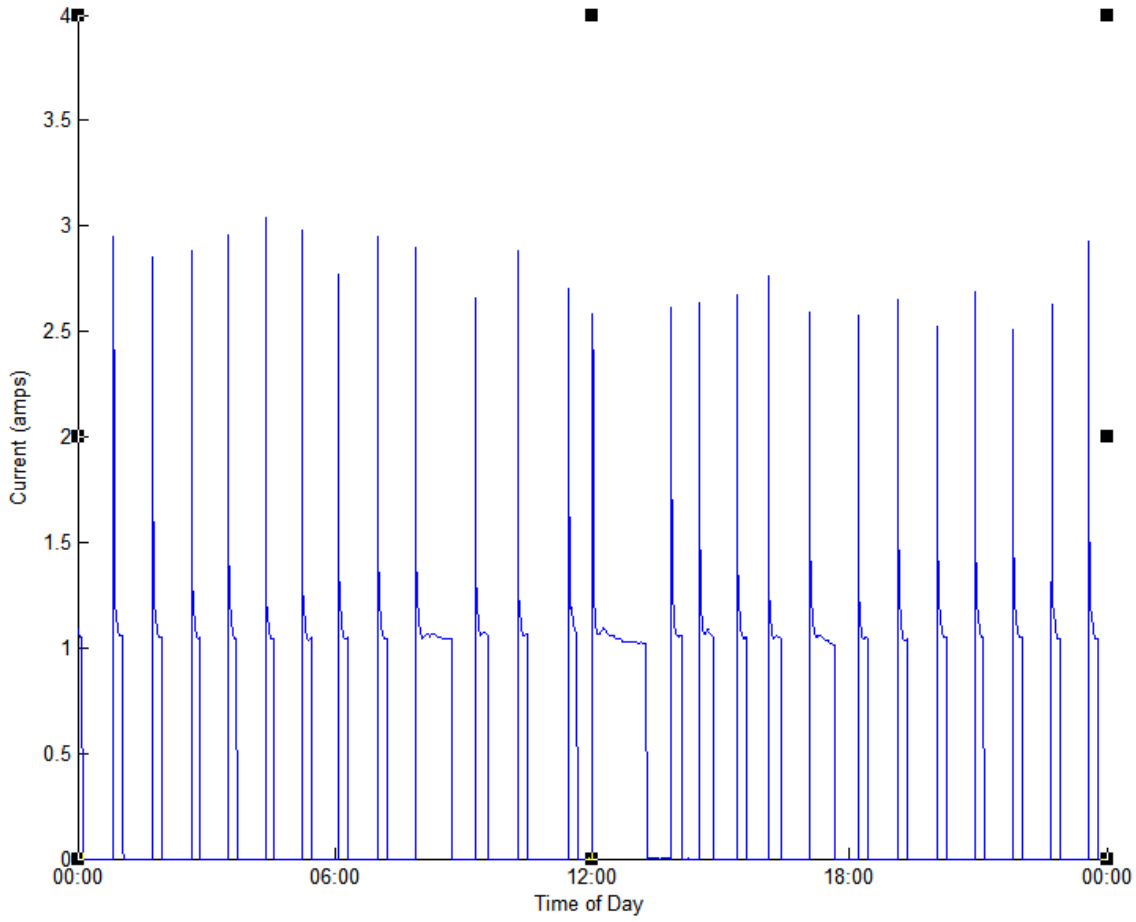

Figure 45 - Typical weekday metered current profile for Circuit #6 (DHW heater)

Figure 46 shows the current data for one of the Office receptacle circuits (Circuit #12). Here, many items are turning ON/OFF throughout the day, as well as some items appear to be on at all times. Constant receptacle energy demands are commonly referred to as phantom loads, or the small loads associated with transformers and devices that operate in standby mode and consume small amounts of electrical power at all times. For model calibration purposes, all of the energy used on this circuit is confined to one model zone (office) and one end-use (receptacles), and therefore, considered one item (N=1) for the purposes of processing.

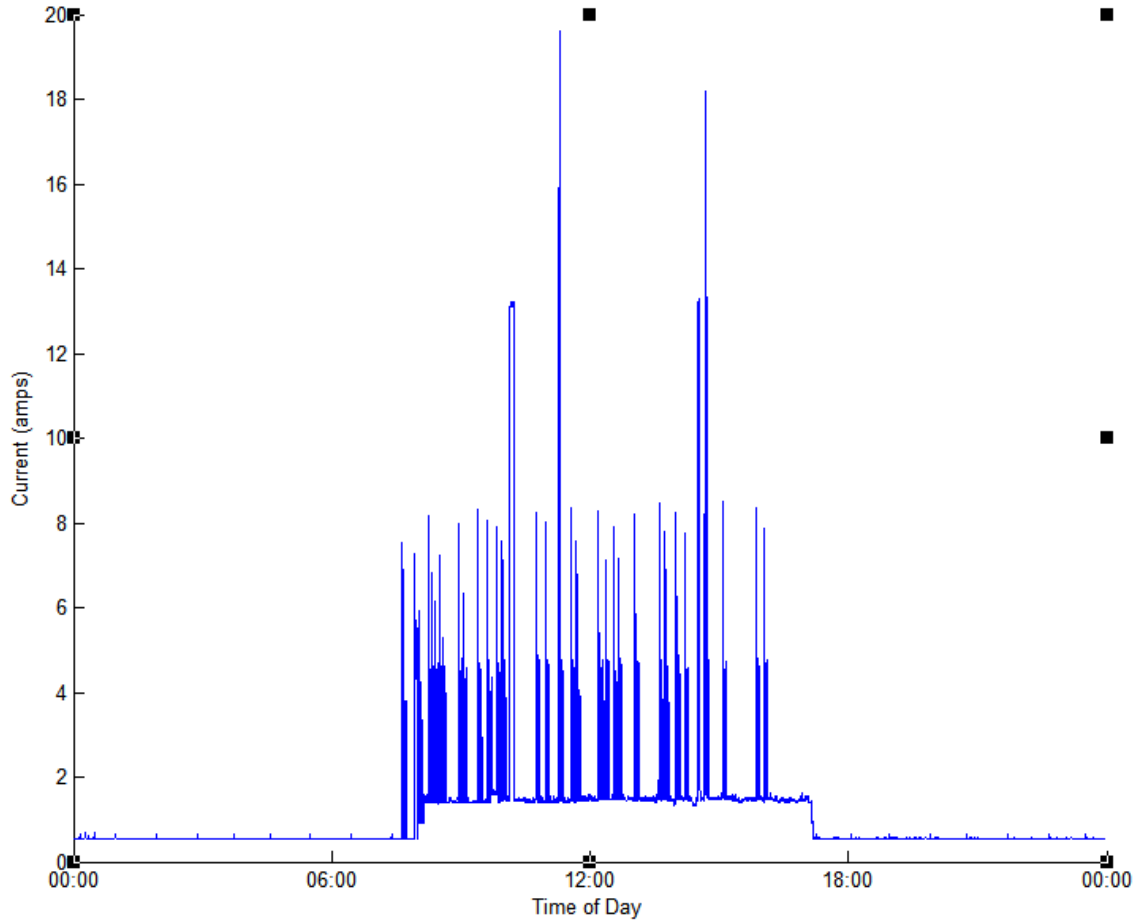

Figure 46 - Typical weekday metered current profile for Circuit #12 (Office S&W Plugs)

5.2.2 Electrical Data Processing Routine Overview

Figure 47 provides a high-level outline of the software routine developed to process electrical sub-meter data into hourly interval data, formatted for use in the eQUEST program. For channels with only one electrical consuming item (N=1), calculating interval current values using Equation (14) is straightforward. For channels with more than one electrical consuming items (N>1), additional processing (outlined in the dashed red box) is needed to disaggregate and allocate metered information by zone and end-use.

The additional work to disaggregate energy use was needed since the lighting circuits serve multiple model zones and include other end-uses. Interior lighting is a major component of building energy use, and for the study building, is estimated to account for 30% of total building energy use (see results described in Chapter 6). Though not necessarily practical for a small commercial building which only consumes ~20,000kWh/year ($1,600/year @ $0.08/kWh), the algorithms used here extend the information gathered by the electrical sub-metering system; primarily, the ability to identify energy use according to model zone and end-use.

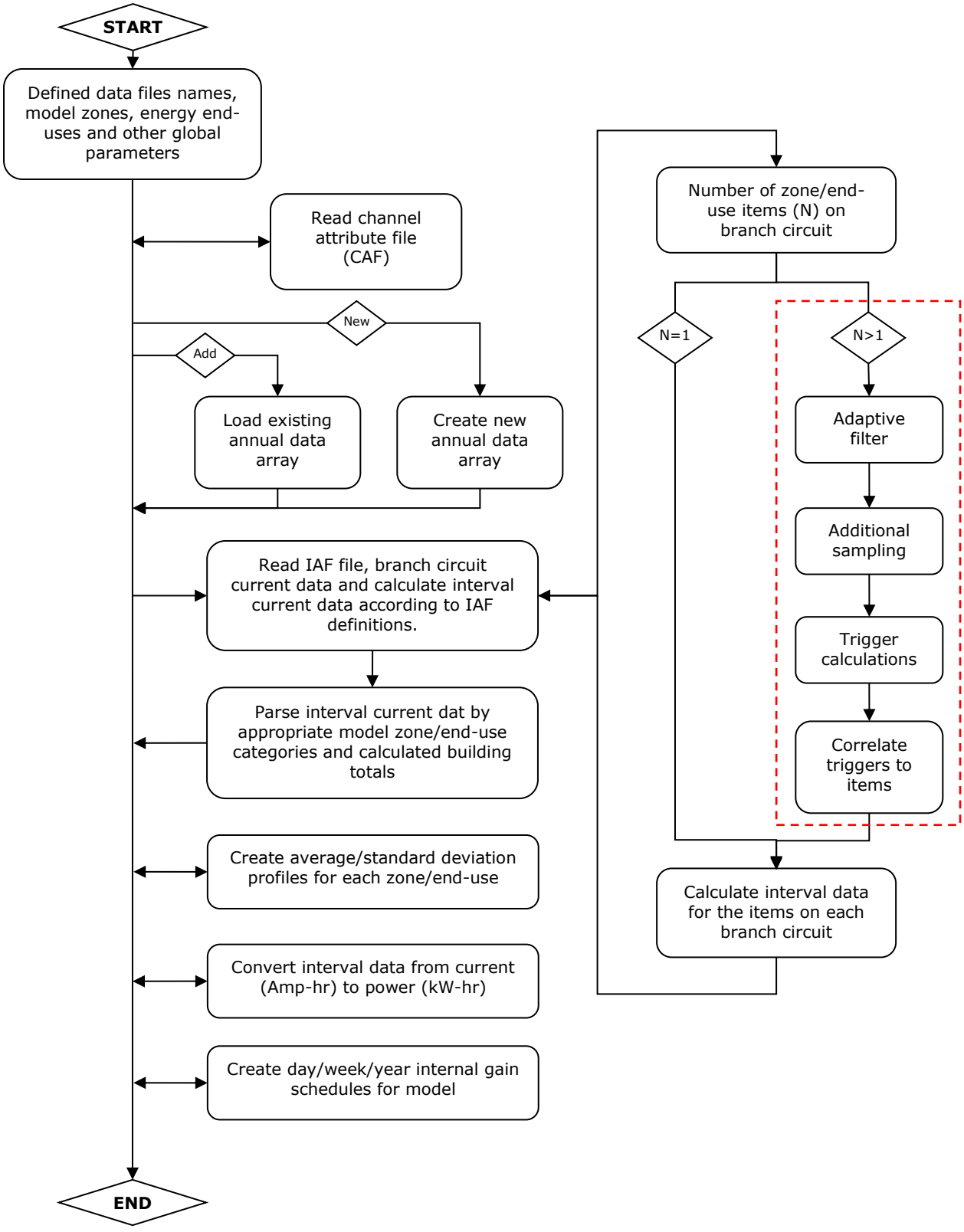

Figure 47 - Electrical data processing routine flow chart

5.2.3 Item Attribute File (IAF)

Data logged by the DAQ system is stored in a CSV file, organized by channel. After initialization of the data processing routine, the first step is to read the item attribute file (IAF). This file describes the attributes of electrical items, their corresponding end-uses/model zones, and other data processing definitions for each DAQ channel. This file is defined in a spreadsheet, exported to a CSV file, and then parsed by the Matlab code prior to reading any of the raw branch circuit data.

For channels with more than one electrical consuming item (N>1), the metered data are disaggregated into separate data streams; one stream for each electrical item. The disaggregation is performed automatically by analyzing the current level and correlating step changes in the current amplitude, a.k.a 'triggers', with the consumption of the various electrical items on the circuit pre-defined by the program user in the IAF. A trigger event can be positive or negative, corresponding to switching an electrical item ON or OFF. Trigger levels for each item are determined through a trial period, where electrical items are methodically switched ON/OFF and the change in current amplitude is observed on the DAQ system and recorded. The IAF is then created to include the following attributes of each electrical item on the circuit:

- A string description of the item
- The average trigger value, in Amps
- The trigger tolerance, which defines the range above or below the average trigger value of an item.
- The initial state (ON/OFF) of the item when data logging began.
- The nominal current amplitude of the item when it is ON.
- If more than one item has the same average trigger magnitude, an assigned fractional priority, i.e. a weighting factor, is used to describe the probability of each item being turned ON/OFF, compared to other items with the same average trigger.

- The zone and end-use(s) the item is mapped to. If the electrical item corresponds to more than one end-use, fractions for each end-use are defined.
- Other information, such as power factor and correction factors used for converting measured current to power.

Figure 48 shows the IAF for Circuit #8, the office lighting circuit, as well as a graphical representation of the average trigger level and tolerances of the four electrical items.

Chnl Description Office and Bath Lts
Units Amps

Start of input

	0	1	2	3	4	5	6	7	8	9	10	11	12	13
; #	Description	Average Trigger (amps)	Priority	Trigger Tolerance (amps)	Initial State	Static Load (amps)	Power Factor (PF)	Correction Factor (CF)	zone	enduse1	fraction1	enduse2	fraction2	
1	Office Lts	5.86	0	2.828	0	5.39	1	1.04	1	1	1	0	0	
2	Office Bath Lts+Fan	1	0.9	0.354	0	1.11	1	1.04	2	1	0.65	8	0.35	
3	WH Bath Lts+Fan	1	0.1	0.354	0	1.11	1	1.04	3	1	0.65	8	0.35	
4	Front Ext Lt	0.1	0	0.071	1	0.086	1	1.04	999	3	1	0	0	

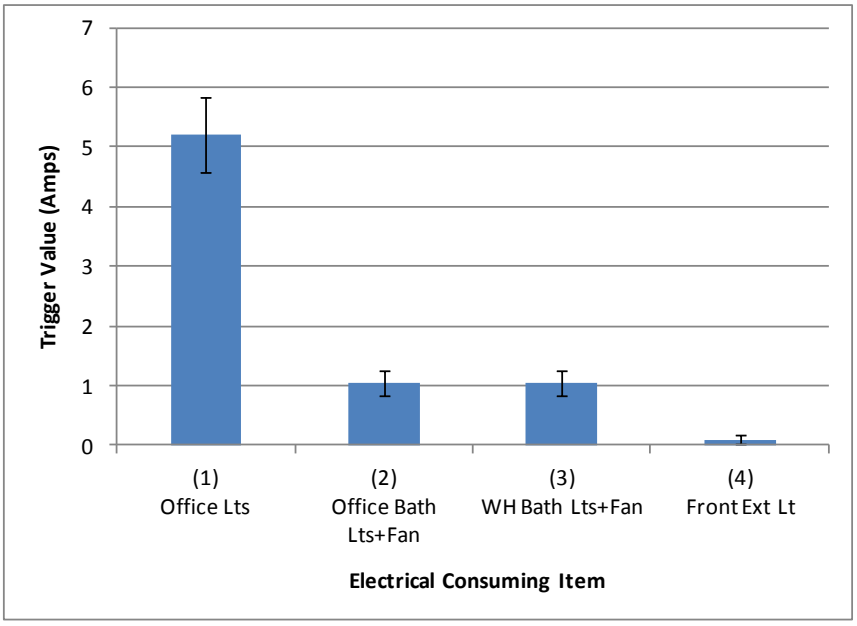

Figure 48 - IAF and average and tolerance of average trigger values for Circuit #8

Matlab routines were written to use the parameters defined by the IAF and automatically identify individual items on the two circuits with more than one item (Circuit #8 and #4) by comparing trigger values and to the corresponding electrical consuming item. In developing these routines, a few additional steps were found to result in reliable processing over the various different monitoring periods.

5.2.3.1 Smoothing

Figure 49 shows the measured current, sampled at a frequency of 1 second, for (a) Circuit #8 (Office Lights) and (b) Circuit #4 (Warehouse Lights), both of which have more than one electrical consuming item on the circuit. The periods shown in the plots cover ~20 minutes of a typical weekday morning. Step changes corresponding to different circuit items are indicated by the numbered lines.

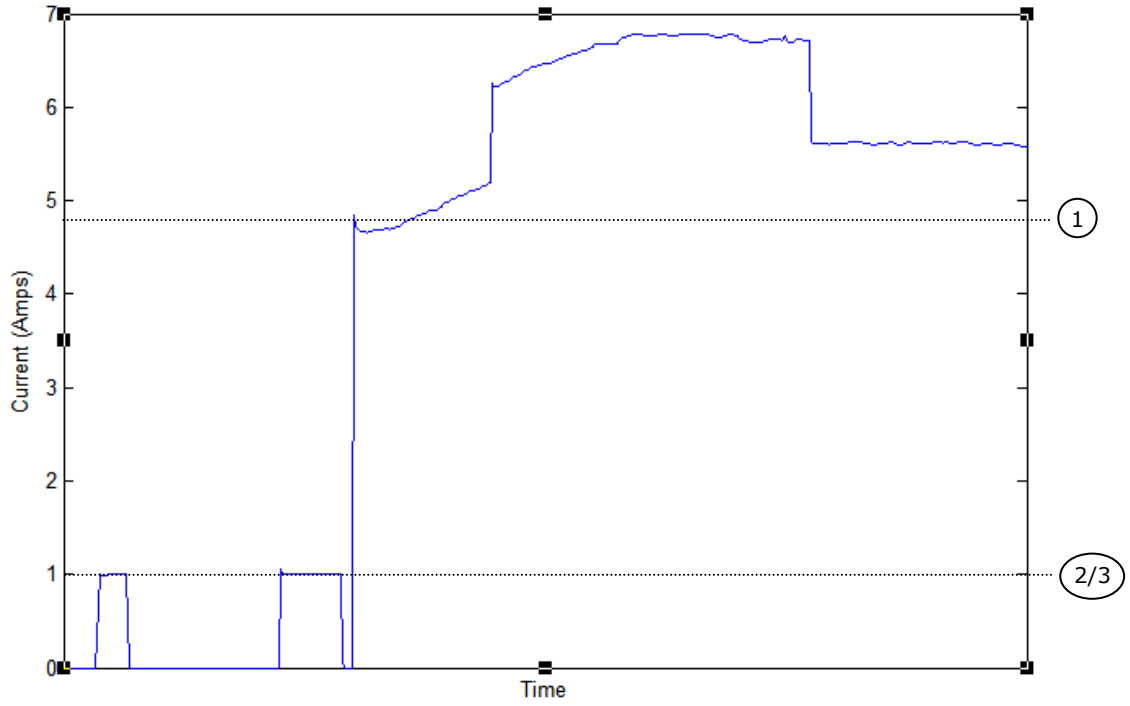

(a)

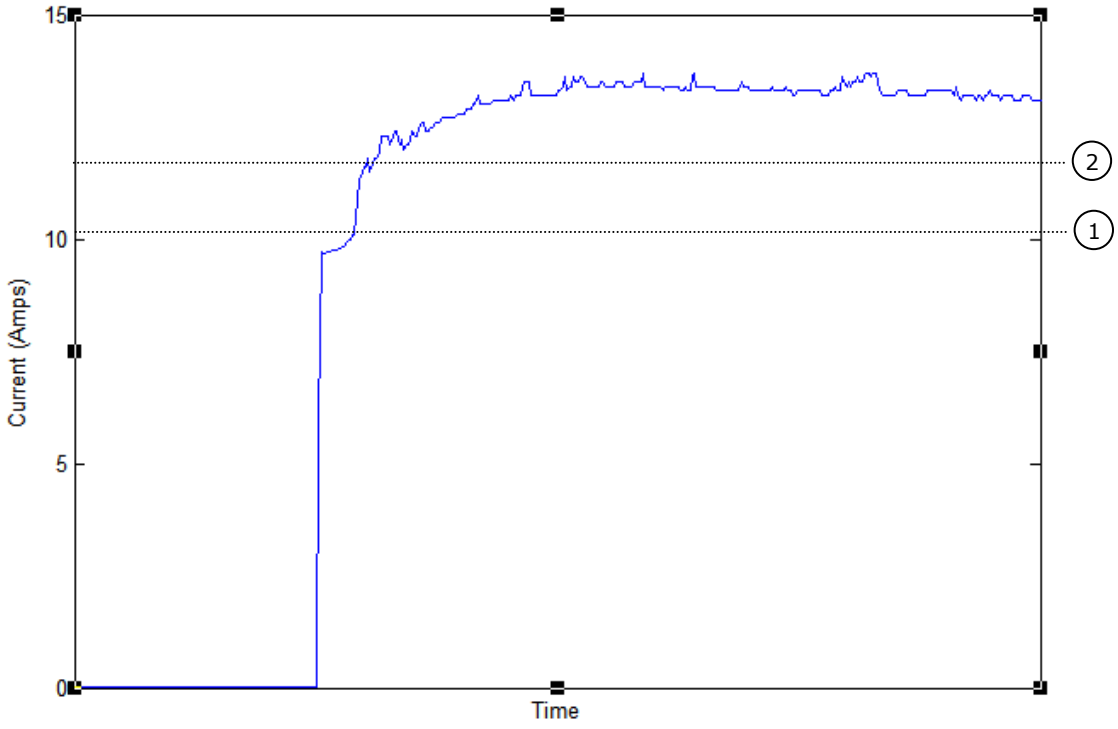

(b)

Figure 49 - Metered current data for Circuit #8 (a) Circuit #4 (b)

The first thing to note is the slight fluctuations in the current draw, and in the case of Circuit #4, what appears to be noise in the current signal. Initial attempts to disaggregate different items on the two circuits failed because small changes in the current amplitude would "confuse" the processing routine. For this reason, a method to smooth data streams was investigated.

The principal method investigated was moving average smoothing. In this case, new data points are calculated by averaging the values within a defined 'window' around the point of interest. See Figure 50 for a basic illustration of this principal.

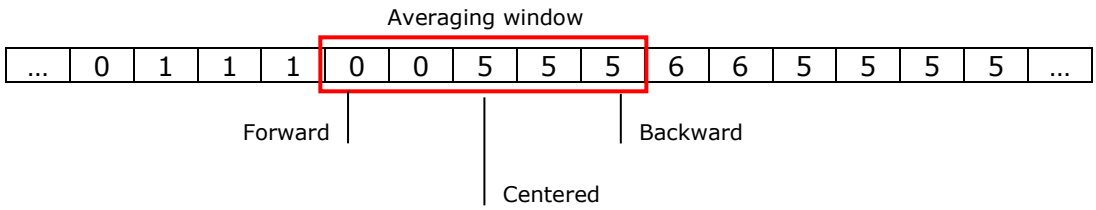

Figure 50 - Simple moving average window.

The moving average window can be backward, centered, or forward looking, and when processing values that have already been measured (i.e. not streamed "live" from the DAQ system), any of these windowing methods can used. A "simple" moving average assumes the values in the averaging window have the same weight. However, the moving average can be influenced using linear, exponential, and other functions to weight values included in the window, assigning more or less importance to the values around the point calculation.

Figure 51 shows the impact of using a forward looking, unweighted moving average smoothing technique on data of two circuits. The window width is held constant at 30 values, which for this example, is a 30 second period of time. The moving average method effectively smooths data, however it also distorts the step changes associated with items

turning ON and OFF. For this reason, an adaptive approach was used to start and stop the moving average smoothing around trigger events. Specifically, the width of the moving average window is narrowed and widened to not include the trigger event, and at at large step changes in electrical current amplitude, the actual values are retained. The indicator used to stop and start moving average smoothing is determined by evaluating an approximation of the 2nd derivative (described in Section 5.2.3.3) at each point. However, the 2nd derivatve threshold for the adaptive smoothing process is defined lower than that used in identifying trigger events, which helps ensure the step changes of true electrical items is preserved. The impact of using this adaptive moving average is illustrated in Figure 52. The result is a smoothed yet good representation of metered data.

5.2.3.2 Additional Sampling

In addition to moving average smoothing, undersampling is another approach to filtering data while attempting to preserve the amplitude of changes. In this case, data smoothed using the adaptive moving average technique is re-sampled at a frequency less than the original metering frequency. Undersampling helps remove small deviations that may be retained by the adaptive filtering method, as demonstrated in Figure 52(b).

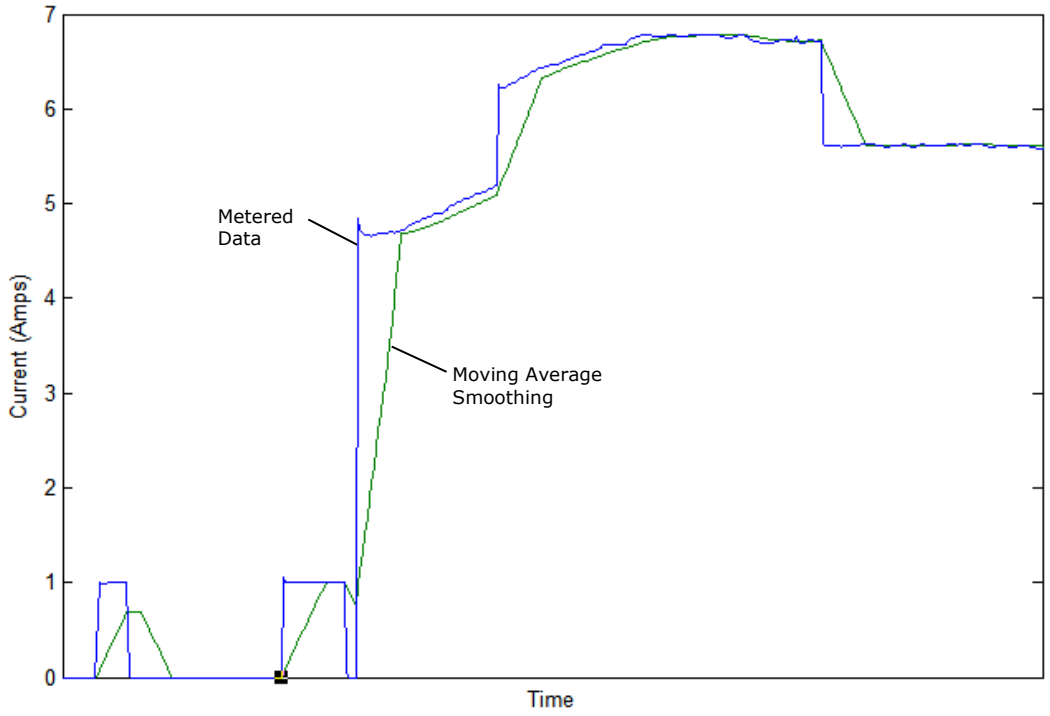

(a)

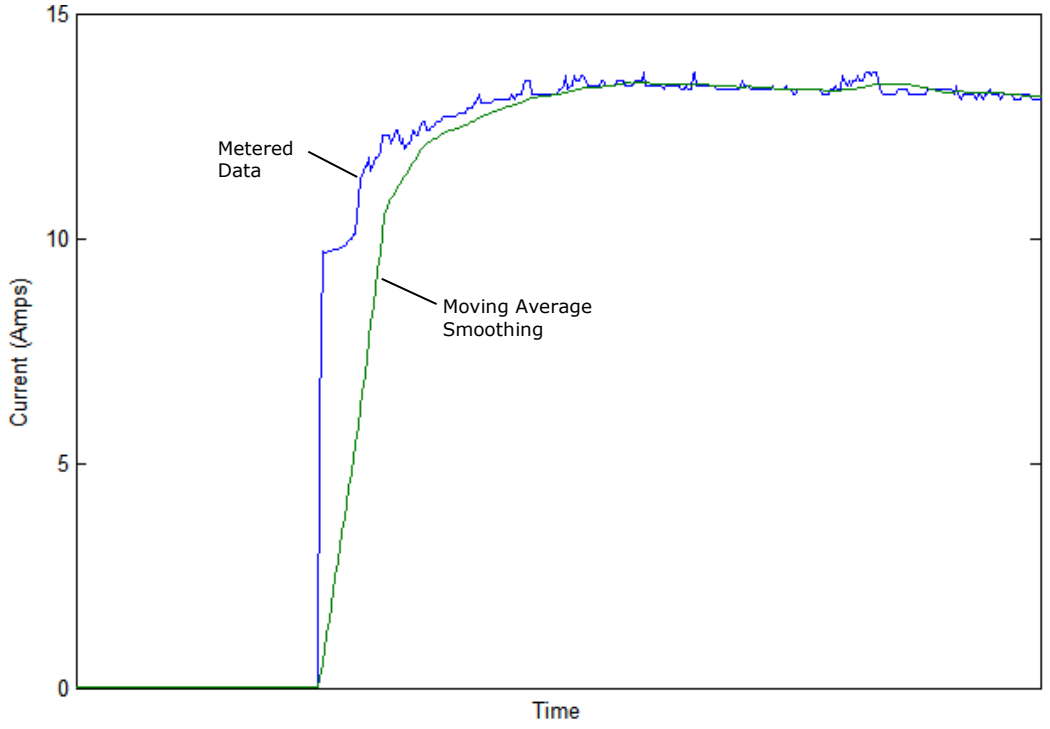

(b)

Figure 51 - Simple moving average smoothing for Circuit #8 (a) Circuit #4 (b)

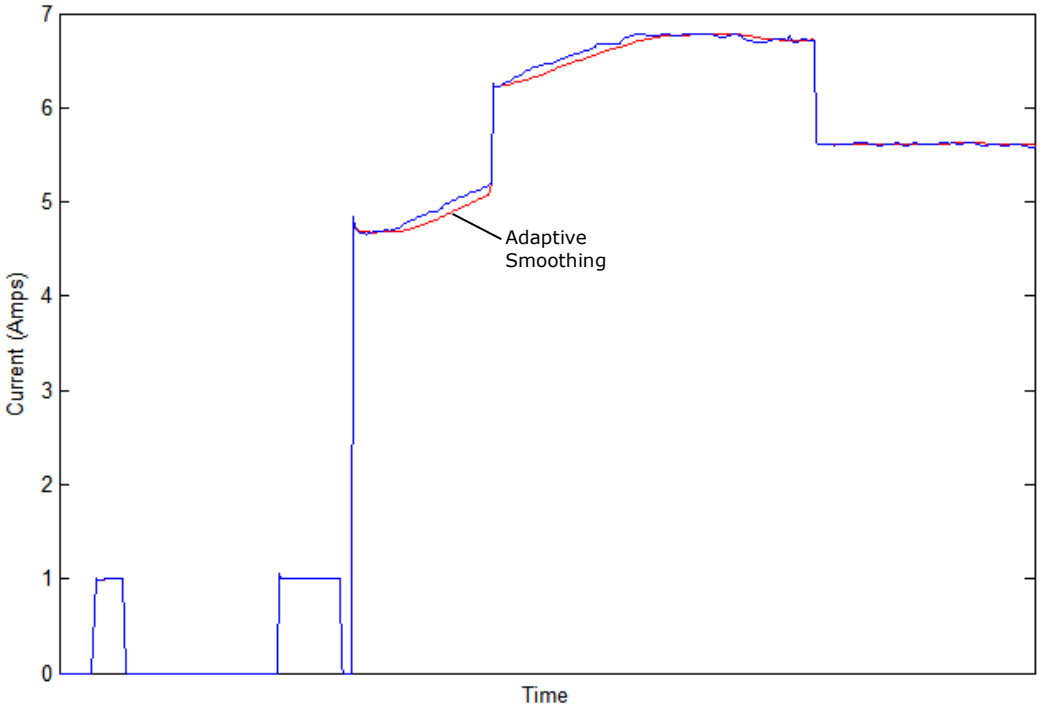

(a)

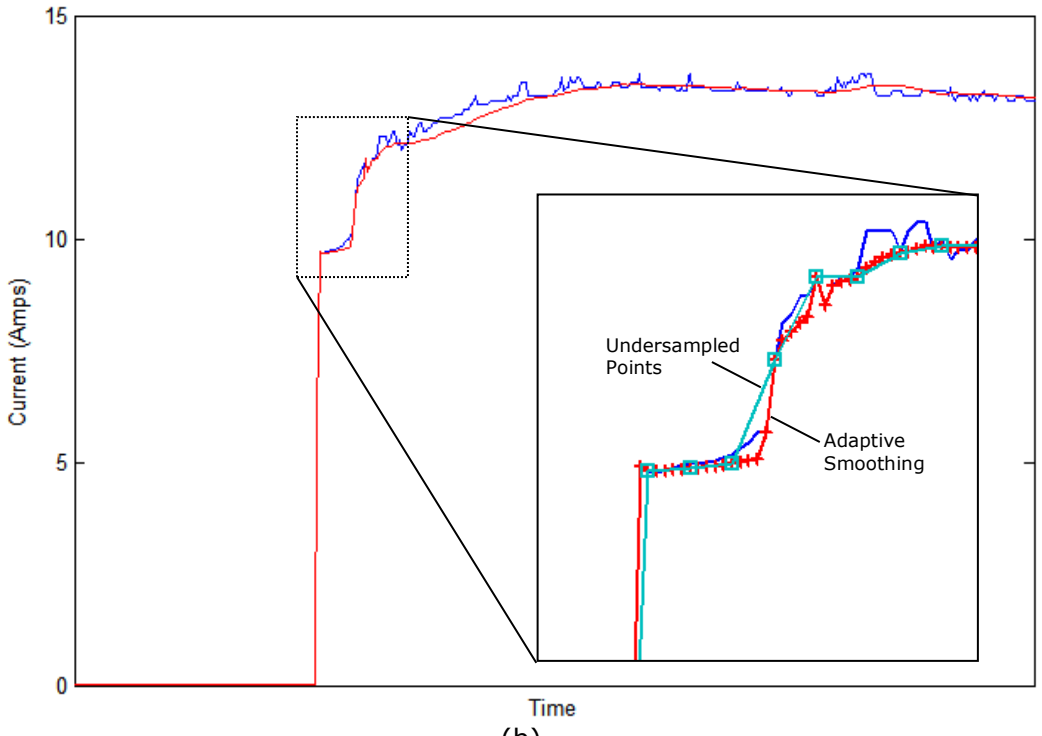

(b)

Figure 52 - Adaptive smoothing and undersampling for (a) Circuit #8 (b) Circuit #4

5.2.3.3 Trigger and Second Derivative Calculations

As defined earlier, a "trigger" event is one that corresponds to one or more of the electrical consuming items on a particular circuit switching ON or OFF. After the sub-metered electrical current data have been smoothed and under-sampled, they are reanalyzed to identify which changes in amplitude correspond to different electrical items.

Detection of abrupt changes in time-varying data is a signal processing application encountered in other engineering contexts (Step Detection 2013). The method used in this study relies on evaluating a numerical approximation of the second derivative (I'') at each point of the electrical current data stream. The second derivative calculation, shown in Equation (15), ignores the actual time between points, and thus the result of interest, the magnitude of the calculation, is independent of the sampling rates used in data logging or processing.

$$I''(n) = [(I_n - I_{n-1}) - (I_{n-1} - I_{n-2})] \quad (15)$$

The second derivative was used for the following reasons:

- The sign (+/-) of the derivative is indicative of the direction of change. For example, in the case of positive step change, the second derivative is initially positive, corresponding to a convex shaped curve.
- At the end of the step change, the second derivative switches in sign, and the magnitude is equal (or nearly equal for inexact step changes) in magnitude to the second derivative at the start of the step change, thus acting as an indicator the step change event has completed.

These characteristics are used to identify the trigger events, and the magnitude and direction of the overall change in current amplitude is stored in memory for the next data processing steps.

5.2.3.4 Correlate Triggers to Individual Items On a Circuit

Once identified, trigger events are correlated to the electrical items attached to the circuit. This is done by comparing average trigger value of each item on the circuit, plus or minus the trigger tolerance, to the magnitude of each trigger event. A tolerance is needed since trigger events did not consistently have the same magnitude. The variation in trigger magnitude was attributed to:

- The change is current amplitude is not a true step-wise function at trigger events.
- External influences causing non-linear current consumption. In the case of fluorescent lighting, the temperature of the lamp has a noticeable influence on the current draw.

After correlating the trigger event to an electrical consuming item, the status (ON/OFF -> 1/0) is retained in memory, and at each trigger event, the status of the item is compared to the event action. Tracking of item status allows the processor to maintain logical consistency in the state of each item. That is, if items are already ON, it cannot be turned ON again, and if two items have similar or the same trigger value, the status of each can be used to identify which of the items can be switched ON or OFF. Items with the same trigger value, as is the case for the office and warehouse bathrooms (Items #2 and #3) on Circuit #8 (see Table 10), are assigned weighted probabilities for being switched. For example, in the case of the study building, the warehouse has fewer employees than the office, and therefore, that bathroom was assigned a lower probability of use. In general, the probabilities are informed by engineer's judgment or knowledge of building operations. Finally, the processor is also capable of detecting linear combinations of items being turn ON at the same time (currently limited to two items).

With the status of each item on the circuit known, it is also possible to determine an expected value of branch circuit current use by multiplying the nominal current draw of each

item (defined in the IAF file) times the item's integer status value (1/0). Therefore, at all times the analysis routine maintains an expected value of the current amplitude, which can be compared to the actual metered value. A quality assurance (QA) comparison of the expected to actual value is made at intermediate intervals (typically every 5 min), and the discrepancy is compared once again to the trigger value (± trigger tolerance) of each item on the circuit. If a match is made, the status of the matching item is updated, thus helping to ensure the expected and actual values are corrected before determining future switching events.

5.2.3.5 Trigger Calculation Results

Figure 53 presents the actual metered current for Circuit #8 (Office Lights), after smoothing/sampling, as it compares to the current estimated by multiplying the integer status of individual items times the item's nominal current draw. The actual and calculated values correlate well; on a daily basis, the difference in total measured current was typically observed within 1% of the total metered value. One notable difference is the current draw of the office lights (Item 1) decreases throughout the day. This correlates with the expected, temperature dependent performance of linear fluorescent lighting (Bleeker and Veenstra 1990). Analyzing the switching events has other possible applications, though these were not directly applied in this study:

- Switching of office lighting (Item #1) is manual, so the hours the lights are ON should correlate well with occupancy.
- A wall-mount occupancy sensor (OS) controls switching of office and warehouse bathroom lights. If replaced with a manual toggle switch, the energy consumption before and after could be compared to develop an estimate of energy savings from installing the OS. Typically, this type of study would require a separate state/change data logger.

- As previously indicated, lighting is one of the study building's largest energy end-uses. The number of lighting hours plays a critical role in the potential energy savings from lighting and control upgrades. This method provides resolution on the number of hours lighting is switched ON. In the case of Circuit #8, the priority would be to upgrade the office lighting, since it is the largest magnitude and is on the most hours of a given day.

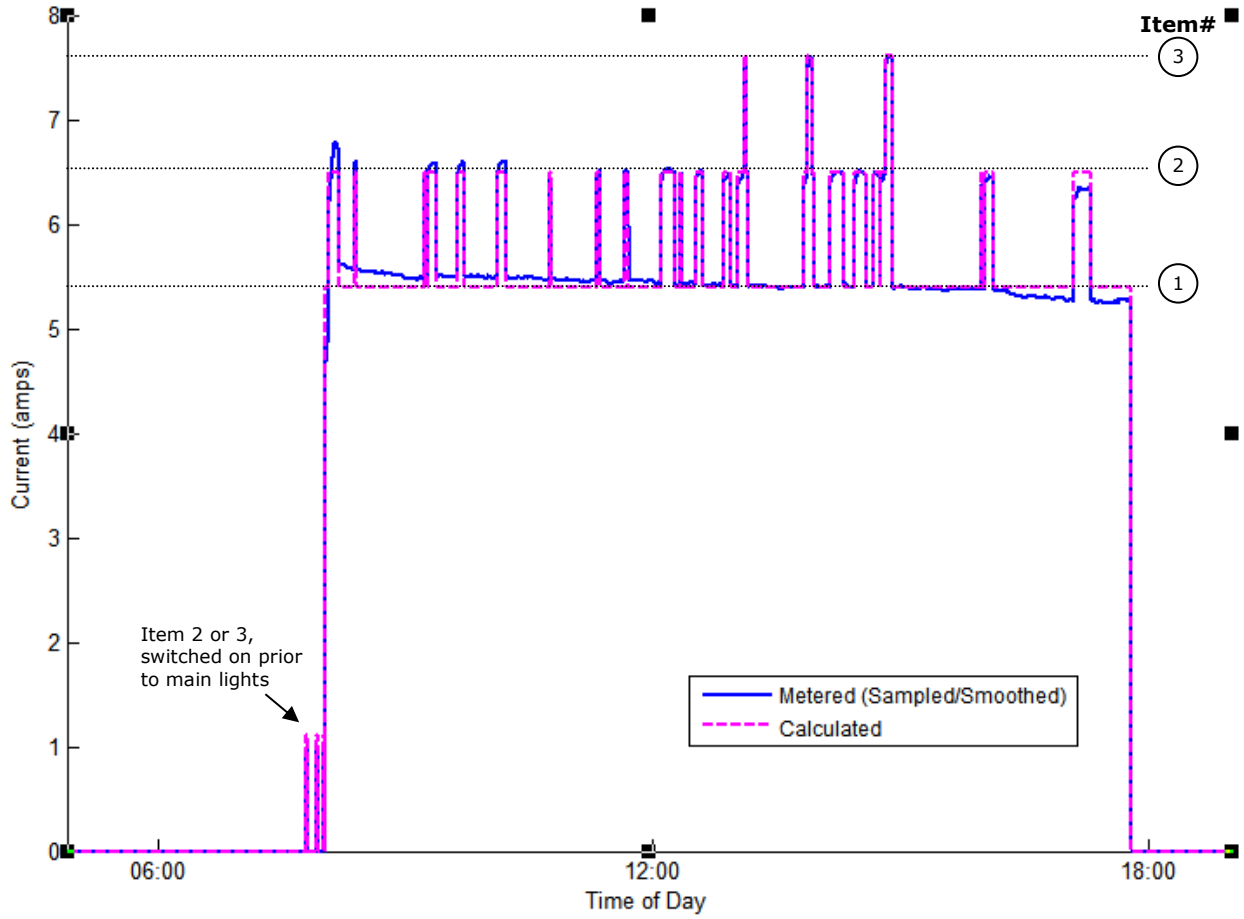

Figure 53 - Comparison of metered (smoothed/sampled) current data to the calculated total current used by all items

5.2.3.6 Interval Calculations

Once disaggregated, the final processing step for circuits with more than one electrical consuming item is the same as circuits with only one item: calculation of the current draw for hourly intervals. The same calculations defined in Section 5.1.2 are used, though the interval calculation are made for each individual item using the current values calculated in previous steps.

5.2.3.7 Trigger Calculation Parameters

Reliable processing of data channels with multiple items (trigger calculations) was sensitive to many of the parameters defined and discussed here. Optimization of these parameters was not a principal goal of this study, rather, trial and error and informal sensitivity analyses were used to find parameters that yielded acceptable results. However, a few of the key parameters are noted for future study:

> Sampling Rate: For this study, the DAQ sampling rate was set to 1 sample/second for each monitoring period. This was the highest frequency the DAQ multiplexer was capable of when monitoring 16 different channels. The high sampling rate was chosen to give flexibility in post-processing data, and ensured that very short electrical events, such as briefly turning on lights in the bathroom, were observed. However, when metering over the course days, weeks, or even years, high sample frequencies results in large data files and longer data processing times. Through experimentation with a "virtual" sampling rate, that is, under-sampling the raw data to mimic acquisition at a lower frequency, it was found lower frequencies still yielded adequate resolution on switching events while not having a notably negative affect on estimating total building power. The virtual rate used for the final processing of raw current data was 1 sample every 10 seconds, or $f = 0.10$. This seemed to offer a reasonable balance between processing reliability and speed.

Step Detection: The magnitude of the second derivative is used to determine when step changes in the data occur (i.e. trigger events). The same method is also used in the adaptive smoothing method to determine when the moving average window is reduced or enlarged. Though shown to be acceptable for this study, the thresholds defined for the second derivative are sensitive to the relative magnitudes of each item's current amplitude. Therefore, the thresholds need to be tailored to each circuit (i.e. DAQ channel).

5.2.4 Parsing Interval Current Data by Model Zone/End-use

Once the raw DAQ current data streams are processed into arrays of hourly interval values, it is parsed into an m x n array structure that better correlates with the BEM program. The dimensions of the array structure are described below, and for this specific project, are listed in Table 11:

- Model Zones (m): BEM models are composed of thermal zones, which often correlate to the physical building spaces, and are where the definitions of internal loads are typically defined. For this project, additional zone categories, such as 'Exterior Usage' and 'All Zones Total' are also calculated.
- Model End-Uses (n): BEM models define internal loads and tabulate results by energy end-use. The same convention is followed in this data structure to enable comparison of metered energy use to model outputs. Similar to totalizing energy use for all model zones, an additional category 'All End-uses Total' reflects the total metered end-use current for each zone.

Table 11 - List of model zones and end-uses

Zones (m=11)	End-Uses (n=12)
Office	Interior Lighting
Office Bathroom	Task Lighting
Warehouse Bath	Exterior Lighting
East Warehouse	Receptacles
West Warehouse	Space Heating
Office Attic	Space Cooling
Office Bath Attic	HVAC Fans
Warehouse Bath Attic	Exhaust Fans
Exterior Usage	Domestic Hot Water
	Refrigeration
All Zones TOTAL	**All End-uses TOTAL**

After parsing into model zones/end-uses, the individual data streams are written to the annual data array, created earlier in this process. The processor performs this task for each day of available metered information. At the end of this process, all the various raw data files are processed into hourly interval values and stored to the annual data arrays.

5.2.5 Create Average/Standard Deviation Profiles

In this study, metering was performed in short-term (approximately one-week) intervals, and was not performed throughout the entire year. In general, continuous metering is preferred for model calibration exercises, however, availability of equipment and engineering resources may limit the amount of metered information available. For this reason, a processing step was implemented to generate average daily profiles from available metering data. In later steps, when annual schedules are developed for the calibrated energy model, the average day profiles are assumed for all days that actual, metered information is unavailable.

Average hourly profiles were created for the following categories, which correspond to the schedule definitions of most energy modeling programs:

- Each individual day of the week (Sun-Sat) and Holiday (Hol)
- Weekdays (composite of all Mon-Fri days)
- Weekend and holidays (composite of all Sat-Sun-Hol days)

In addition to average profiles, the standard deviation of the profiles was calculated to illustrate the magnitude of hourly variation among days in the same schedule category.

The average day profiles are generated after processing all raw DAQ data files, and the annual data arrays are populated with available metered data. This ensures the average daily profiles are determined from the largest subsets of daily profiles. The hourly average and standard deviation values are determined using Equations (16) and (17) (Black 2012), which rely on calculating running totals of the hourly interval current values.

$$\mu_I = \frac{1}{N}\sum_{i=0}^{N-1} I_{hour} \tag{16}$$

$${\sigma_I}^2 = \frac{1}{N-1}\left[\sum_{i=0}^{N-1} I_{hour}^2 - \frac{1}{N}\left(\sum_{i=0}^{N-1} I_{hour}\right)^2\right] \tag{17}$$

where:
I_{hour} = interval current measurement (Amp-hr)
N = number of samples in averaging category
μ_I = average hourly value (Amp-hr)
σ_I = standard deviation of average values (Amp-hr)

5.2.6 Conversion of Current to Power

Current sensors were used to measure branch circuit electrical consumption, and this study relies on the idea that current can be used as a proxy for power. To convert sub-metered current data to power, a method similar to that described by Pacific Gas and Electric (2010) was used.

5.2.6.1 Spot Measurements of Current and Power

Using the DAQ system, spot measurements of current (I_i) were measured on different days and when different end-uses were active. At the same time, the following values were recorded using a portable power analyzer:

1. RMS Current, I_{RMS} (Amps)
2. RMS Voltage, V_{RMS} (Volts)
3. Power Factor, PF (ratio)
4. Power, P (Watts or kW, recorded for reference only)

Using the series of measurements for each DAQ channel, a weighted (by current amplitude) average ratio of I_i to I_{RMS} and circuit PF was calculated. The resulting values for each circuit are listed in Table 12 below. The monitored office heater circuit (#7) was one phase of the heater's two-phase power supply. For this reason, the calculated current ratio, 0.95, was multiplied times 2, thereby accounting for the equal current drawn on both phases. Finally, from all measurements of V_{RMS}, the average building supply voltage was calculated to be 122.9 Volts.

Table 12 - Weighted average current ratio and power factor (PF) from spot current and power factor measurements

Circuit #	DAQ Ch#	Zone	End-use	Current Ratio	Avg PF
3	11[1]	E Warehouse	Receptacles	1.71[3]	0.52[3]
4	12	Office	Interior lighting, exterior lighting, receptacle	0.99	0.99
7	11[1,2]	Attic space over office/bathrooms	Space heating	1.90	1.00
6	9	Office, warehouse and office bathrooms	DHW	1.04	1.00
8	10	Office (north wall)	Interior lighting, exterior lighting, exhaust fans	0.99	1.00
10	15	Server room (Office bathroom)	Receptacles	1.31	0.69
11	14	Office (south & west wall)	Receptacles	1.03	0.86
12	16	E Warehouse (packing area)	Receptacles	1.41	0.78
14	13	E Warehouse (north wall)	Receptacles	1.71	0.52

1. Circuits monitored for separate monitoring periods using the same DAQ channel.
2. Circuit is one phase of two-phase heater. Reported current ratio measured value for circuit multiplied by 2.
3. No spot measurements made, however, the primary electrical consuming item on this circuit during the monitoring period was the refrigerator, which was moved from circuit #14 to circuit #3 between monitoring periods.

5.2.6.2 Calculation of Power

With the relationship between current measured by the DAQ system and the actual power measured using a power analyzer defined, an estimate of hourly energy use was calculated using Equation (18).

$$P_{hour} = \frac{(I_{hour} \times I_{ratio}) \times AvgV_{RMS} \times AvgPF}{1000} \quad (18)$$

where:
P_{hour} = interval power calculation (kW-hr)
I_{hour} = interval current measurement (Amp-hr)
I_{ratio} = Current ratio for circuit
$AvgV_{RMS}$ = Average RMS voltage, all circuits (Volts)
AvgPF = average power factor for circuit

5.2.6.3 Comparison of Calculated Power to Utility Data

With the metered current converted to power, it was possible to compare the calculated values to the actual building energy use, as defined by the building utility meter. Figure 54 shows a comparison of the hourly interval values for both.

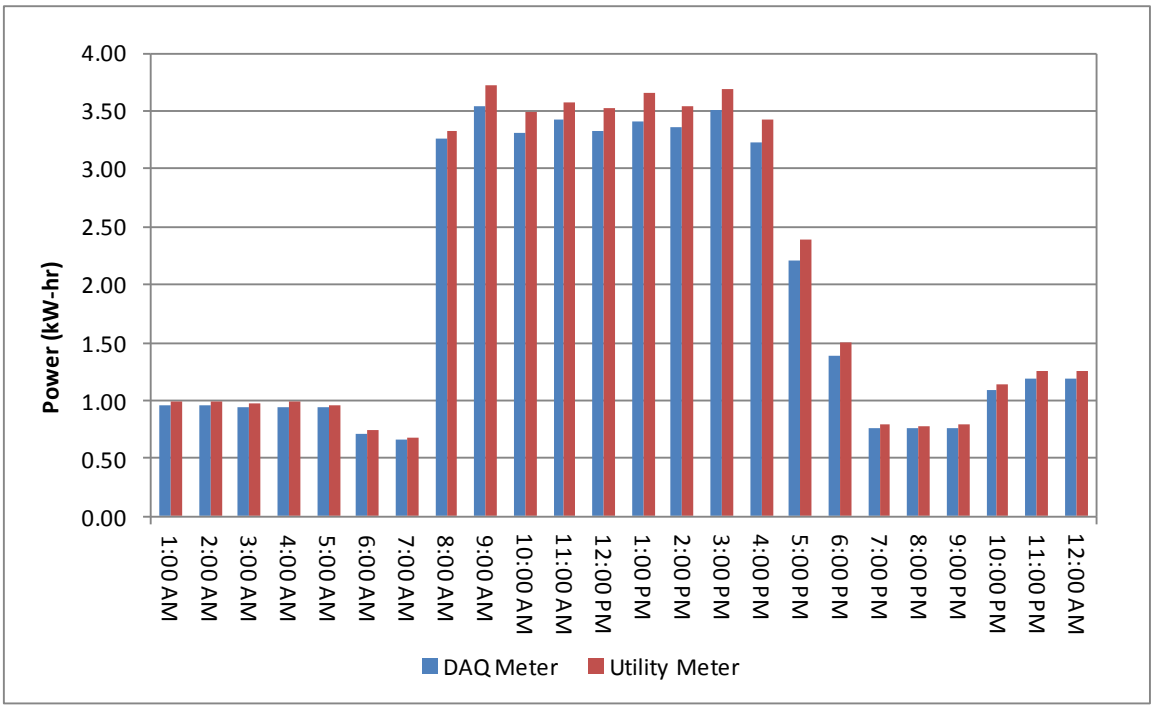

Figure 54 - Comparison of interval power calculated from DAQ meter to utility meter, no adjustment

The DAQ calculated power was observed to be consistently around 5% less than the utility measurement. Therefore, a constant multiplier of 1.05 was applied to all hourly DAQ power measurements. After making this adjustment, the difference in power was <1% (see Figure 55), which was assumed to be well within the margin of error for model calibration purposes.

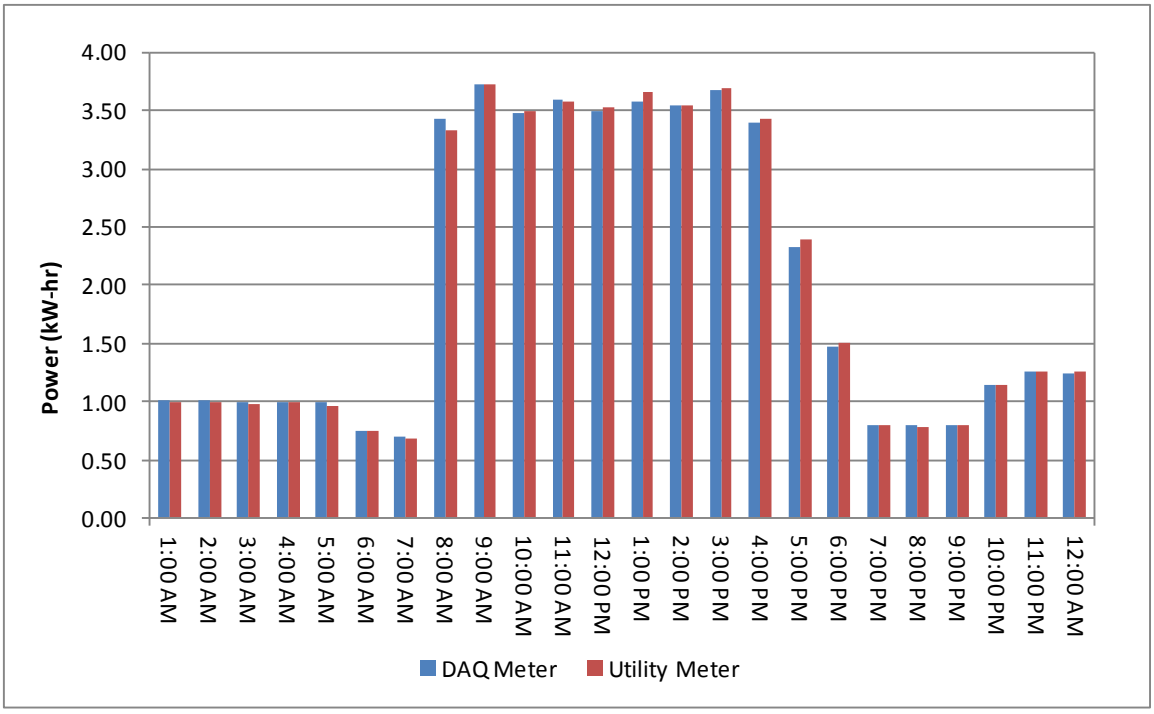

Figure 55 - Comparison of interval power calculated from DAQ meter (with a 1.05 multiplier) to utility meter

The conversion to power was performed for each of the daily zone/end-use data arrays contained in the annual data array file, as well as the average days calculated previously. Once converted, the data arrays are stored in a separate file for use in the final step of the processing routine.

5.2.7 Creation of Model Schedules

After completing conversion of current data to hourly interval power, the final step was to write the model/end-use data into a format compatible with the BEM software, eQUEST/DOE-2.2.

The eQUEST software easily facilitates defining operational schedules which vary on a daily basis, but it is not well suited to describing a continuous stream of schedule values, as is the case when load profiles are developed from measured data. As such, a Matlab routine was developed to write (to text file) an annual eQUEST schedule for each model zone/end-use.

The process begins with creating a week schedule (WEEK-SCHEDULE-PD) for every week of the year. Then, daily (Sun-Sat and Holiday) day schedules are defined by profiles developed from metered data, or for days where measurements were not made, by the average daily profiles. In this process, it is critical to assign the day schedules to the proper day of the week for the given analysis year. This ensures the hourly model inputs and outputs can be directly compared to the utility and weather data for each calendar day. Figure 56 illustrates the eQUEST daily schedules (DAY-SCHEDULE-PD) that comprise a typical weekly schedule (WEEK-SCHEDULE-PD). In this case, the week is made up of both metered day schedules (annotated with the actual date) and average day schedules (annotated with the term "Avg"). For this study, the following additional assumptions were made for the eQUEST input schedules:

- The Holiday schedule is the same as the average Sunday schedule.
- The heating design day (HDD) schedule for all internal gains is zero for all hours of the day.
- The cooling design day (CDD) schedule for all internal gains is assumed the average weekday profile for the given zone/end-use.

Once week schedules are defined, an annual eQUEST schedule is developed, ensuring the end month/days of each weekly schedule period align with the actual calendar days of the analysis year. An example year schedule is shown in Figure 57.

```
$ ------ Example day schedules --------
$ Model zone: S-MnOfc__ = Main Office
$ Model enduse: Iltg = Interior Lighting
$ DT = Day type (1 = Monday, 2, = Tuesday, etc)

"S-MnOfc_ILtg__DT-1_Avg" = DAY-SCHEDULE-PD
   TYPE              = MULTIPLIER
   VALUES            = ( 0, 0, 0, 0, 0, 0, 0, 0, 0.6668, 0.6886, 0.6886,
         0.6886, 0.6886, 0.6886, 0.6886, 0.6886, 0.6886, 0.544, 0, 0, 0, 0,
         0, 0 )
   ..
"S-MnOfc_ILtg__DT-2_100629" = DAY-SCHEDULE-PD
   TYPE              = MULTIPLIER
   VALUES            = ( 0, 0, 0, 0, 0, 0, 0, 0, 0.3397, 0.6886, 0.6886,
         0.6886, 0.6886, 0.6886, 0.6886, 0.6886, 0.6886, 0.4614, 0, 0, 0, 0,
         0, 0 )
   ..
"S-MnOfc_ILtg__DT-3_100630" = DAY-SCHEDULE-PD
   TYPE              = MULTIPLIER
   VALUES            = ( 0, 0, 0, 0, 0, 0, 0, 0.0092, 0.6886, 0.6886, 0.6886,
         0.6886, 0.6886, 0.6886, 0.6886, 0.6886, 0.6886, 0.3592, 0, 0, 0, 0,
         0, 0 )
   ..
"S-MnOfc_ILtg__DT-4_100701" = DAY-SCHEDULE-PD
   TYPE              = MULTIPLIER
   VALUES            = ( 0, 0, 0, 0, 0, 0, 0, 0, 0.5853, 0.6886, 0.6886,
         0.6886, 0.6886, 0.6886, 0.6886, 0.6886, 0.6886, 0.6886, 0.1561, 0,
         0, 0, 0, 0 )
   ..
"S-MnOfc_ILtg__DT-5_100702" = DAY-SCHEDULE-PD
   TYPE              = MULTIPLIER
   VALUES            = ( 0, 0, 0, 0, 0, 0, 0, 0, 0.0046, 0.6886, 0.6886,
         0.6886, 0.6886, 0.6886, 0.6886, 0.6886, 0.6886, 0.2089, 0, 0, 0, 0,
         0, 0 )
   ..
"S-MnOfc_ILtg__DT-6_100703" = DAY-SCHEDULE-PD
   TYPE              = MULTIPLIER
   VALUES            = ( 0, 0, 0, 0, 0, 0, 0, 0, 0, 0, 0, 0, 0, 0, 0, 0, 0, 0,
         0, 0, 0, 0, 0, 0 )
   ..
"S-MnOfc_ILtg__DT-7_Avg" = DAY-SCHEDULE-PD
   TYPE              = MULTIPLIER
   VALUES            = ( 0, 0, 0, 0, 0, 0, 0, 0, 0, 0, 0, 0, 0, 0, 0, 0, 0, 0,
         0, 0, 0, 0, 0, 0 )
   ..

$ ----- Example week schedule -------

"S-MnOfc_ILtg__2010_Wk27" = WEEK-SCHEDULE-PD
   TYPE              = MULTIPLIER
   DAY-SCHEDULES     = ( "S-MnOfc_ILtg__DT-1_Avg",       $ Monday
                         "S-MnOfc_ILtg__DT-2_100629",    $ Tuesday
                         "S-MnOfc_ILtg__DT-3_100630",    $ Wednesday
                         "S-MnOfc_ILtg__DT-4_100701",    $ Thursday
                         "S-MnOfc_ILtg__DT-5_100702",    $ Friday
                         "S-MnOfc_ILtg__DT-6_100703",    $ Saturday
                         "S-MnOfc_ILtg__DT-7_Avg",       $ Sunday
                         "S-MnOfc_ILtg__DT-7_Avg",       $ Holiday
                         "HDDDay",                       $ Heating Design Day (HDD)
                         "S-MnOfc_ILtg__DT-AvgWD_Avg" )  $ Cooling Design Day (CDD)
   ..
```

Figure 56 - Example eQUEST day and week schedule input

```
$ ------ Example day schedules --------
$ Model zone: S-MnOfc__ = Main Office
$ Model enduse: Iltg = Interior Lighting


"S-MnOfc_ILtg__2010" = SCHEDULE-PD
   TYPE              = MULTIPLIER
   $ Arrays of end month/day of each of week schedules listed below.
   MONTH             = ( 1, 1, 1, 1, 1, 2, 2, 2, 2, 3, 3, 3, 3, 4, 4, 4, 4, 5,
         5, 5, 5, 5, 6, 6, 6, 6, 7, 7, 7, 7, 8, 8, 8, 8, 8, 9, 9, 9, 9, 10,
         10, 10, 10, 10, 11, 11, 11, 11, 12, 12, 12, 12, 12 )
   DAY               = ( 3, 10, 17, 24, 31, 7, 14, 21, 28, 7, 14, 21, 28, 4,
         11, 18, 25, 2, 9, 16, 23, 30, 6, 13, 20, 27, 4, 11, 18, 25, 1, 8,
         15, 22, 29, 5, 12, 19, 26, 3, 10, 17, 24, 31, 7, 14, 21, 28, 5, 12,
         19, 26, 31 )
   WEEK-SCHEDULES    = ( "S-MnOfc_ILtg__2010_Wk1", "S-MnOfc_ILtg__2010_Wk2",
         "S-MnOfc_ILtg__2010_Wk3", "S-MnOfc_ILtg__2010_Wk4",
         "S-MnOfc_ILtg__2010_Wk5", "S-MnOfc_ILtg__2010_Wk6",
         "S-MnOfc_ILtg__2010_Wk7", "S-MnOfc_ILtg__2010_Wk8",
         "S-MnOfc_ILtg__2010_Wk9", "S-MnOfc_ILtg__2010_Wk10",
         "S-MnOfc_ILtg__2010_Wk11", "S-MnOfc_ILtg__2010_Wk12",
         "S-MnOfc_ILtg__2010_Wk13", "S-MnOfc_ILtg__2010_Wk14",
         "S-MnOfc_ILtg__2010_Wk15", "S-MnOfc_ILtg__2010_Wk16",
         "S-MnOfc_ILtg__2010_Wk17", "S-MnOfc_ILtg__2010_Wk18",
         "S-MnOfc_ILtg__2010_Wk19", "S-MnOfc_ILtg__2010_Wk20",
         "S-MnOfc_ILtg__2010_Wk21", "S-MnOfc_ILtg__2010_Wk22",
         "S-MnOfc_ILtg__2010_Wk23", "S-MnOfc_ILtg__2010_Wk24",
         "S-MnOfc_ILtg__2010_Wk25", "S-MnOfc_ILtg__2010_Wk26",
         "S-MnOfc_ILtg__2010_Wk27", "S-MnOfc_ILtg__2010_Wk28",
         "S-MnOfc_ILtg__2010_Wk29", "S-MnOfc_ILtg__2010_Wk30",
         "S-MnOfc_ILtg__2010_Wk31", "S-MnOfc_ILtg__2010_Wk32",
         "S-MnOfc_ILtg__2010_Wk33", "S-MnOfc_ILtg__2010_Wk34",
         "S-MnOfc_ILtg__2010_Wk35", "S-MnOfc_ILtg__2010_Wk36",
         "S-MnOfc_ILtg__2010_Wk37", "S-MnOfc_ILtg__2010_Wk38",
         "S-MnOfc_ILtg__2010_Wk39", "S-MnOfc_ILtg__2010_Wk40",
         "S-MnOfc_ILtg__2010_Wk41", "S-MnOfc_ILtg__2010_Wk42",
         "S-MnOfc_ILtg__2010_Wk43", "S-MnOfc_ILtg__2010_Wk44",
         "S-MnOfc_ILtg__2010_Wk45", "S-MnOfc_ILtg__2010_Wk46",
         "S-MnOfc_ILtg__2010_Wk47", "S-MnOfc_ILtg__2010_Wk48",
         "S-MnOfc_ILtg__2010_Wk49", "S-MnOfc_ILtg__2010_Wk50",
         "S-MnOfc_ILtg__2010_Wk51", "S-MnOfc_ILtg__2010_Wk52",
         "S-MnOfc_ILtg__2010_Wk53" )
   ..
```

Figure 57 - Example eQUEST year schedule input

At this point, it is important to note the metered and average day schedule values have not been normalized. That is, they represent the estimated energy consumed (kWh) for each model zone/end-use. eQUEST internal gains are described by an hourly design value (in W/ft^2 or kW), multiplied times the schedule value. For this reason, all zones with these custom schedules are defined to have a design load of 1 kW.

5.3 Processing Measured Temperature and Solar Data

5.3.1 Temperature Data

This study included seven interior and one exterior temperature sensors located at various points throughout the building site. Logging of interior space temperatures was intended for comparison to space temperatures predicted by the model. However, sensor locations were restricted to limit interference with occupant movement, and thus positioned near the ceiling or on a column.

Figure 58 below plots spot measurements of temperature at various heights below the ceiling mounted sensors in the office and attached bathroom at 5:30pm on July 14, 2010. The space was not occupied, heating systems were not active, and windows were closed for roughly 30 minutes prior to taking measurements. The plots illustrate stratification in the vertical temperature, an expected phenomena in spaces without significant air movement. Vertical measurements of temperature during other times of the day or year were not obtained, so the degree of temperature stratification for other conditions is unknown. The energy modeling software outputs space temperatures on an hourly basis, however, the space is assumed to be well-mixed and therefore uniform in temperature. Without expanded knowledge of temperature stratification in the office and bathroom spaces, the DAQ measured temperatures were simply averaged for each hourly interval and used (without adjustment) as a qualitative comparison to the modeled space temperature.

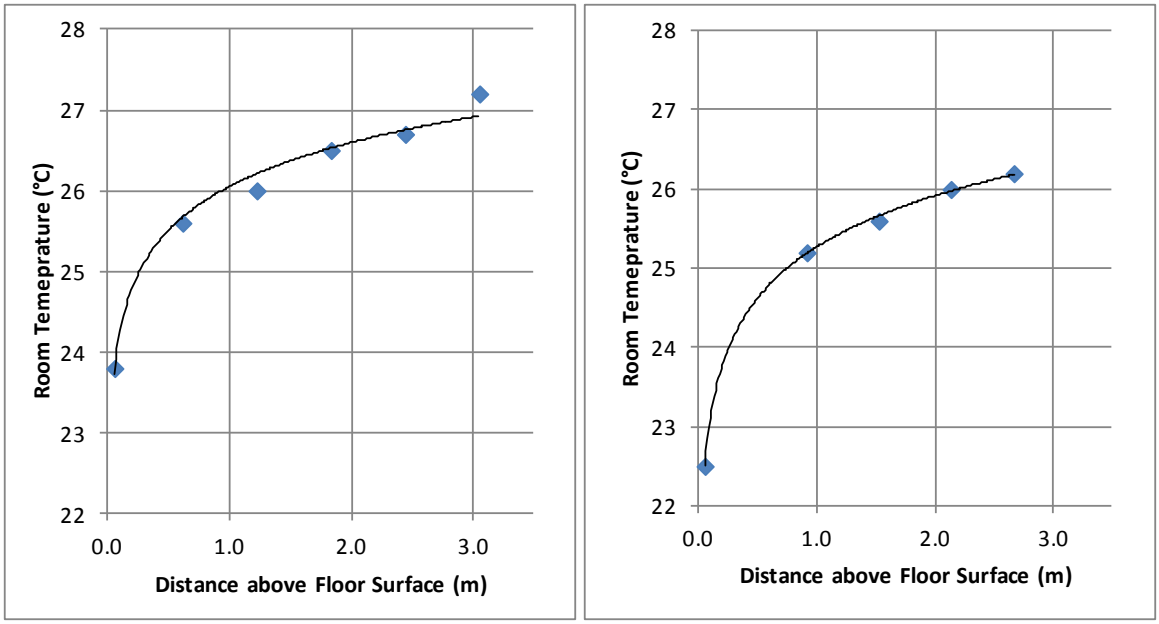

Figure 58 - Spot measurements of temperatures at various heights in the (a) Office and (b) Office Bathroom spaces.

In the warehouse, vertical stratification and variation of temperatures within the large, open unconditioned space was observed on a regular basis. Sensors were mounted vertically on a column in the center of the East Warehouse at increments of 5ft, as well as one additional sensor suspended from the ceiling at 10ft, approximately 5ft from the east exterior wall (see Chapter 3.4.3). As shown in Figure 59, the stratification is predominant during daytime hours, with a 3-5°C variation in height observed as the exterior temperature and solar radiation increase. For the purposes of this study, the four DAQ measured temperatures were averaged on an hourly basis, and compared to the modeled temperatures of the East Warehouse space.

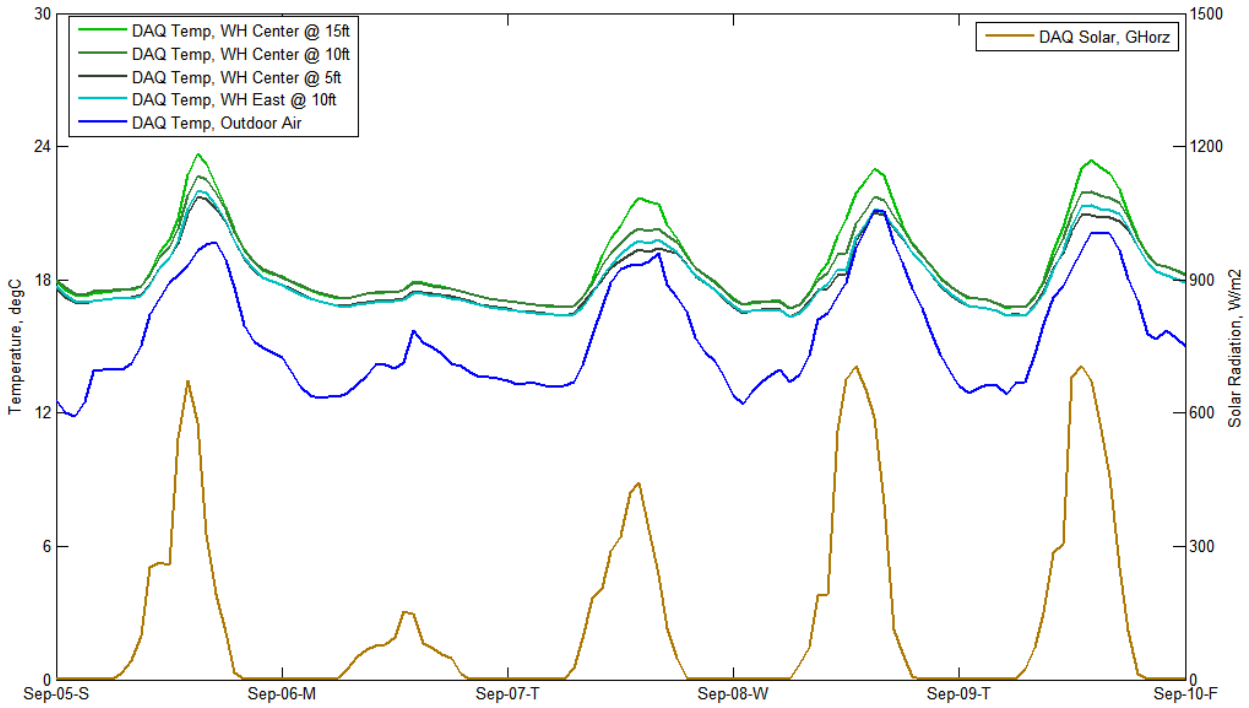

Figure 59 - Measured outdoor air, solar, and East Warehouse space temperature profile

Finally, the outdoor air temperature (OAT) was also logged by the DAQ system. As described in Chapter 4.2.2.2, direct solar radiation affected the outdoor air (OA) sensor in the late afternoon hours of the summer. After approximately September 1, the afternoon sun was low enough in the sky for the OA sensor to be shaded throughout the entire day. Temperatures measured throughout each hour were averaged for comparison to the instantaneous OA temperature recorded in the simulation weather file.

5.3.2 Solar Radiation

Hourly global horizontal solar radiation was measured at the same time that temperature and electrical sub-metering occurred. Again, for comparison to the values included in the simulation weather file, the DAQ measurements of solar radiation were averaged for each interval hour.

5.3.3 Summary of Metered Information

Data logging for this study occurred intermittently from 6/13/2010 to 12/19/2010. In total, 152.7 days, or 3,665 hours of data logging were processed to generate a detailed description of dynamic model inputs or for comparison to simulation outputs. Table 13 below summarizes the dates/times covered in each logging period. For all monitoring periods, each of the 16 DAQ channels was sampled at a frequency of one sample/second, resulting in ~2.8 GB of comma-delimited data files. The total time to process all data files according to the procedures described in this chapter was approximately 20 minutes.

Table 13 - Summary of DAQ logging periods

Data file name	Start time	End Time	Interval Start	Interval End	Day Start	Day End	Elapsed Days	Elapsed Hours
100613_2110.CSV	06/13/2010 21:20	06/21/2010 01:29	06/13/2010 22:00	06/21/2010 01:00	164	172	7.13	171
100621_0129.CSV	06/21/2010 01:29	06/28/2010 00:03	06/21/2010 02:00	06/28/2010 00:00	172	179	6.92	166
100628_0023.CSV	06/28/2010 00:04	07/04/2010 10:48	06/28/2010 01:00	07/04/2010 10:00	179	185	6.38	153
100714_0457.CSV	07/14/2010 04:57	07/19/2010 23:15	07/14/2010 05:00	07/19/2010 23:00	195	200	5.75	138
100719_2314.CSV	07/19/2010 23:15	07/28/2010 00:18	07/20/2010 00:00	07/28/2010 01:00	200	209	8.04	193
100728_0017.CSV	07/28/2010 00:19	08/03/2010 11:03	07/28/2010 01:00	08/03/2010 11:00	209	215	6.42	154
100805_1310-1.CSV	08/05/2010 13:10	08/07/2010 00:00	08/05/2010 14:00	08/07/2010 00:00	217	219	1.42	34
100805_1310-2.CSV	08/10/2010 00:00	08/12/2010 17:31	08/10/2010 01:00	08/12/2010 17:00	222	224	2.67	64
100816_1455.CSV	08/16/2010 14:55	08/18/2010 15:13	08/16/2010 15:00	08/18/2010 15:00	228	230	2.00	48
100819_1146.CSV	08/19/2010 11:46	08/30/2010 14:26	08/19/2010 12:00	08/30/2010 14:00	231	242	11.08	266
100830_1932.CSV	08/30/2010 19:32	09/10/2010 17:46	08/30/2010 20:00	09/10/2010 17:00	242	253	10.88	261
100910_1744.CSV	09/10/2010 17:46	09/17/2010 16:59	09/10/2010 18:00	09/17/2010 16:00	253	260	6.92	166
100917_1734.CSV	09/17/2010 17:33	09/22/2010 08:10	09/17/2010 18:00	09/22/2010 08:00	260	265	4.58	110
100922_0812.CSV	09/22/2010 08:11	09/28/2010 22:04	09/22/2010 09:00	09/28/2010 22:00	265	271	6.54	157
100928_2212.CSV	09/28/2010 22:12	10/06/2010 07:58	09/28/2010 23:00	10/06/2010 07:00	271	279	7.33	176
101006_2356.CSV	10/06/2010 23:57	10/07/2010 18:07	10/07/2010 00:00	10/07/2010 18:00	279	280	0.75	18
101013_1454.CSV	10/13/2010 14:54	10/18/2010 11:51	10/13/2010 15:00	10/18/2010 11:00	286	291	4.83	116
101018_1800.CSV	10/18/2010 18:00	10/31/2010 22:18	10/18/2010 19:00	10/31/2010 22:00	291	304	13.13	315
101031_2218.CSV	10/31/2010 23:18	11/07/2010 01:59	11/01/2010 00:00	11/07/2010 02:00	304	311	6.08	146
101110_1646.CSV	11/10/2010 16:46	11/24/2010 22:24	11/10/2010 17:00	11/24/2010 22:00	314	328	14.21	341
101124_2224.CSV	11/24/2010 22:25	11/29/2010 20:43	11/24/2010 23:00	11/29/2010 20:00	328	333	4.88	117
101204_1746.CSV	12/04/2010 17:46	12/19/2010 13:19	12/04/2010 18:00	12/19/2010 13:00	338	353	14.79	355
						Total	**152.71**	**3,665**

5.4 Processing Utility Interval Data

Utility energy consumption is often the benchmark (i.e. measured value) for calibrating the energy model. Errors in human meter readings and other anomalies in reported utility consumption are possible; however, the building in question was outfitted with a new, digital AMR meter, described in Chapter 3.4.1. In this case, the interval values reported by the utility are the average power (in kW) for each 15-minute period of a clock hour. To calculate hourly energy consumption, the sub-hourly interval values were downloaded from the utility website; for every hour with a complete set of interval data (4 reported values greater than zero), the average power was calculated. Numerically, the average hourly power (in kW) and hourly energy consumption (kWh) are the same value.

6 Model Development and Calibration

6.1 Overview

This chapter defines the steps taken to build and to calibrate the energy model of the building described in previous chapters. The general approach was to start with a model based on "default" static and dynamic assumptions generated by the modeling software and basic user inputs, followed by incremental addition of details and adjustments based on measurements and other evidence gathered for this study. The main objective is to illustrate the relative change in model calibration as assumptions are informed by actual audit and measured information. Calibration will be determined by comparing the predicted and measured whole building energy use over hourly, daily, and monthly intervals, using the statistical methods described in this Chapter.

6.1.1 Revision Control

In this study, changes to the energy model were archived using TortoiseSVN (2013), an open-source software that integrates an Apache Subversion (SVN) client management as a Microsoft Windows shell extension. This tool facilitates making incremental, user annotated "snapshots" of the model information, which can be easily accessed and compared at any time throughout the model calibration process. In addition to using Subversion, model parameters adjusted to achieve calibration were described using DOE-2.2's Building Description Language (BDL) expressions. The BDL language allows specification of global variables, as well as the use of IF/THEN, SWITCH/CASE, and other expressions to define the values of DOE-2 keywords (i.e. model inputs). For this study, global "flag" variables were defined, with the status of the flag value (0, 1, 2, etc.) corresponding to a different assumptions. Figure 60 provides an example of the syntax used to define the interior LPD of a modeled space (i.e. room), changing it from the Wizard default value to the value calculated from the building survey. These expressions, combined with the eQUEST

parametric run manager, allow each of the major model calibration runs to be simulated consecutively and results compared using the native eQUEST reports.

```
$ Example global flag variables
$ ------------------------------------------------------
$              Global Parameters
$ ------------------------------------------------------
PARAMETER
   "AuditLPD Flag"          = 0  ..
PARAMETER
   "AuditWallTypes Flag"    = 0  ..
PARAMETER
   "MeteredSchedules Flag"  = 0  ..

$ Example syntax for switching wall construction assignments using IF/THEN expression

"EL1 East Wall (ML.NE1.E1)" = EXTERIOR-WALL
   CONSTRUCTION     =
{if(#pa("AuditWallTypes Flag")==1)
   then #si("EWT1 Cons","EXTERIOR-WALL","CONSTRUCTION")            $ Audit construction
 else #si("EL1 EWall Construction","EXTERIOR-WALL","CONSTRUCTION") $ Wizard construction
 endif}

$ Example syntax for switching space lighting power density

"S-E WH__ (ML.s1)" = SPACE
…
   LIGHTING-W/AREA  = (
{if(#pa("MeteredSchedules Flag")>=1)
   then 0
 else if(#pa("AuditLPD Flag")==1)
  then 6*192/#l("AREA")            $ Audit LPD = # fixtures * fixture power / space area
 else 1.19                         $ Wizard LPD
 endif endif} )
```

Figure 60 - Example global variables and BDL expressions

6.1.2 Calibration Statistics

To quantify model calibration, mean bias error (MBE) and coefficient of variation of the root mean square error (CVRSME) were calculated. MBE describes the variation of the measured and simulated mean values, while CVRSME is a gauge of how well the simulation matches the variation in measured values. These metrics are described by the following formulae:

$$\overline{M_T} = \frac{\sum_{i=1}^{N_T} M_i}{N_T} \tag{19}$$

$$MBE_{(T)} = \frac{\sum_{i=1}^{N_T} (M_i - S_i)}{\overline{M_T}} \tag{20}$$

$$CVRSME_{(T)} = \frac{\sqrt{\frac{\sum_{i=1}^{N_T} (M_i - S_i)^2}{N_T}}}{\overline{M_T}} \tag{21}$$

where:
M_i = measured interval value at instance i
S_i = simulated interval value at instance i
T = the interval (e.g. monthly, daily, hourly)
$\underline{N_T}$ = number of values at interval T
$\overline{M_T}$ = average of the measured data

In addition, the absolute percent error (APE) is also a useful metric. The APE was calculated at each interval, and plotted as a surface to understand the relative magnitude of model error throughout the year.

$$APE = \sqrt{\left(\frac{M_i - S_i}{M_i}\right)^2} \tag{22}$$

When using whole building simulation to predict actual performance, ASHRAE Guideline 14 (2002) recommends the following thresholds for MBE and CVRSME[4]:

- For monthly calibration data (T = monthly), CVRSME = 15% and MBE = 5%.
- For hourly calibration data (T = hourly), CVRSME = 30% and MBE = 10%.

[4] MBE and CVRSME formulae in ASHRAE Guideline 14 include an adjustment of number of values (N_T) by the number of model parameters (p). For calibrated simulations, the Guideline indicates to use a value of p=1. For hourly calibrations, this adjustment has a small impact on the statistics, so it was omitted for comparison to other work, such as Raftery (2011 (2)).

6.1.3 Calibration Period

Another important specification is the calibration period over which the measured and modeled data are compared. The duration of calibration studies is typically at least 12 months. However, for this study, the calibration period is defined from June 1st 2010 to December 31st, 2010 for the following reasons:

- The building was purchased in early 2010, and regular daily operations did not begin until March.
- The monitoring equipment for the study was not installed and tested until late May 2010, and monitoring did not begin until 6/13/10.
- The seven month calibration period is still long enough to cover range of typical environmental and operational conditions.

The 214 day (5,136 hour) calibration period was shortened further to 205.8 days (4,940 hours) due to intermittent gaps in the 15-minute utility interval data. In addition to describing the calibration statistics for this period, a summary of calibration results for the hours that electricity sub-metering data were available is included in Chapter 6.5. The sub-metering periods, as described in Chapter 5.3.3, cover 152.7 days (3,665 hours), or 71% of the calibration period.

6.2 Initial Model

With the building survey, weather file, and meter data gathered and processed, the next step undertaken in this study was to create the energy model. For this project, a DOE-2.2 (also referred to here as DOE-2) model was created, edited, and simulated using the eQUEST software.

6.2.1 eQUEST

eQUEST is likely the most commonly used graphical interface to the DOE-2 simulation engine. In addition to graphical access to DOE-2 model input and output, the program also includes a model creation "Wizard", described by the program authors (James J. Hirsh and Associates 2010):

> *"The building creation wizard guides you through a series of steps designed to allow you to fully describe the principal energy-related features of your design. The wizard then creates a detailed description of the proposed design in the format required by the DOE-2 simulation program. At each step of describing your building design, the wizard provides easy-to-understand choices of component and system options."*

In general, the eQUEST Wizard is a powerful tool for quickly creating model geometry and defining starting points for the large amount of detail necessary for simulations. eQUEST's Design Development (DD) Wizard provides the greatest flexibilty, and steps users through a series of screens where detail is specificied by building category (geometry, envelope, lighting, etc). Modelers can specify their own information, but also have the option to accept default assumptons for pre-defined building types.

6.2.2 Wizard Model

The floor plan and envelope geometry of initial wizard model was developed from the original construction drawings and audit information. Figure 61 shows the 3-D rendering of

the model, as it compares to the actual building. A few simplifications to the building description were made:

- The model roof is flat, as opposed to the low slope incorporated into the actual roof. The approximate average floor-to-roof height was used to define the volume of zones throughout the building. This simplification does slightly reduce the total roof surface area, and alters the orientation of the roof with respect to incident solar radiation.
- The warehouse doors are modeled as opaque door objects. The amount of door glazing is approximately 15%, and though the sectional door panels are insulated, there is no thermal break in metal framing members.

The impact of these model simplifications on calibration was not determined in this study, but is believed to be small.

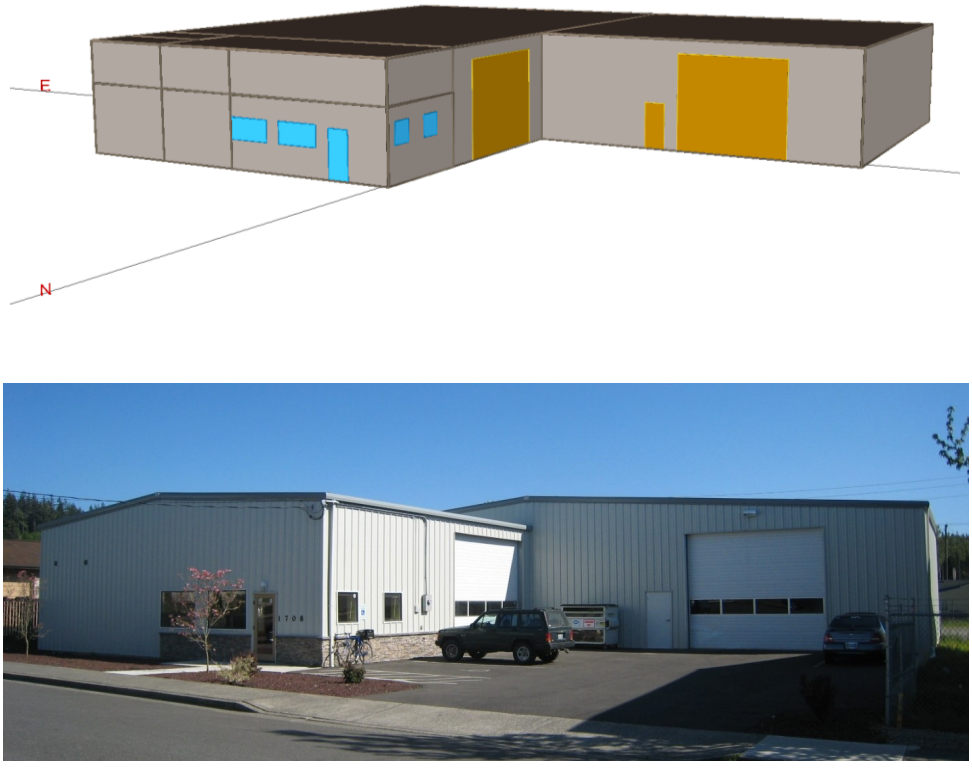

Figure 61 - 3D rendering of energy model and image of actual building

The Wizard was used to allocate activity area descriptions (office, restrooms, etc) to model zones, as well as a preliminary specification of building envelope, HVAC, and DHW systems (see Figure 62). From this information, the eQUEST program generates default schedules, internal load assumptions, and other detail, which is populated to the text file structure compatible with the DOE-2 simulation engine.

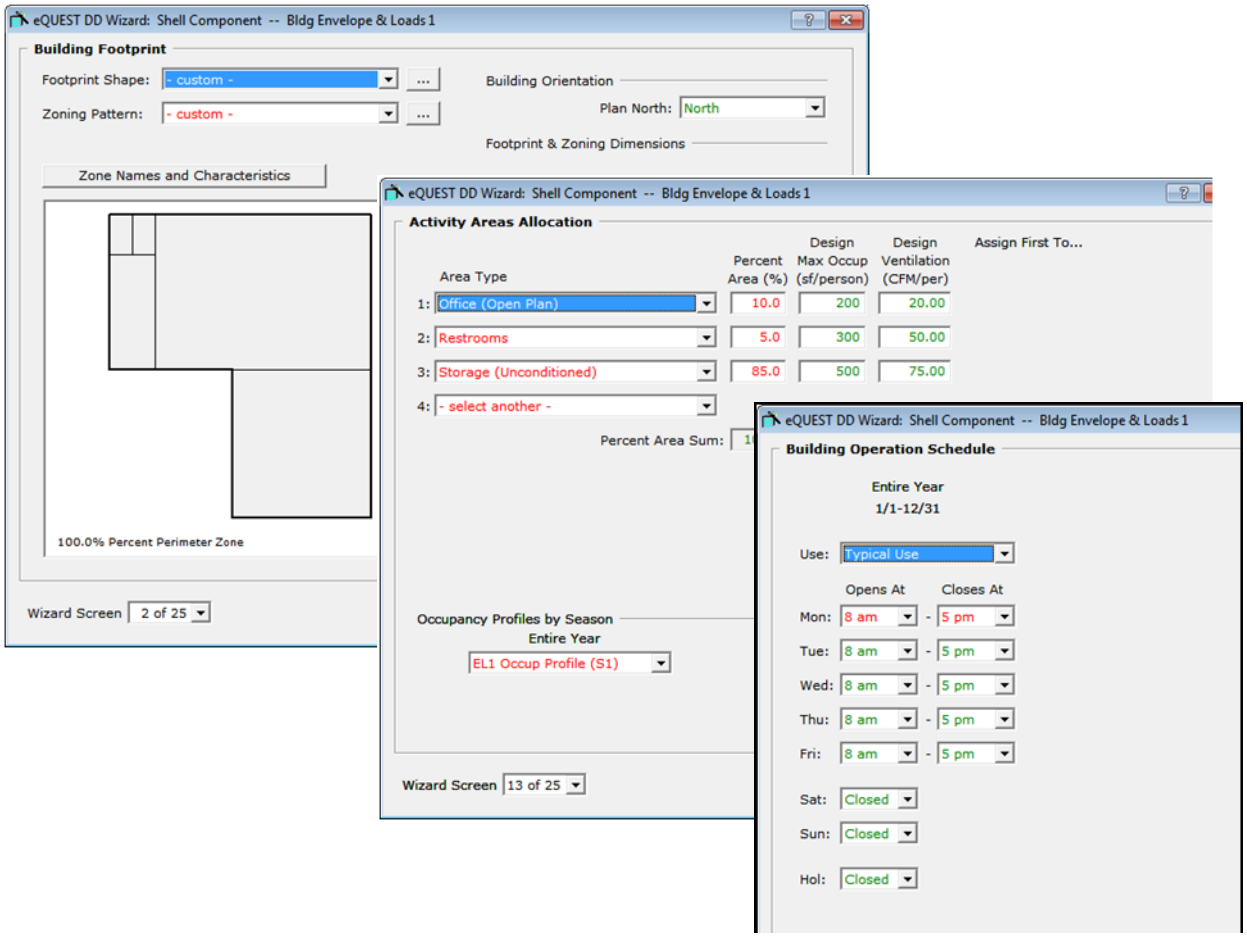

Figure 62 - Example eQUEST Wizard input screens

After exiting the eQUEST Wizard, a few basic revisions to the model were made:

- Specifying the custom weather file developed in Chapter 4.
- Rotate building 90 degress to represent actual orientation.
- Renamed spaces and assigned actual capacities of office electric resitance space heaters, and disabled baseboard heaters in bathroom (based on audit observations).
- Defined hourly reports to output electricity energy use, thermal zone space temperatures, and weather file variables.

This model served as a starting point for the calibration procedure.

6.3 Calibration Steps

6.3.1 Run 0: Wizard Model

The first step of the calibration process was to run an annual simulation and calculate the model statistics for the Wizard-based model. Figure 63 shows the hourly APE plotted for the calibration period, while Figure 64 displays the results for an entire annual simulation under 2010 weather conditions.

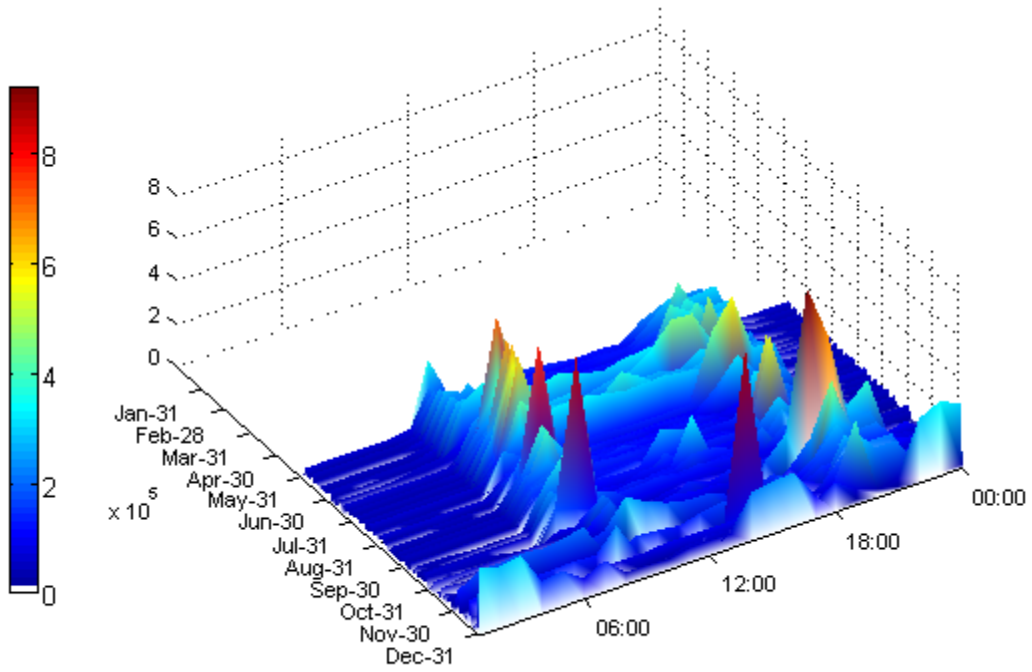

Figure 63 - Run 0 hourly absolute percent error (APE) plot

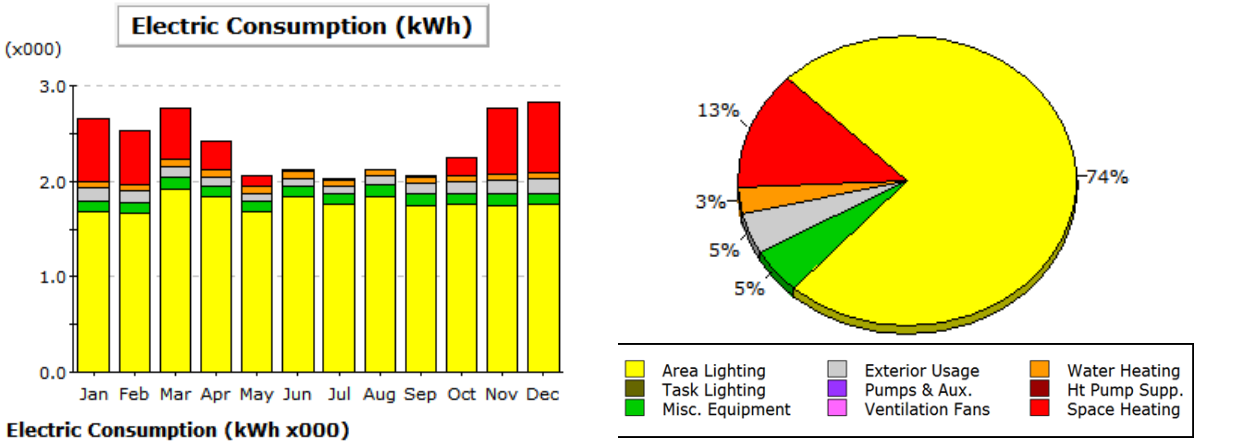

Electric Consumption (kWh x000)

	Jan	Feb	Mar	Apr	May	Jun	Jul	Aug	Sep	Oct	Nov	Dec	Total
Space Cool	-	-	-	-	-	-	-	-	-	-	-	-	-
Heat Reject.	-	-	-	-	-	-	-	-	-	-	-	-	-
Refrigeration	-	-	-	-	-	-	-	-	-	-	-	-	-
Space Heat	0.66	0.57	0.53	0.29	0.11	0.03	0.00	0.00	0.02	0.19	0.70	0.74	3.86
HP Supp.	-	-	-	-	-	-	-	-	-	-	-	-	-
Hot Water	0.07	0.07	0.08	0.08	0.07	0.07	0.07	0.07	0.06	0.07	0.07	0.07	0.83
Vent. Fans	-	-	-	-	-	-	-	-	-	-	-	-	-
Pumps & Aux.	-	-	-	-	-	-	-	-	-	-	-	-	-
Ext. Usage	0.14	0.12	0.11	0.09	0.08	0.07	0.08	0.09	0.10	0.12	0.13	0.15	1.31
Misc. Equip.	0.11	0.11	0.13	0.12	0.11	0.12	0.12	0.12	0.12	0.12	0.12	0.12	1.44
Task Lights	-	-	-	-	-	-	-	-	-	-	-	-	-
Area Lights	1.67	1.67	1.91	1.83	1.67	1.83	1.75	1.83	1.75	1.75	1.75	1.75	21.19
Total	2.67	2.54	2.76	2.42	2.05	2.13	2.02	2.12	2.06	2.25	2.78	2.83	28.63

Figure 64 - Run 0 monthly building end-use energy and fractions

The initial Wizard model results indicate substantial (>100%) error for most of the daytime hours, and the default Wizard lighting assumptions indicate nearly three quarters of total building energy use is for interior lighting. The initial calibration metrics were MBE -54.8% and CVRSME 114.4%. These results indicate that the model is overestimating total energy use, and given the large interior lighting fraction, the Wizard lighting power assumptions were reviewed next.

6.3.2 Run 1: Audit LPDs

The first adjustment to the model was to update the default lighting power assumptions with the values determined from the audit. Table 14 summarizes the Wizard and audited LPDs.

Table 14 - Summary of building area LPDs

Building Area	Wizard LPD (w/ft2)	Audit LPD (W/ft2)
Office	1.24	1.22
Restrooms	0.77	0.87
Warehouse	1.19	0.34

The Wizard default LPDs were reasonable assumptions for the office and restrooms, however in this case, the default "Storage, Unconditioned" assumption was roughly three times the actual warehouse installed lighting power. If the default assumptions were used to estimate the impacts of a lighting retrofit, the savings would have been dramatically over-estimated. The building LPD revisions substantially improved the MBE and CVRSME to 19.8% and 47.3% respectively. However, as shown in Figure 65, the simulated building energy use as a function of outdoor air temperature (energy-OAT plot) did not correlate well with the measured performance. The fact that the simulated energy use is close to or zero for many hours of the calibration period does not match the measured performance, pointing to a discrepancy in the simulated constant electrical loads.

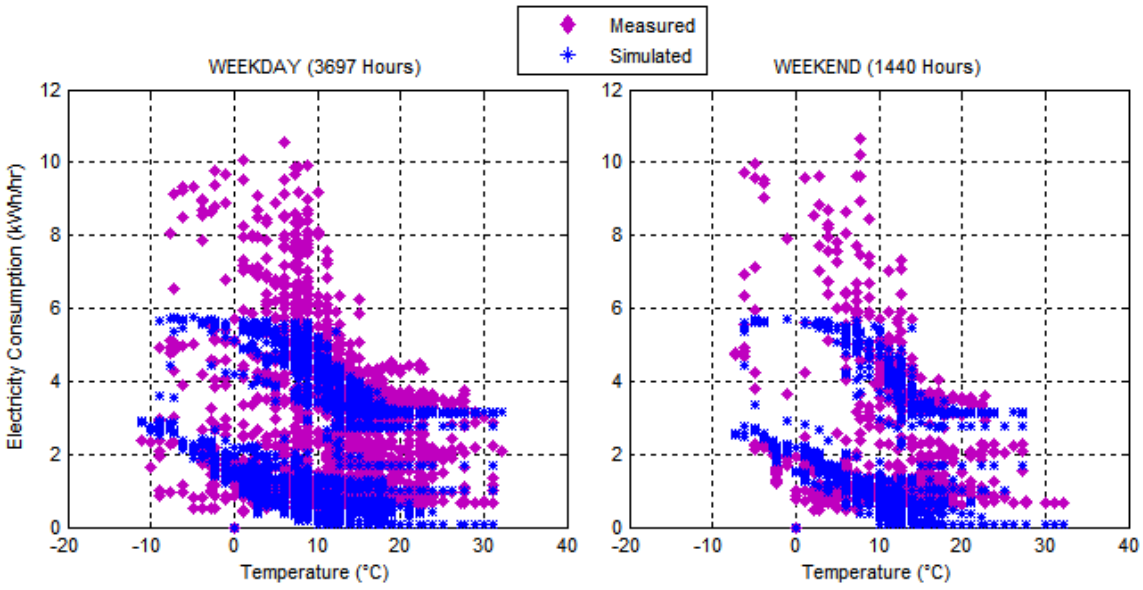

Figure 65 - Run 1 energy-OAT plot

6.3.3 Runs 2-4: Audit Wall Types, Windows, and Occupancy

Before incorporating sub-metered electrical load information into the model (i.e. addressing dynamic model inputs), additional envelope and occupancy information obtained from the building survey and known to be different than Wizard default values was included. Table 15 summarizes the changes to the model, as well as the impact on MBE and CVRSME. The combination of audit information moved calibration metrics in the right direction, but did not reduce error to acceptable levels. Without significantly more audit information to incorporate, Run 5 marks the point at which a modeler might start "turning the knobs" on unknown model parameters such as operating schedules, receptacle loads and infiltration to obtain model calibration. Figure 66 indicates the predicted annual building energy use is 45% less than Run 0. The fraction of energy used for lighting has reduced, though it is still predicted to account for 50% of annual energy consumption.

Table 15 - Run 2-4 audit wall type, window, and occupancy adjustments

Run #	Run Title	Description	Statistics
2	Audit Wall Types	Revised exterior wall and door constructions. Average wall U-factors: Above-grade walls Wizard = U-0.100, Audit = U-0.090 Roofs Wizard = U-0.088, Audit = U-0.160	MBE = 17.5% CVRSME = 46.7%
3	Audit GTCs	Revised window U/SHGC values and revised window modeling method from SHADING-COEF to GLASS-TYPE-CODE. Average U-factors Wizard = U-0.59, Audit = 0.38	MBE = 17.7% CVRSME = 46.8%
4	Audit Occupancy Densities	Revised design number of occupants in select spaces: Warehouse Wizard = 11.4 people, Audit = 1.9 people Office Wizard = 2.8 people, Audit = 3.7 people	MBE = 18.0% CVRSME = 46.8%

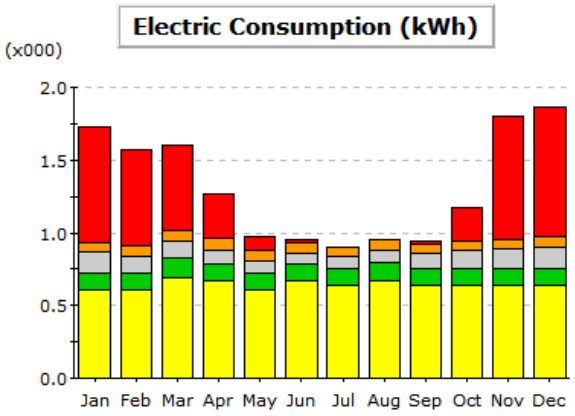

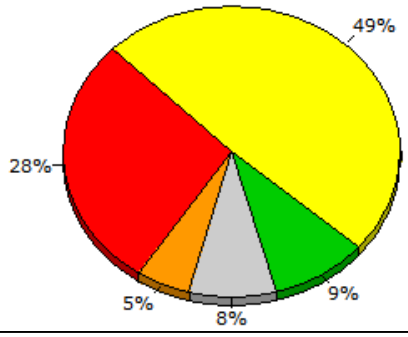

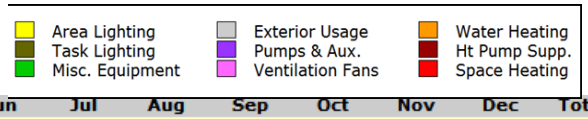

Electric Consumption (kWh x000)

	Jan	Feb	Mar	Apr	May	Jun	Jul	Aug	Sep	Oct	Nov	Dec	Total
Space Cool	-	-	-	-	-	-	-	-	-	-	-	-	-
Heat Reject.	-	-	-	-	-	-	-	-	-	-	-	-	-
Refrigeration	-	-	-	-	-	-	-	-	-	-	-	-	-
Space Heat	0.80	0.66	0.58	0.31	0.10	0.02	0.00	0.00	0.02	0.23	0.84	0.88	4.44
HP Supp.	-	-	-	-	-	-	-	-	-	-	-	-	-
Hot Water	0.07	0.07	0.08	0.08	0.07	0.07	0.07	0.07	0.06	0.07	0.07	0.07	0.83
Vent. Fans	-	-	-	-	-	-	-	-	-	-	-	-	-
Pumps & Aux.	-	-	-	-	-	-	-	-	-	-	-	-	-
Ext. Usage	0.14	0.12	0.11	0.09	0.08	0.07	0.08	0.09	0.10	0.12	0.13	0.15	1.31
Misc. Equip.	0.11	0.11	0.13	0.12	0.11	0.12	0.12	0.12	0.12	0.12	0.12	0.12	1.44
Task Lights	-	-	-	-	-	-	-	-	-	-	-	-	-
Area Lights	0.61	0.61	0.70	0.67	0.61	0.67	0.64	0.67	0.64	0.64	0.64	0.64	7.70
Total	1.73	1.57	1.60	1.27	0.97	0.95	0.90	0.95	0.94	1.17	1.80	1.86	15.72

Figure 66 - Run 4 monthly building end-use energy and fractions

6.3.4 Run 5: Schedules and Internal Loads Based on Sub-Meter Data

The next step in this calibration process was to utilize the schedules and loads developed from sub-metered information to describe the primary dynamic inputs of the model. Given the large amount of unconditioned building area, and the presence of a heating-only system in the Office space, intuition suggests building energy use is likely driven by lighting and plug load end-uses. In this case, all lighting is manually switched ON/OFF by the occupants except for the use of wall mounted occupancy sensors in the bathrooms. The office and warehouse areas both include computer workstations, which are used regularly during the day, but intermittently shut off at night. Entering this study, it was expected the accurate

specification of these occupant-dependent model assumptions would be a critical step before honing assumptions for more difficult to predict/measure variables like infiltration.

Figure 67 summarizes the updated hourly APE using the schedules developed from sub-metering lighting, receptacle equipment, exhaust fans, and domestic hot water (DHW) heating circuits.

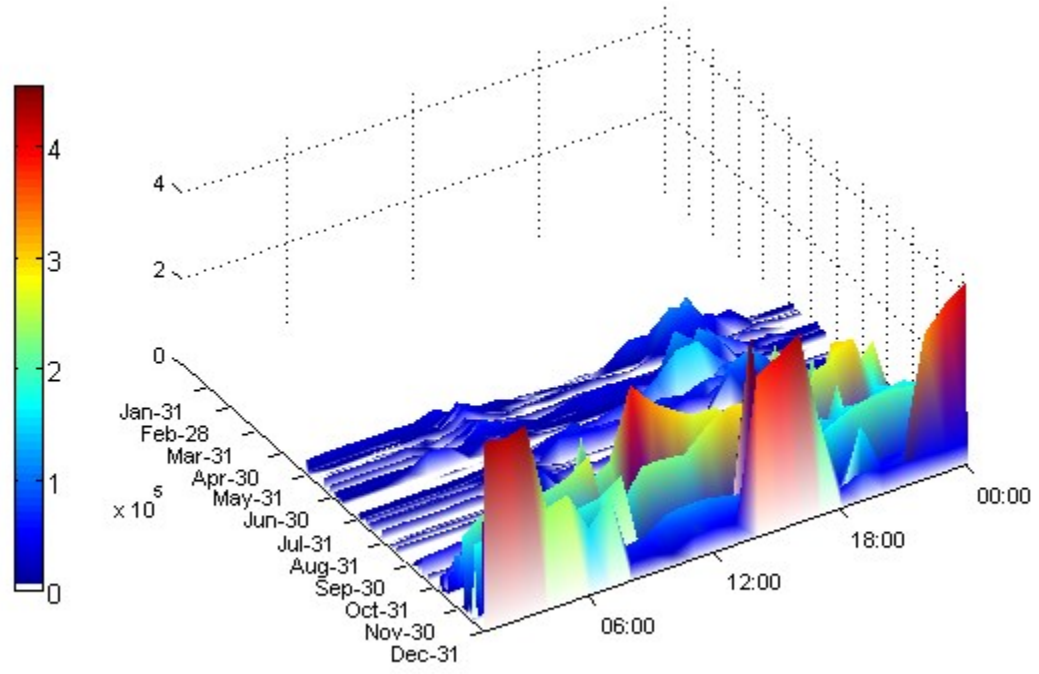

Figure 67 - Run 5 hourly APE and building end-use energy fractions

The use of metered schedules resulted in another step change of the calibration metrics, reducing MBE and CVRSME to 2.9% and 38.9%, respectively. When only including hours with sub-metering data, the MBE and CVRSME were 1.9% and 36.0%, respectively. In both cases, the use of measured electrical data brings model calibration close to the goals for hourly calibration. Comparing Figure 68 with the results for Run 4 shows the receptacle based (Misc.) equipment is a larger fraction than lighting, and the DHW energy fraction has shrunk. However, inspection of the energy-OAT (Figure 69) plots clearly indicates the

model still under-predicts energy consumption at lower outdoor air temperatures, pointing to increased office heater operation in the fall/winter. This discrepancy was confirmed by reviewing time series plots of heater energy use measured by the DAQ system.

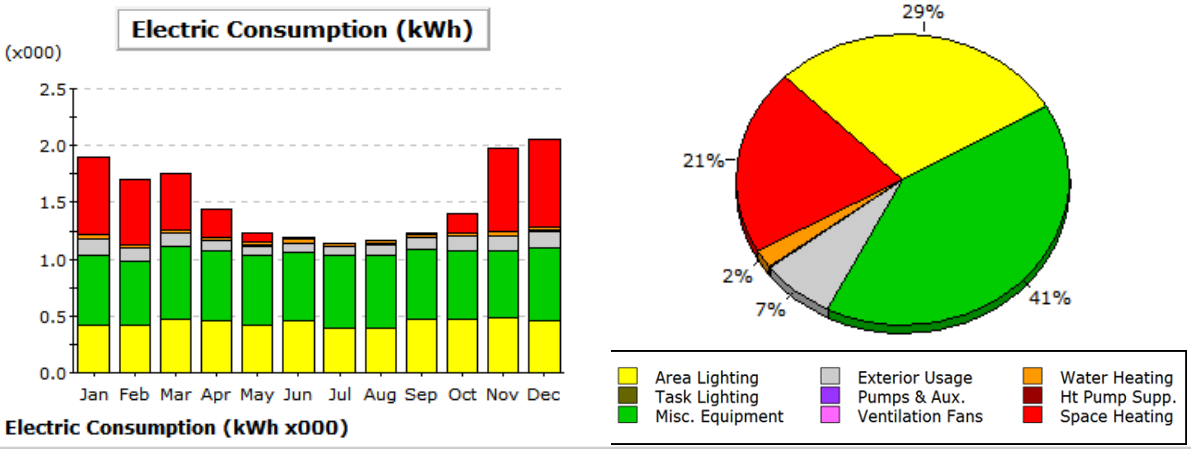

Electric Consumption (kWh x000)

	Jan	Feb	Mar	Apr	May	Jun	Jul	Aug	Sep	Oct	Nov	Dec	Total
Space Cool	-	-	-	-	-	-	-	-	-	-	-	-	-
Heat Reject.	-	-	-	-	-	-	-	-	-	-	-	-	-
Refrigeration	-	-	-	-	-	-	-	-	-	-	-	-	-
Space Heat	0.69	0.57	0.49	0.24	0.07	0.02	0.00	0.00	0.01	0.17	0.74	0.77	3.77
HP Supp.	-	-	-	-	-	-	-	-	-	-	-	-	-
Hot Water	0.03	0.03	0.03	0.03	0.03	0.03	0.03	0.03	0.03	0.03	0.03	0.04	0.38
Vent. Fans	0.00	0.00	0.00	0.00	0.00	0.00	0.00	0.00	0.00	0.00	0.00	0.00	0.02
Pumps & Aux.	-	-	-	-	-	-	-	-	-	-	-	-	-
Ext. Usage	0.14	0.12	0.11	0.09	0.08	0.07	0.08	0.09	0.10	0.12	0.13	0.15	1.31
Misc. Equip.	0.62	0.57	0.64	0.61	0.62	0.61	0.64	0.65	0.62	0.60	0.59	0.64	7.39
Task Lights	-	-	-	-	-	-	-	-	-	-	-	-	-
Area Lights	0.42	0.41	0.48	0.46	0.42	0.46	0.39	0.39	0.47	0.47	0.48	0.46	5.32
Total	1.90	1.71	1.75	1.44	1.22	1.19	1.14	1.17	1.23	1.40	1.98	2.05	18.18

Figure 68 - Run 5 monthly building end-use energy and fractions

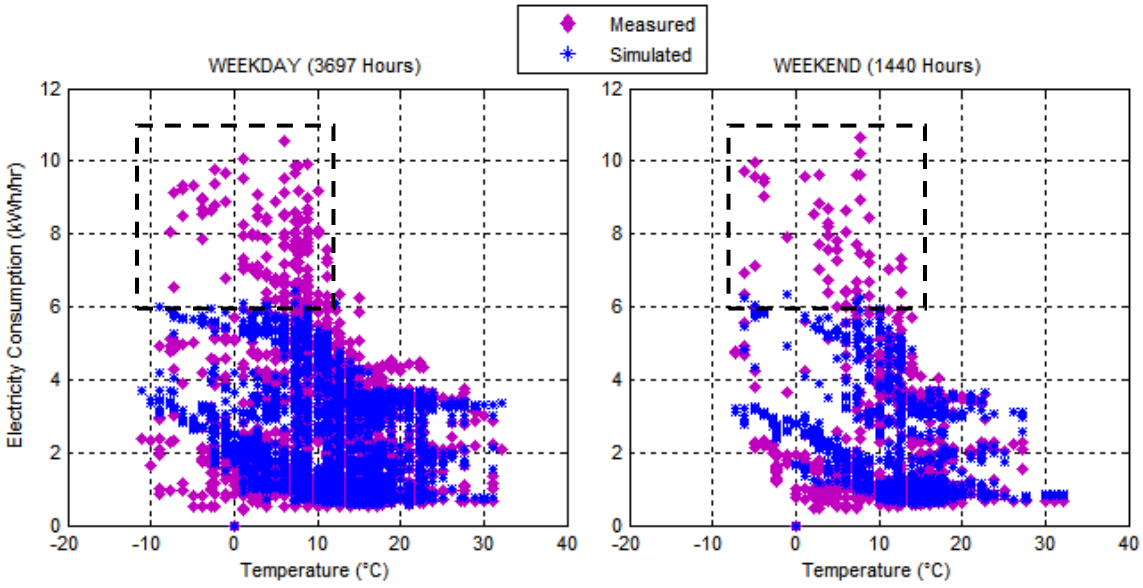

Figure 69 - Run 5 Energy-OAT plot

6.3.5 Run 6-7: Adjustment of Office Envelope Performance

With indication the office heating energy was under-estimated, a brief infrared thermography study was undertaken to identify thermal bridges in the opaque envelope. Infrared thermography is a common tool for identifying locations of elevated envelope heat loss and air leakage that cannot be normally detected with other measurement tools. Important observations include:

1. Numerous cavities of the framed office walls were found to be under- or un-insulated (see Figure 70 and Figure 71). One inferred scenario for exterior wall voids is that the batt insulation is not confined to the cavity of the wood-framed walls built inside of the metal-frame building structure, and therefore the batt insulation has collapsed down into the lower portion of the walls. Another scenario is batt insulation was simply not installed in these wall cavities.
2. No perimeter or under-slab insulation was identified in the plans, which was reflected in the Wizard model inputs. However, thermography (see Figure 72 and Figure 73)

revealed the top edge of the slab was exposed to the ambient air along the north and east perimeter of these heated spaces. This was assumed to result in greater heat loss than calculated by the Wizard defined un-insulated slab-on-grade floor assembly.

To account for these observed thermal bridges, the heat loss (U) factor of the conditioned space wall and floor assemblies was reduced. A detailed thermal imaging study to quantify the total affected surface area and calculation of the under-insulated wall performance was outside the scope of this study. Instead, as an estimate, the wall insulation performance of all the office vertical walls was reduced by 20%.

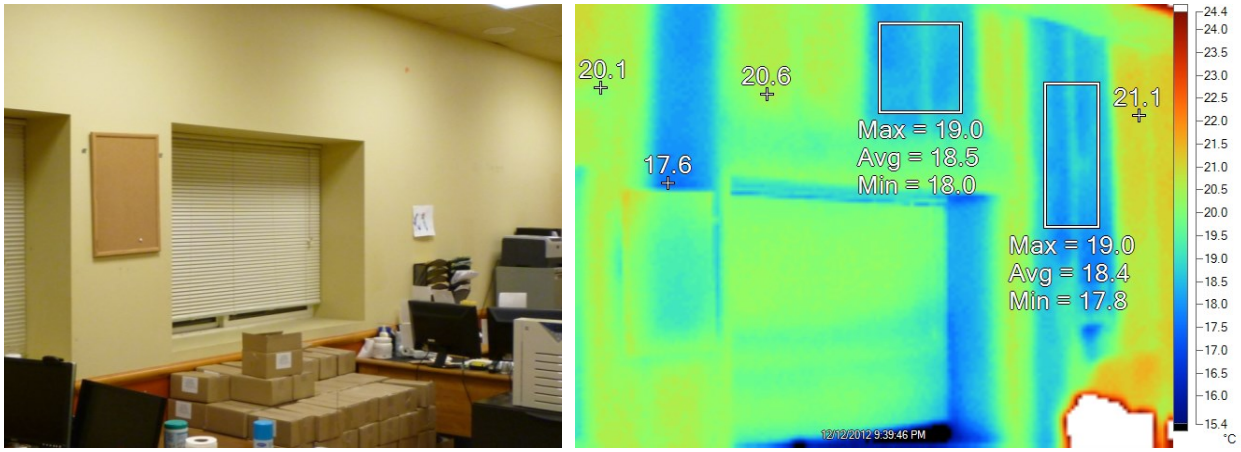

Figure 70 - Thermal and photo images of north Office wall

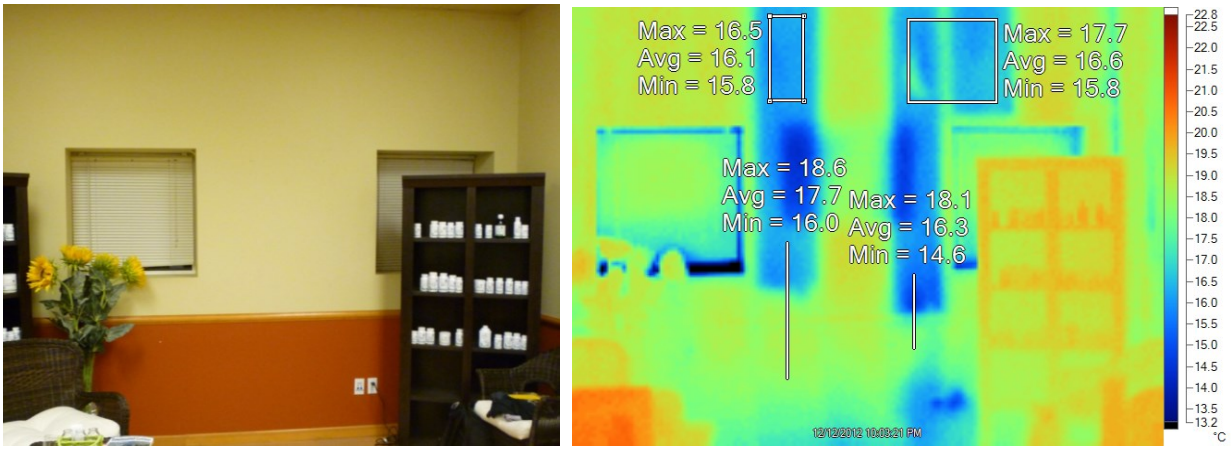

Figure 71 - Thermal and photo images of west Office wall

Figure 72 - Thermal and photo images of Office floor at north wall

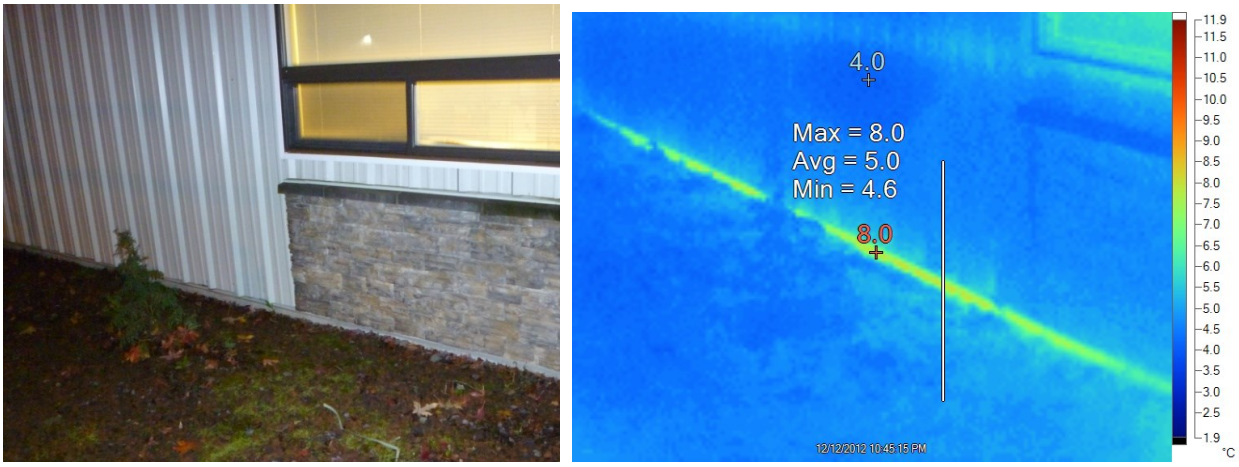

Figure 73 - Thermal and photo images of north exterior wall of Office at slab

These adjustments improved the calibration metrics to MBE 1.5% and CVRSME 38.4%, but as shown in Figure 74, still did not account for the large number of hours of elevated energy consumption below 10°C.

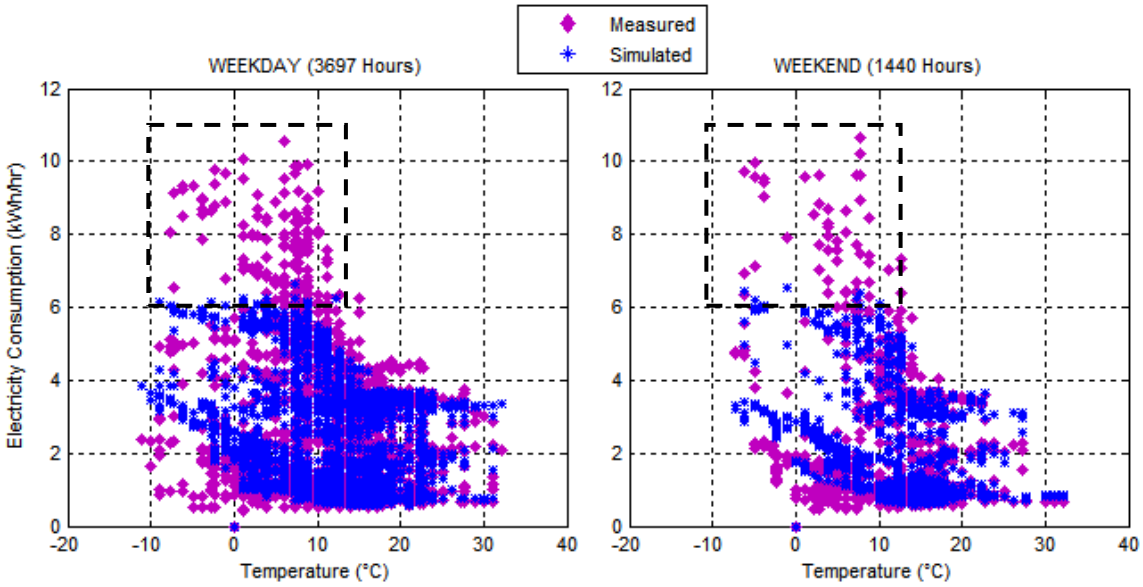

Figure 74 - Run 7 energy-OAT plot

6.3.6 Run 8: Office Thermostat Schedule

Closer inspection of DAQ time series data revealed the office temperatures measured during colder periods often spiked higher than the programmed thermostat set points. A thermostat controls the office heaters, and the thermostat was programmed per the owner's preferences at the start of the study. Despite this step, occupants still had the ability to adjust temperature set points as they pleased. Figure 75 illustrates the profile of the measured vs. simulated values for a representative time period, including the indoor/outdoor air temperatures and office heating energy consumption. The measured office temperatures were used to guide development of new heating setpoint schedules, summarized in Table 16.

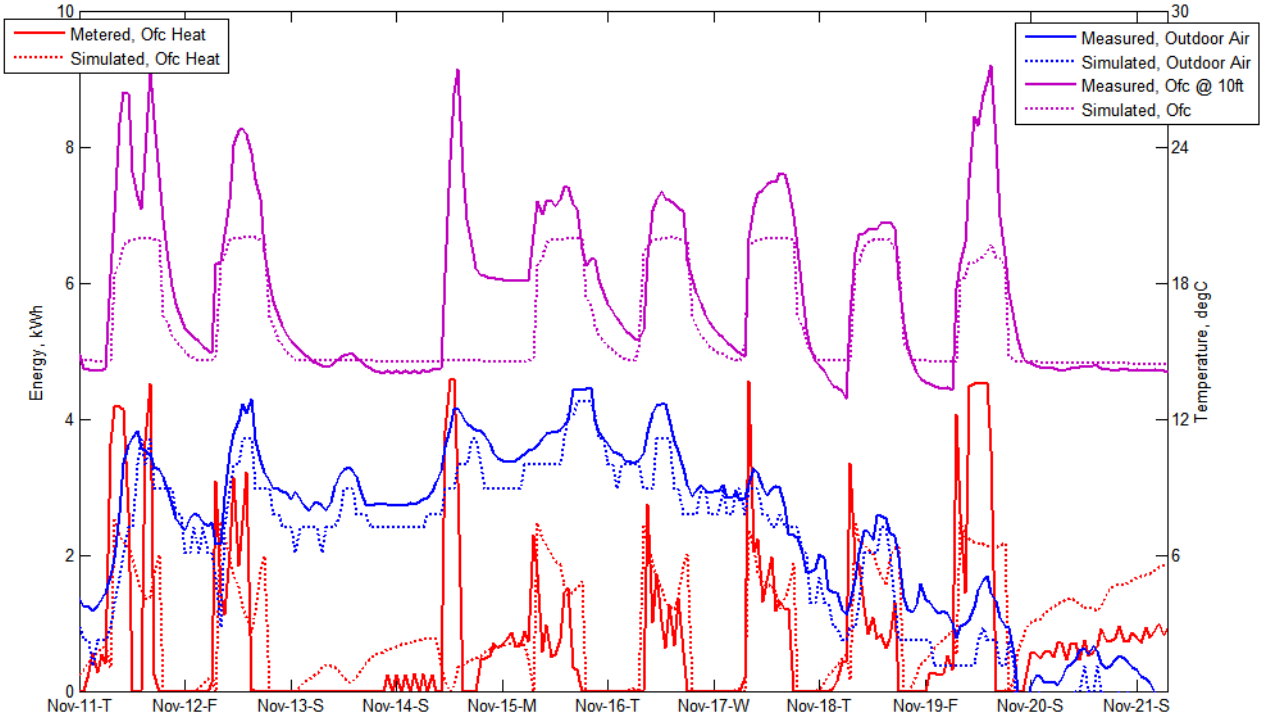

Figure 75 - Office heating energy and temperature profiles

Table 16 - Run 8 Office heating thermostat schedules

Original Thermostat Schedule Runs 1-7	New Thermostat Schedule Runs 8+
Entire period (6/1 – 12/31/10) WD: 7am-6pm = 68°F, setback to 58°F WEH = 58°F all hours	6/1 – 10/31/10) WD: 7am-6pm = 68°F, setback 58°F WEH = 58°F all hours 11/1 – 11/19/10) WD: 7am-6pm = 70°F, setback to 52°F WEH = 52°F all hours 11/20 – 12/31/10) WD: 7am-6pm = 75°F, setback to 52°F WEH = 52°F all hours

Implementing this schedule in the model decreased MBE and CVRSME to 0.6% and 35.5%, respectively. Figure 76 shows the revised hour APE end-use fraction plots, indicating model error during the last 2 months of the year has decreased, and the heating energy fraction increased by 3%. Figure 77 indicates the thermostat schedule adjustments account for a

large portion of the additional energy used below 10°C. However, there is still a void in simulated energy use above 8kW and below the 10°C.

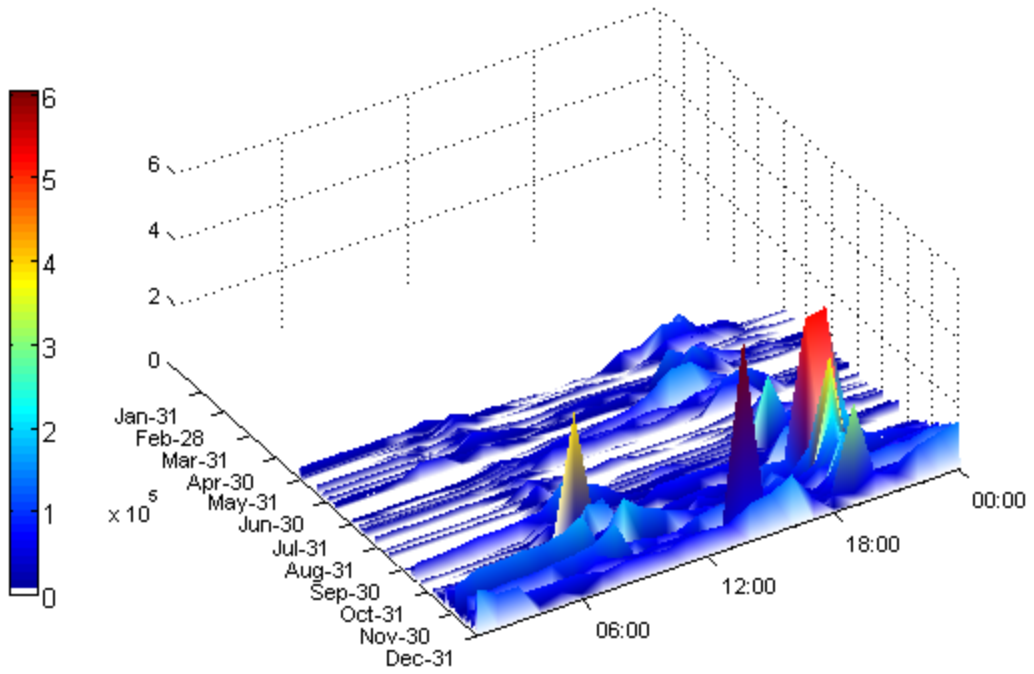

Figure 76 - Run 8 hourly APE and building end-use energy fractions

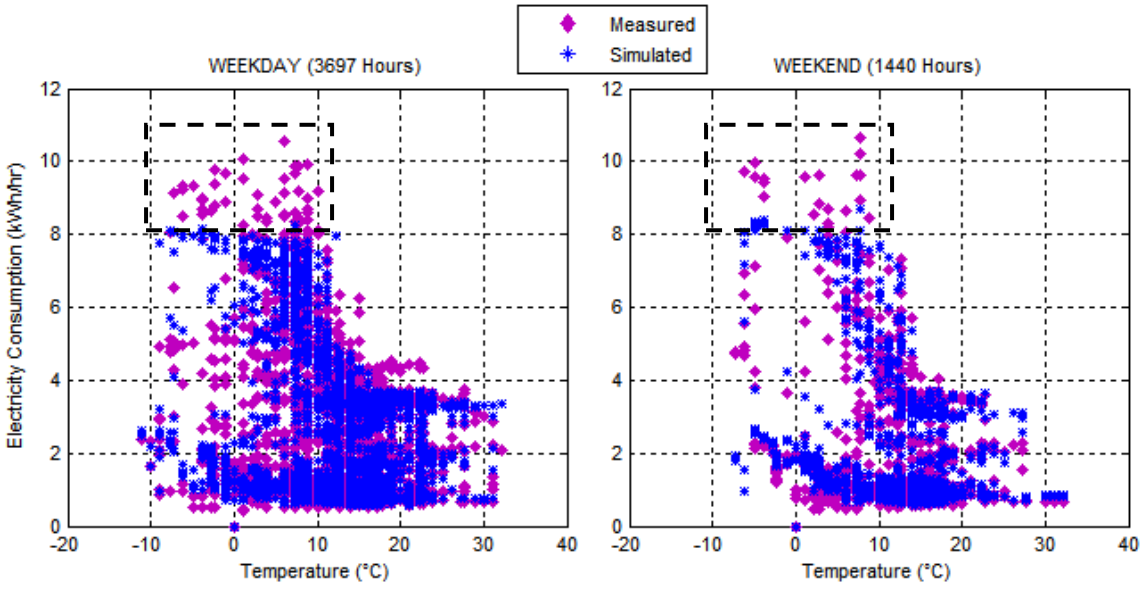

Figure 77 - Run 8 energy-OAT plot

6.3.7 Run 8.1-2: Infiltration Sensitivity Analysis

Up until this point of the modeling process, no adjustments to the building outdoor air infiltration rates and schedules had been made. The Wizard specification for "Loose", or 0.25 room air changes per hour (ACH) was assumed for simulation runs 0-8, which when combined with the annual weekday/weekend schedule multiplier specified by the Wizard, results in an average infiltration rate of ~0.26 ACH. With model calibration close to industry targets, a brief infiltration sensitivity analysis was performed to understand their impact on overall energy use, data scatter, and calibration metrics. For runs 8.1 and 8.2, the infiltration rate in all spaces was increased and decreased by 50%, respectively. Table 17 summarizes the calibration metrics for Runs 8.0 through 8.2. A ±50% change in the Wizard defined infiltration rate results in approximately a ±1% impact on building energy use over the calibration period, and CVRSME did not change substantially. This brief sensitivity analysis suggests infiltration rates do not explain the discrepancy below 10°C, and unless the office thermostat set points can be concretely defined for a portion of the calibration period, it is difficult to justify adjusting the rates outside these preliminary boundaries.

Table 17 - Run 8.0-8.2 infiltration rate adjustments

Run #	Run Title	Description	Statistics
8.0	Office Thermostat Schedule	Average infiltration rate of 0.26ACH	MBE = 0.6% CVRSME = 35.5%
8.1	Infiltration +50%	Infiltration rates increased from 0.26ACH to 0.39ACH.	MBE = -0.7% CVRSME = 35.8%
8.2	Infiltration -50%	Infiltration rates decreased from 0.26ACH to 0.13ACH.	MBE = 2.0% CVRSME = 35.5%

To this point, the plot of building energy as a function of outdoor air temperature has been an important tool for visualizing the measured vs. simulated performance. Given the unknown discrepancy in energy use, it was decided to use the same visualization method to evaluate the Office heating energy as a function of OAT (see Figure 78). It was found the

measured data were more scattered, though the relative magnitude and trend predicted by the simulation is similar. Since the office heater load is likely the most significant, temperature dependent load in the building, this clue pointed to another temperature dependent load outside the context of the Office.

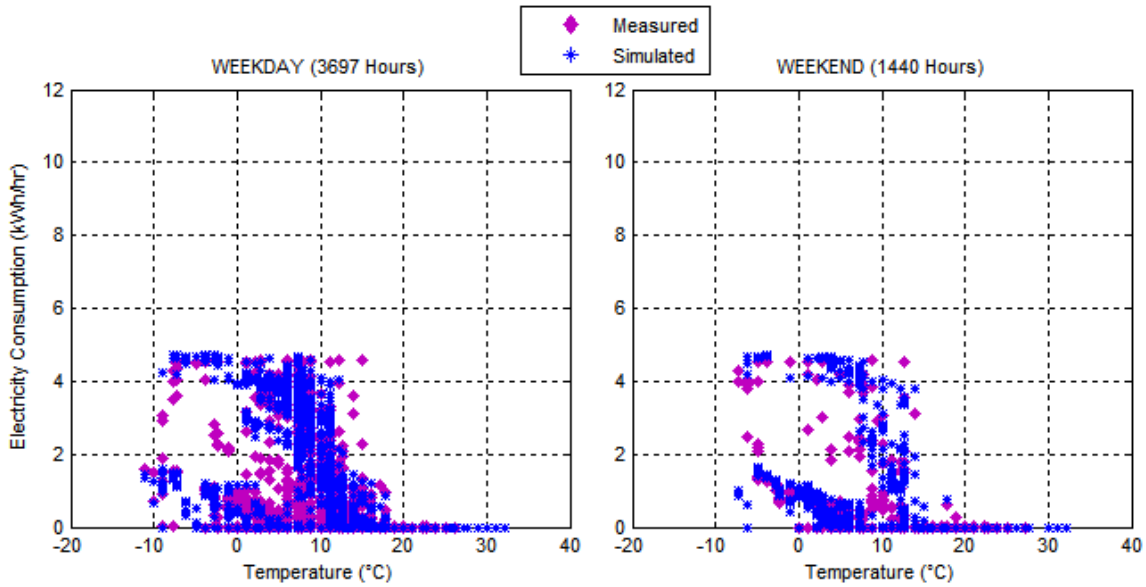

Figure 78 - Run 8 Office heating energy-OAT plot

6.3.8 Run 9: Warehouse Heating

In addition to office occupants adjusting the thermostat heating setpoint, another important building variable was identified and believed to contribute to the energy discrepancy below 10°C. After beginning this study, a 2kW electric radiant panel heater was installed over the warehouse packing station (see Figure 79). The heater is turned ON using a manual switch located near the center of the East Warehouse space. The maximum timer setpoint is 15 minutes, meaning occupants can run the heater for no longer than 15 minutes before they have to restart the timer.

Figure 79 - Picture of radiant heaters mounted over the E Warehouse packing area

The warehouse heater was not sub-metered, and given its manual control, there was no direct information upon which to base model inputs/adjustments. Since higher building loads were only observed below 10°C, the model was updated to include a 2KW heater in the warehouse space, modeled to turn ON every other hour during normal working hours when the warehouse space temperature was below 8.9°C (48°F). Compared to Run 8, this revision did account for a change in the calibration metrics (MBE -0.7%, CVRSME 36.7%), including a slight increase in the CVRSME. However, it did augment the distribution of simulated energy use in the range identified below 10°C and above 8 kWh/hr (see Figure 80).

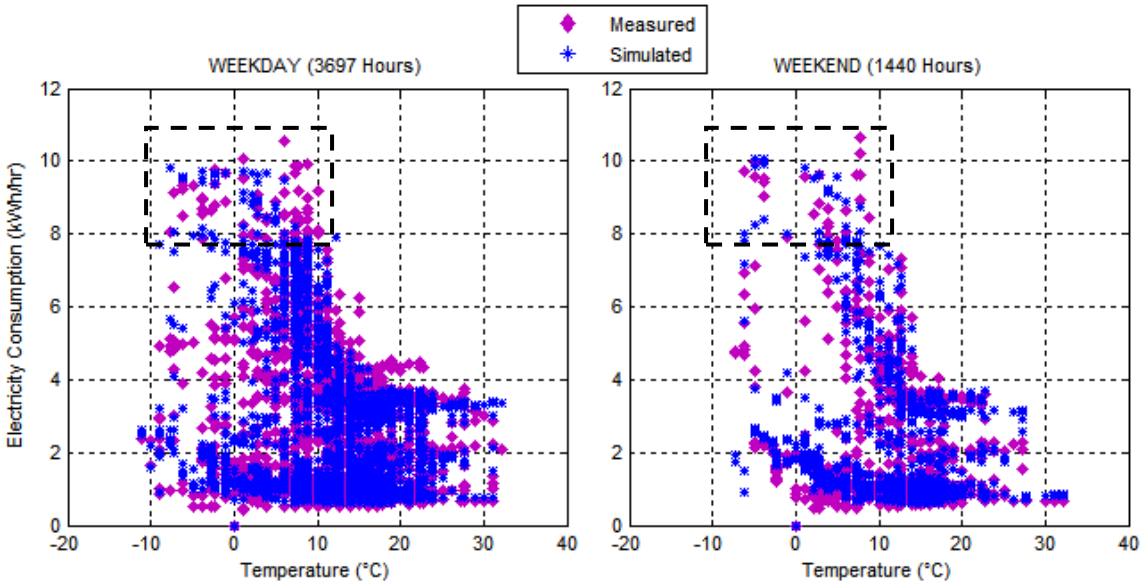

Figure 80 - Run 9 energy-OAT plot

6.3.9 Run 10: DOE-2 Domestic Hot Water Heating

Since Run 5, the domestic hot water heating (DHW) energy was simulated using the sub-metered hourly energy use of the heater, rather than relying on the DOE-2 water heating model. Prior to re-implementing the DOE-2 DHW model, the modeled DHW energy use of the original Wizard model was compared to the DAQ measured values using a time series plot (Figure 81). The Wizard weekday hourly DHW load results in roughly 2-3 times more electrical energy use than the actual sub-meter information showed. The load is also quite intermittent, as would be expected for a small office building with only 3-5 people. The time-series plot also shows the night and weekend energy use is lower than measured, indicating the original Wizard default tank stand-by losses are less than the actual heater performance.

Using this information, the DHW design load, usage schedule, and tank standby losses were modified to mimic the DAQ measured profile and total heater energy use as close as possible. Table 18 summarizes the Wizard default inputs and the revised values. Using the

DOE-2 model and the new model parameters, the energy profile during both peak and off-peak hours matched reasonably well (see Figure 82), and the measured and simulated DHW heating energy for the metering period were the same (159 kWh). Calibration metrics changed slightly, MBE -0.8% and CVRSME 36.7%, indicating the DOE-2 model and inputs values are an acceptable approximation of the heater performance. Finally, Figure 83 summarizes the monthly building end-use energy and fractions for reference to earlier simulation runs.

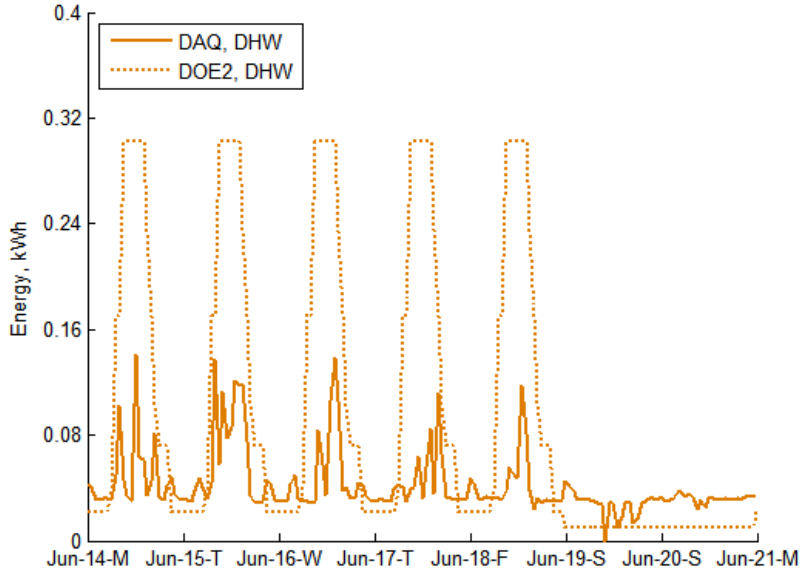

Figure 81 - Run 0-4 (Wizard) DHW load profile compared to actual sub-metered data

Table 18 - Run 10 DHW model inputs

Original (Wizard) DHW Inputs Runs 0-4	Revised DHW Inputs Runs 10+
Tank Setpoint = 135°F Tank Volume = 6 gallons Heating Efficiency = 100% Design Load = 1.62 gal/hr WD full load hours = 9.05 WEH full load hours = 0.36 Tank heat loss (UA) = 0.25 Btu/hr-°F	Tank Setpoint = 135°F Tank Volume = 6 gallons Heating Efficiency = 100% Design Load = 0.64 gal/hr WD full load hours = 2.70 WEH full load hours = 0 Tank heat loss (UA) = 1.63 Btu/hr-°F

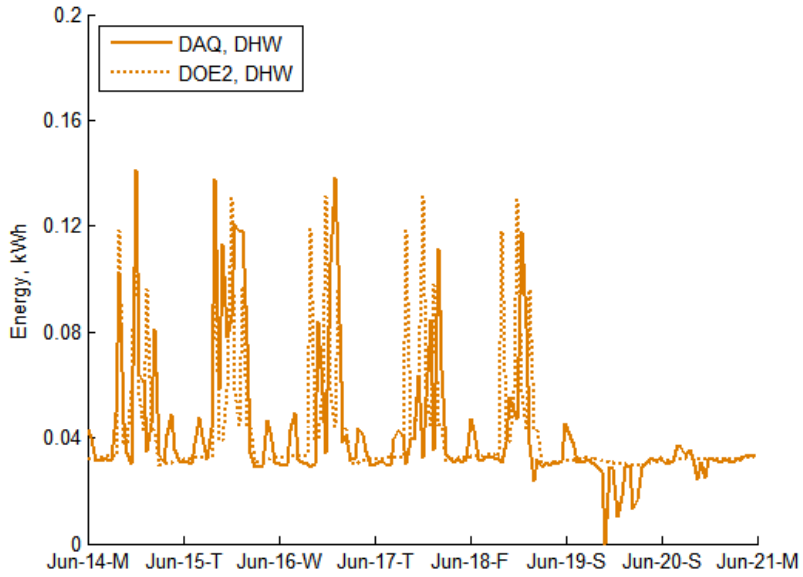

Figure 82 - Run 10+ (Revised) DHW load profile compared to actual sub-metered data

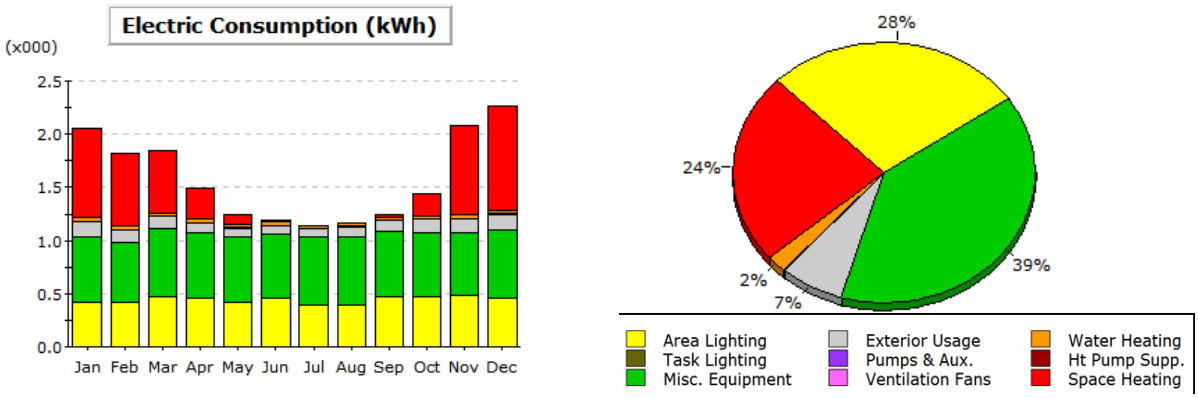

Electric Consumption (kWh x000)

	Jan	Feb	Mar	Apr	May	Jun	Jul	Aug	Sep	Oct	Nov	Dec	Total
Space Cool	-	-	-	-	-	-	-	-	-	-	-	-	-
Heat Reject.	-	-	-	-	-	-	-	-	-	-	-	-	-
Refrigeration	-	-	-	-	-	-	-	-	-	-	-	-	-
Space Heat	0.83	0.68	0.58	0.29	0.09	0.02	0.00	0.00	0.02	0.20	0.84	0.98	4.55
HP Supp.	-	-	-	-	-	-	-	-	-	-	-	-	-
Hot Water	0.04	0.03	0.04	0.03	0.03	0.03	0.03	0.03	0.03	0.03	0.03	0.04	0.39
Vent. Fans	0.00	0.00	0.00	0.00	0.00	0.00	0.00	0.00	0.00	0.00	0.00	0.00	0.02
Pumps & Aux.	-	-	-	-	-	-	-	-	-	-	-	-	-
Ext. Usage	0.14	0.12	0.11	0.09	0.08	0.07	0.08	0.09	0.10	0.12	0.13	0.15	1.31
Misc. Equip.	0.62	0.57	0.64	0.61	0.62	0.61	0.64	0.65	0.62	0.60	0.59	0.64	7.39
Task Lights	-	-	-	-	-	-	-	-	-	-	-	-	-
Area Lights	0.42	0.41	0.48	0.46	0.42	0.46	0.39	0.39	0.47	0.47	0.48	0.46	5.32
Total	2.05	1.82	1.84	1.49	1.24	1.19	1.14	1.16	1.24	1.43	2.08	2.27	18.98

Figure 83 - Run 10 monthly building end-use energy and fractions

As another evaluation of calibration, Figure 84 illustrates the relative linear correlation between measured and simulated energy use on weekday and weekend days.

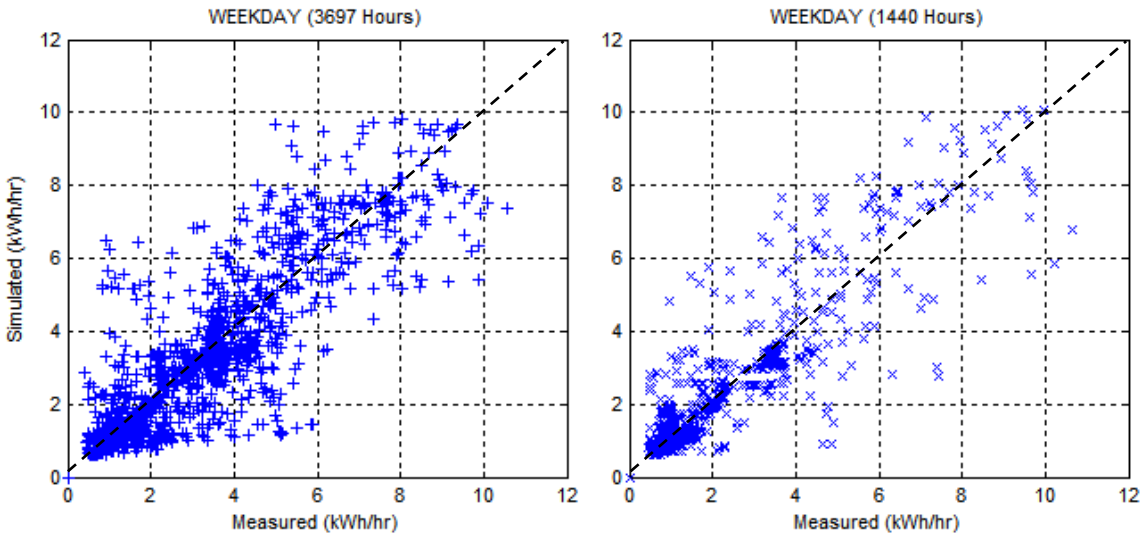

Figure 84 - Scatter plot of measured vs. simulated energy use for Run 10

6.3.10 Discussion of Results for Runs 0-10

At this point in the study, it became clear that improving the calibration metrics likely would require additional processing of the measured data. The hourly calibration metrics for the Runs 0-10 are summarized in Table 19, and metrics for Runs 1-10 are plotted in Figure 85. Both include the MBE and CVRSME for the entire calibration period (All), as well as the sub-metering period (Mtr). Run 10 time-series plots of office temperature and heating power indicate the schedules implemented in Run 8 improved predictions on some days, but could not account for occupants frequently manipulating the space heating setpoint; the likely principal source of model error. This emphasizes the importance of either controlling HVAC system set points, or monitoring them to incorporate additional detail into calibrated models.

Table 19 - Summary of hourly calibration statistics for Runs 0-10

Title	Run	MBE - All	CVRSME - All	MBE - Mtr	CVRSME - Mtr
Wizard Model	0	-54.8%	114.4%	-57.1%	120.0%
Audit LPDs	1	19.8%	47.3%	19.1%	46.8%
Audit Wall Types	2	17.5%	46.7%	17.0%	46.6%
Audit Windows	3	17.7%	46.8%	17.2%	46.7%
Audit Occupancy	4	18.0%	46.8%	17.4%	46.7%
Sub-Metered Schedules	**5**	**2.9%**	**38.9%**	**1.9%**	**36.0%**
Ofc Wall Insulation -20%	6	1.9%	38.7%	1.0%	35.9%
Ofc Floor Insulation -20%	7	1.5%	38.5%	0.6%	35.8%
Ofc TStat Schedule	8	0.6%	35.5%	0.2%	33.2%
Warehouse Heating	9	-0.8%	36.7%	-1.1%	34.4%
DOE-2 DHW	10	-0.8%	36.7%	-1.1%	34.4%

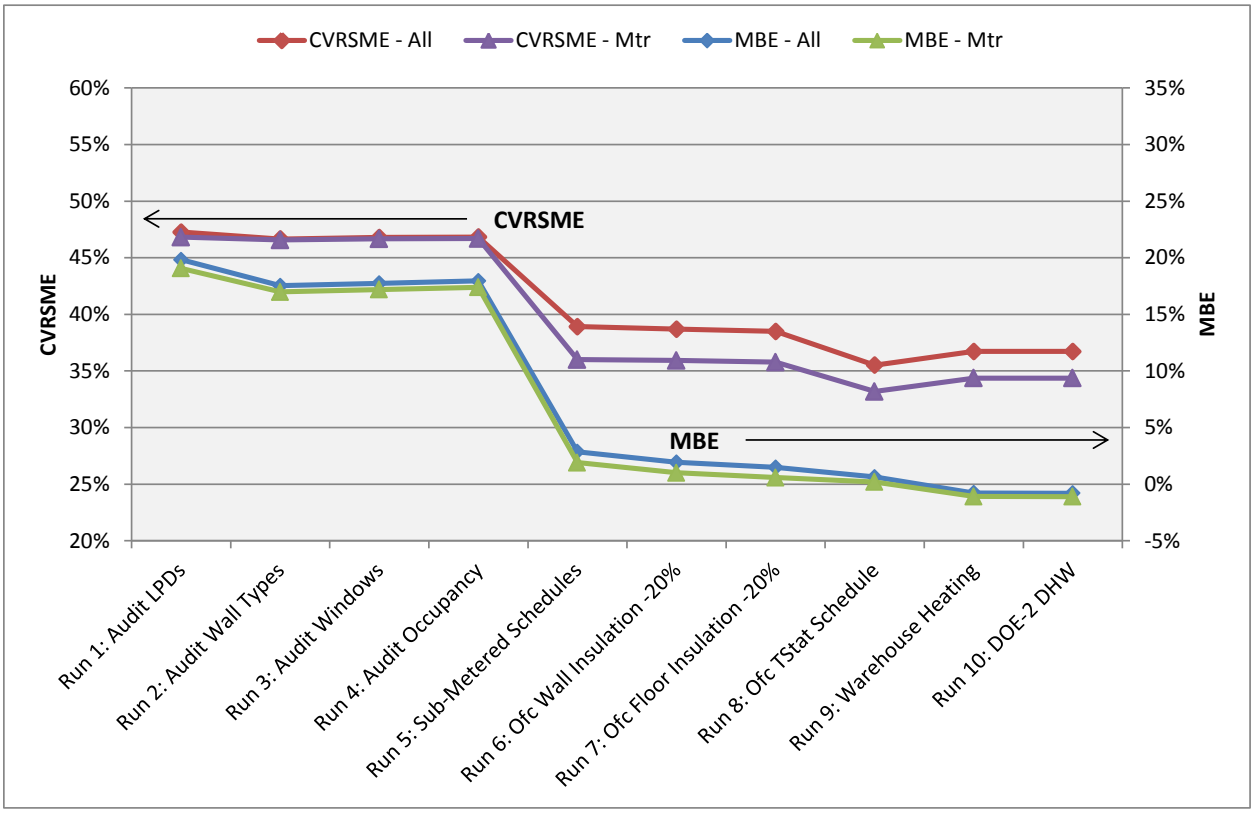

Figure 85 - Plotted hourly calibration statistics for Runs 1-10

The integration of electrical data processed using the methods described in this study did indeed result in a large step change improvement of calibration metrics. Using additional evidence gathered from interior space temperature measurements led to the next largest improvements in calibration. The results of additional infiltration sensitivity runs 9.1 and

9.2 suggest the modeled infiltration rate may be less than the assumed 0.25 ACH. However, without better definition of actual office heating set points and other unmetered loads, no definitive conclusions could be made. Though "turning knobs" on model parameters was useful to understanding the sensitivity of model parameters, the step-wise integration of measured and observed evidence proved to steadily advance calibration.

Inspecting the results for Run 10, the final CVRSME metric fell short of the 30% calibration target, yet from Run 5 and beyond, the MBE was well within the established target. To determine model calibration outside the influence of occupants changing heating set points, the calibration period was shortened to the months of year when demand for space heating was less. Table 20 summarizes the calibration metrics for four periods, varying in length from four months to seven months (the full period defined for the study).

Table 20 - Summary of calibration statistics for

Period Start	Period End	Calibration Statistics (All)	Calibration Statistics (Mtr)
6/1/2010	9/30/2010 (4 months)	MBE = 2.7% CVRSME = 19.2%	MBE = 3.2% CVRSME = 15.7%
	10/31/2010 (5 months)	MBE = 2.3% CVRSME = 23.1%	MBE = 2.6% CVRSME = 21.7%
	11/30/2010 (6 months)	MBE = 0.8% CVRSME = 32.2%	MBE = 0.5% CVRSME = 32.2%
	12/31/2010 (7 months)	MBE = -0.8% CVRSME = 36.7%	MBE = -1.1% CVRSME = 34.4%

The results illustrate that the model achieved calibration targets through October 2010, and suggests that if data were available to better quantify the set points of the heating systems, model calibration for the complete period could be improved. Using information acquired in this study, one proposed approach would be to correlate variables believed to be directly or indirectly proportional to system set points (space temperature, time of day/week, light switching behavior, etc.), and generate custom office and warehouse system availability and thermostat schedules. Unfortunately, development and implementation of this additional

model detail could not be completed in the timeframe of this study, leaving Run 10 as the last model iteration intended to improve model calibration.

Figure 86 illustrates the change in annual building end-use energy predictions for Runs 0 through 10, while Figure 87 shows the end-use fractions for key calibration milestones in the study. It is clear that conclusions on end-use energy fractions changed significantly with the incorporation of the model schedules based on disaggregated electrical data. The interactive effect of lighting and receptacle equipment energy on space heating systems is similar, so the correct distribution of these fractions might never have been realized if not for the detailed monitoring. Though not included in the scope of this study, the predictions on the impact of energy efficiency measures targeting these end-uses would have likely yielded different conclusions, and subsequently misled a design team and the owner from selecting measures with the highest impacts.

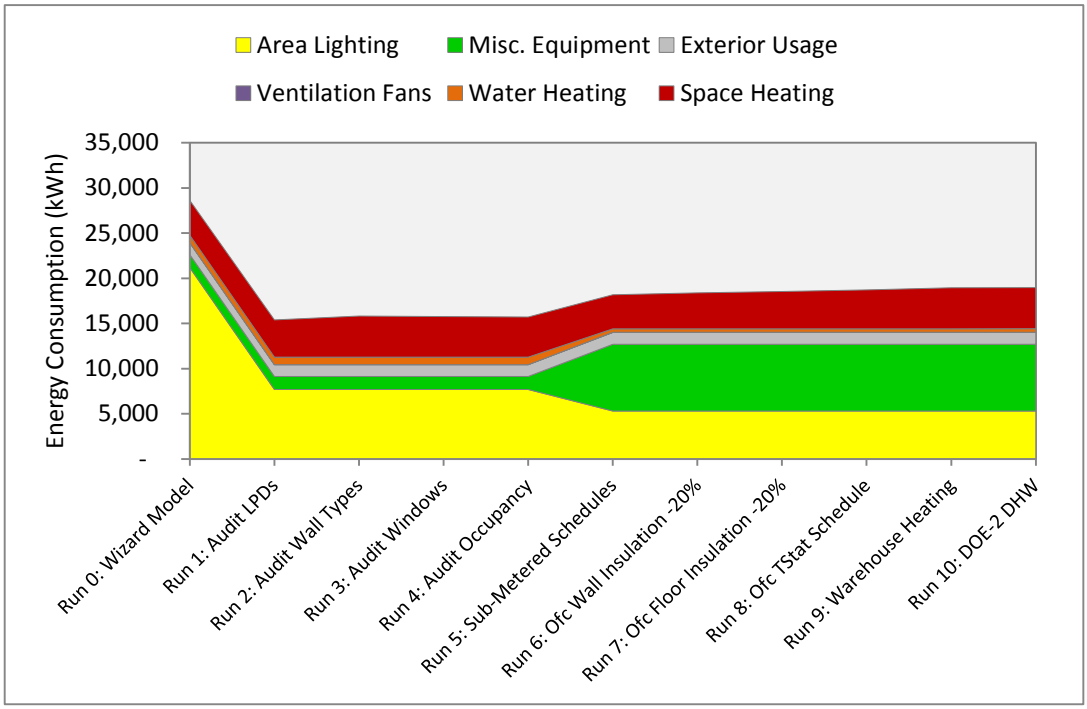

Figure 86 - Individual end-use energy components for Runs 0-10

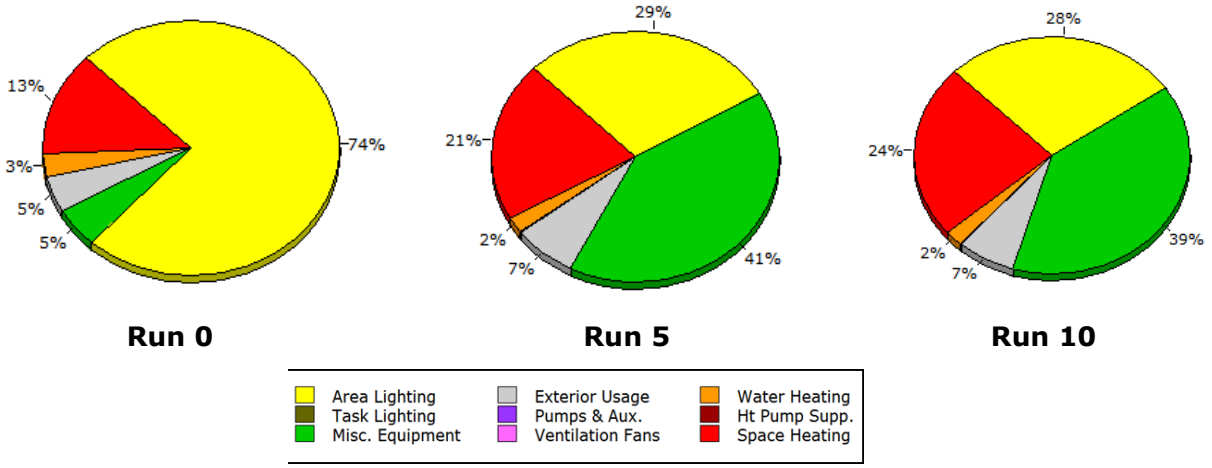

Figure 87 - End-use energy fractions for Runs 0, 5, and 10

6.4 Weather Files and Average Day Schedules

After Run 10, attention was turned to evaluating the impact of other previously defined assumptions, such as weather files and the detail used to define driving inputs.

For reference in the following discussions on weather files, Table 21 summarizes a few key statistics calculated for the different weather sources.

Table 21 - Summary of weather file statistics

	360ZH1	WxA[5]	TMY3
Heating Degree Hours/Day (Base 65)	5178	5223	5914
Cooling Degree Hours/Day (Base 65)	143	157	143.5
Average Daily Solar Radiation (Btu/ft2/day)	Global = 1005 Direct = 968	Global = 1096 Direct = 1114	Global = 1047 Direct = 980
Average Wind Speed (mph)	6.7	6.7	7.3

6.4.1 Run 11: WxA Weather File

Simulation Run 11 utilized the WxA weather file (described in Chapter 4). The use of the WxA weather file resulted in a slight change in the calibration metrics; MBE decreased from -0.8% to 0.1%, CVRSME increased from 36.7% to 37.6%. Building heating energy increased by 5%, likely explained by the slightly higher heating degree hours. Nonetheless, the overall results are comparable with the custom weather file developed for this study.

6.4.2 Run 12: TMY3 Weather File

In addition to evaluating the WxA weather file, the readily available TMY3 weather file for Bellingham International Airport was also simulated. The heating energy increased by 30%, indicative of the higher heading degree hours and average wind speed. Expectedly, the

[5] The WxA weather summary file provides values in SI units (18°C base). For consistency with DOE-2 .bin weather file statistics, these values were calculated using hourly DOE-2 outputs in IP units.

calibration metrics were worse; MBE increased from -0.8% to -3.2%, CVRSME increased from 36.7% to 40.7%.

6.4.3 Run 13: Average Day Schedules

The last run of this study focused on evaluating the impact of using "average" day schedules developed from the sub-metered data. In this case, the average day schedules were developed from a large subset of metered information. However, the mean daily schedule profiles were largely unchanged by increasing the dataset. Therefore, if only a few weeks of sub-meter data were available to generate a description of the dynamic model inputs, it was inferred that model calibration would not dramatically suffer. Indeed, the use of the average profiles did affect model calibration; MBE reduced from -0.8% to -0.5%, and CVRSME increased from 37.6% to 39.6%. However, this result suggests short-term sub-metering provides valuable input to the model calibration process. It is likely the duration of monitoring is dependent on variability in building operations throughout a year, and for buildings with regular seasonal changes in operation, the development of average schedules for different periods may be critical to improving model calibration.

6.5 Results Summary

Table 22 through Table 24 summarize the calibration metrics for hourly, daily, and monthly periods for both the entire calibration period (All) and the hours where sub-metered data were available (Mtr). A noteworthy result is monthly metrics for model Run 5 and subsequent model runs are within the specified uncertainty targets.

Table 22 - Summary of hourly calibration statistics

Title	Run	MBE - All	CVRSME - All	MBE - Mtr	CVRSME - Mtr
Wizard Model	0	-54.8%	114.4%	-57.1%	120.0%
Audit LPDs	1	19.8%	47.3%	19.1%	46.8%
Audit Wall Types	2	17.5%	46.7%	17.0%	46.6%
Audit Windows	3	17.7%	46.8%	17.2%	46.7%
Audit Occupancy	4	18.0%	46.8%	17.4%	46.7%
Sub-Metered Schedules	**5**	**2.9%**	**38.9%**	**1.9%**	**36.0%**
Ofc Wall Insulation -20%	6	1.9%	38.7%	1.0%	35.9%
Ofc Floor Insulation -20%	7	1.5%	38.5%	0.6%	35.8%
Ofc TStat Schedule	8	0.6%	35.5%	0.2%	33.2%
Run 8 -> Infiltration +50%	8.1	-0.7%	35.8%	-1.2%	33.7%
Run 8 -> Infiltration -50%	8.2	2.0%	35.5%	1.6%	33.0%
Warehouse Heating	9	-0.8%	36.7%	-1.1%	34.4%
Run 9 -> Infiltration +50%	9.1	-2.1%	37.2%	-2.5%	35.0%
Run 9 -> Infiltration -50%	9.2	0.6%	36.5%	0.3%	34.0%
DOE-2 DHW	10	-0.8%	36.7%	-1.1%	34.4%
WxA Weather File	11	0.1%	37.6%	0.0%	35.1%
TMY3 Weather File	12	-3.2%	40.7%	-3.0%	39.9%
Average Day Schedules	13	-0.5%	39.6%	-0.6%	38.9%

Table 23 - Summary of daily calibration statistics

Title	Run	MBE - All	CVRSME - All	MBE - Mtr	CVRSME - Mtr
Wizard Model	0	-54.8%	77.6%	-57.1%	93.8%
Audit LPDs	1	19.8%	27.9%	19.1%	32.1%
Audit Wall Types	2	17.5%	26.5%	17.0%	31.0%
Audit Windows	3	17.8%	26.7%	17.2%	31.1%
Audit Occupancy	4	18.0%	26.8%	17.4%	31.3%
Sub-Metered Schedules	**5**	**2.9%**	**18.1%**	**1.9%**	**19.3%**
Ofc Wall Insulation -20%	6	1.9%	17.9%	1.0%	19.4%
Ofc Floor Insulation -20%	7	1.5%	17.8%	0.6%	19.3%
Ofc TStat Schedule	8	0.6%	13.7%	0.2%	15.5%
Run 8 -> Infiltration +50%	8.1	-0.7%	13.9%	-1.2%	16.1%
Run 8 -> Infiltration -50%	8.2	2.0%	13.8%	1.6%	15.3%
Warehouse Heating	9	-0.8%	14.0%	-1.1%	16.0%
Run 9 -> Infiltration +50%	9.1	-2.1%	14.7%	-2.5%	17.2%
Run 9 -> Infiltration -50%	9.2	0.6%	13.6%	0.3%	15.3%
DOE-2 DHW	10	-0.8%	14.0%	-1.1%	16.0%
WxA Weather File	11	0.1%	14.5%	0.0%	16.4%
TMY3 Weather File	12	-3.2%	18.5%	-3.0%	22.7%
Average Day Schedules	13	-0.5%	16.4%	-0.6%	20.1%

Table 24 - Summary of monthly calibration statistics

Title	Run	MBE - All	CVRSME - All	MBE - Mtr	CVRSME - Mtr
Wizard Model	0	-54.5%	55.1%	-57.1%	41.1%
Audit LPDs	1	19.9%	20.3%	19.1%	14.2%
Audit Wall Types	2	17.6%	18.0%	17.0%	13.1%
Audit Windows	3	17.8%	18.2%	17.2%	13.2%
Audit Occupancy	4	18.1%	18.4%	17.4%	13.3%
Sub-Metered Schedules	**5**	**2.9%**	**3.6%**	**1.9%**	**2.0%**
Ofc Wall Insulation -20%	6	2.0%	2.9%	1.0%	2.3%
Ofc Floor Insulation -20%	7	1.5%	2.7%	0.6%	2.4%
Ofc TStat Schedule	8	0.7%	3.0%	0.2%	2.9%
Run 8 -> Infiltration +50%	8.1	-0.6%	3.8%	-1.2%	3.6%
Run 8 -> Infiltration -50%	8.2	2.0%	3.0%	1.6%	2.7%
Warehouse Heating	9	-0.7%	4.8%	-1.1%	4.0%
Run 9 -> Infiltration +50%	9.1	-2.1%	6.1%	-2.5%	5.1%
Run 9 -> Infiltration -50%	9.2	0.6%	3.8%	0.3%	3.3%
DOE-2 DHW	10	-0.8%	4.8%	-1.1%	4.0%
WxA Weather File	11	0.1%	5.4%	0.0%	4.5%
TMY3 Weather File	12	-3.2%	6.9%	-3.0%	4.7%
Average Day Schedules	13	-0.4%	4.6%	-0.6%	3.6%

7 Conclusions and Recommendations

This thesis documents an approach to utilize energy and other measured data to improve the calibration of a whole building energy model. Each chapter documents important steps of the process, and provides building energy analysts with insight on how to use this information to improve modeling assumptions, and hence energy model predictions.

7.1 Study Conclusions

Principal conclusions and observations of this study include:

- A detailed and accurate description of dynamic model inputs appears to be the most influential factor affecting energy model calibration. This includes metering of systems dependent on occupant behavior, including manually controlled lighting, receptacle-based equipment, and HVAC set points.
- Envelope and other static characteristics of a building are important information for calibrating models, but when building energy use is predominantly driven by occupant behavior, has a smaller impact on model calibration than driving inputs.
- The availability of energy sub-metering and space temperature measurement is important for a structured, evidence-based approach to improving model calibration.
- The use of current sub-metering, combined with spot measurements of power and 15-minute utility interval data, provides a reasonable estimate of electrical energy. The accuracy of this approach may be undermined for loads with larger variations in power factor, but given the reduced cost of the metering systems, is a worthy consideration.
- Average energy model load and schedule profiles for lighting and receptacle energy end-uses, based on detailed, short-term monitoring, can potentially be an acceptable substitute to long-term monitoring. This observation is assumed to primarily apply to buildings with regular operations, though, average profiles that cover the range of

irregular operations may be acceptable provided there is a way to define when alternate operation schedules should be used.

- A complete evaluation of weather information and its impact on model calibration was not in the scope of this study. However, it appears NCDC weather observations and the use of the Zhang-Huang solar model tailored to local conditions is acceptable and comparable to a commercially available weather file. Proximity to the NCDC/TMY station sites is also assumed a limiting factor.

7.2 Lessons Learned

A "learn by doing" philosophy was taken in gathering and processing information for this study. Though not necessary expanding on the existing knowledge base, many practical lessons were learned. A few important considerations include:

- Data visualization methods, specifically time-series, scatter, and surface plots of monitoring data are critical to integrating monitoring into the energy modeling process. Visualizing information is important for both quality control and for guiding the adjustment of model parameters.
- Archiving software and energy model development using version control is highly recommended. If multiple changes to simulation input are made between iterations, unexpected results can be sometimes occur. The ability to compare the current working revision with past revisions (typically using a text file comparison tool) helps find the root cause of unexpected results quickly.
- In any metering application, it is highly recommended the correct, local standard time always be used and confirmed each time data logging is initiated. Accounting for daylight savings and other time offsets can add significant time to post-processing, and can often be the root cause for incorrect results.
- Most energy models schedules describe alternate conditions for weekday, weekends, and holidays. However, it was observed that occupancy and related energy use

consistently varied on days before and after holidays. On these days when sub-metering was not performed, the assumed average day profiles were the source of significant error. Therefore, when non-continuous data logging is performed, it is recommended that separate profiles for these days be developed.

8 References

Akbari H. 1995. Validation of an algorithm to disaggregate whole-building hourly electrical load into end uses. *Energy* 20:2291-1301.

Armal K., A. Gupta, G. Shrimali, and A. Albert. 2013. Is disaggregation the holy grail of energy efficiency? The case of electricity. *Energy Policy* Vol. 52(C): 213-234.

ASHRAE. 2002. *ASHRAE Guideline 14-2002, Measurement of Energy and Demand Savings*. Atlanta: American Society of Heating, Refrigerating and Air-Conditioning Engineers, Inc.

Bandari M. and S. Shrestha. 2012. Evaluation of weather datasets for building energy simulation. *Energy and Buildings* 49:109-119.

Black T. 2012. Derivations of Applied Mathematics [Internet]. [cited 2013 March 18]. Available from: http://www.derivations.org/derivations.pdf

Bleeker N., and W. Veenstra. 1990. The performance of four foot fluorescent lamps as a function of ambient temperature on 60Hz and high frequency ballasts. *IESNA Annual Conference*, Baltimore (MD).

Buhl F. 1999. DOE-2 Weather Processor. LBNL Simulation Research Group.

California Energy Commission (US). 2008. Nonresidential Compliance Manual [Internet]. [cited 2013 March 18]. Available from: http://www.energy.ca.gov/2008publications/CEC-400-2008-017/CEC-400-2008-017-CMF-REV1.PDF

Chang, W.K., and T. Hong. 2013. Statistical analysis and modeling of occupancy patterns in open-plan offices using measured lighting-switch data. LBNL-6080E. Lawrence Berkeley National Laboratory, Berkeley (CA).

Department of Energy (US). 2011. 2010 Buildings Energy Data Book [Internet]. [cited 2013 March 18]. Available from: http://buildingsdatabook.eren.doe.gov/docs%5CDataBooks%5C2010_BEDB.pdf

Department of Energy (US). 2012. EnergyPlus v7.2. Engineering Reference and Auxiliary Programs, Weather Converter Program documentation

DView [Internet]. Mistaya Engineering Inc. c2012. [cited 2013 March 18]. Available from: http://www.mistaya.ca/software/dview.htm

Diamond R., M. Opitz, T. Hicks, B. Von Neida, and S. Herrra. 2006. Evaluating the energy performance of the first generation of LEED-certified commercial buildings. *Proceedings of the ACEEE 2006 Summer Study*, Pacific Grove (CA), August 13-18..

Duffie J., and W. Beckman. 2006. Solar Engineering of Thermal Processes. 3rd Edition. New Jersey: J. Wiley. 908 p.

Froelich J, E. Larsen, S. Gupta, G. Cohn, M. Reynolds, and S. Patel. 2011. Disaggregated End-Use Energy Sensing for the Smart Grid. *IEEE Pervasive Computing* 10:28-39.

Hart G.W. 1992. Nonintrusive appliance load monitoring. *Proceedings of the IEEE*, Vol. 80(12):1870-91.

Haberl J., and C. Cho. 2004. Literature review of uncertainty of analysis methods (DOE-2 program), ESL-TR-04/11-01, Energy Systems Laboratory Texas A&M University System.

Historical Weather [Internet]. c2013 Weather Undergound, Inc. [cited 2013 March 18]. Available from: http://www.wunderground.com/

Hubler D., K. Tupper, and E. Greensfelder. 2010. Pulling the levers on existing building: A simple method for calibrating hourly energy models. *ASHRAE Transactions* 116(2): 261-268.

Integrated Surface Database. [Internet] National Climatic Data Center (US). [cited 2013 March 18]. Available from: http://www.ncdc.noaa.gov/oa/climate/isd/index.php

James J. Hirsch and Associates. 2010. eQUEST v3.64 Wizard Help Documentation [Internet]. [cited 2013 March 18]. Available from: http://doe2.com/download/equest/eQ-v3-64_Introductory-Tutorial.pdf

Lawrence Berkely National Laboratory, James J. Hirsh And Associates. 2004-2009. DOE-2.2 Building Energy Use and Cost Analysis Program Manuals. Volumes 1-6. Available from: http://doe2.com/DOE2/

Long N. 2006. Real-Time Weather Data Access Guide. NREL/BR-550-34303. National Renewable Energy Laboratory, Golden, CO.

Maile T, V. Basjanac, J. O'Donnell, and M. Garr. 2011. A software tool to compare measured and simulated building energy performance data. *Proceedings of Building Simulation,* Sydney, Australia, Nov 14-16, p. 2341-2347.

Marion W., and K. Urban. 1995. User's Manual for TMY2s. National Renewable Energy Laboratory, Golden, CO.

Mazzuchi R. 1992. End-use profile development from whole-building data combined with intensive short-term monitoring. *ASHRAE Transactions* 98(1), paper number AN-92-15-5, 1180-1184.

Meteorological Assimilation Data Ingest System [Internet]. National Oceanic and Atmospheric Administration. [cited 2013 March 18]. Available from: http://madis.noaa.gov/index.html

Newsham G.R., S. Mancini, and Birt B.J. 2009. Do LEED-certified buildings save energy? Yes, but... *Energy and Buildings* 41: 897–905.

Norford L., and S. Leeb. 1996. Non-intrusive electrical load monitoring in commercial buildings based on steady-state and transient load-detection algorithms, *Energy and Buildings* 24:51-64.

Pacific Gas and Electric Company. 2010. Application Note: Using Current as Proxy for Power. [Internet] [cited 2013 March 18]. Available from: http://www.pge.com/includes/docs/pdfs/about/edusafety/training/pec/toolbox/tll/appnotes/using_current_as_proxy_for_power.pdf

Piguet J. 1987. Measurements and modeling of solar irradiance and luminous efficacy for Seattle [thesis] [Seattle, (WA)]: University of Washington.

Raftery P, M. Keane, and J. O'Donnell. 2011. Calibrating whole building energy models: An evidence-based methodology. *Energy and Buildings* 43: 2356–2364.

Raftery P., M. Keane, and J. O'Donnell. 2011. Calibrating whole building energy models: Detailed case study using hourly measured data. *Energy and Buildings* 43: 3666-3679.

Reddy T.A. 2006. Literature review on calibration of building energy simulation programs: uses, problems, procedures, uncertainty and tools. *ASHRAE Transactions* 112: 226–240.

Soebarto, V. I. 1997. Calibration of hourly energy simulations using hourly monitored data and monthly utility records for two case study buildings. *Proceedings of the 5th International Building Performance Simulation Association Conference*, Madison (WI)

Step Detection [Internet]. Wikipedia. [cited 2013 March 18]. Available from: http://en.wikipedia.org/wiki/Step_detection

Subbarao K. 1988. PSTAR - Primary and Secondary Terms Analysis and Renormalization: A Unified approach to building and energy simulations and short-term testing. TR-254-3175, National Renewable Energy Laboratory, Golden, CO.

Sullivan S., and F. Winkelmann. 1998. Validation studies of the DOE-2 building energy simulation program - Final Report, LBNL-42241.

TortoiseSVN [Internet]. [cited 2013 March 18]. Available from: http://tortoisesvn.net/about.html

Turner C., and M. Frankel. 2008. Energy Performance of LEED for New Construction Buildings. [Internet] Technical Report, New Buildings Institute (US) [cited 2013 March 18]. Available from: http://newbuildings.org/sites/default/files/Energy_Performance_of_LEED-NC_Buildings-Final_3-4-08b.pdf

United States Green Building Council (US). 2012. LEED 2009 For New Construction and Major Renovations [Internet]. [cited 2013 March 18]. Available from: http://new.usgbc.org/sites/default/files/LEED%202009%20Rating_NC-GLOBAL_07-2012_8c.pdf

Wasilowski H., and C. Reinhart. 2009. Modelling an existing building in DesignBuilder/E+: Custom versus default inputs. *Conference Proceedings of Building Simulation 200*9, Glasgow, Ireland.

Weather and Climate Data [Internet] c2013 Weather Analytics (US). [cited 2013 March 18]. Available from: http://www.weatheranalytics.com/weather-products/

Weather Data for Simulation [Internet]. [cited 2013 March 18]. Available from: http://apps1.eere.energy.gov/buildings/energyplus/weatherdata_simulation.cfm

Wilcox S., and W. Marion. 2008. Users Manual for TMY3 Data Sets, NREL/TP-581-43156. National Renewable Energy Laboratory, Golden, CO.

Qingyuan Z., J. Huang, and L. Siwei. 2002. Development of typical year weather data for Chinese locations. *ASHRAE Transactions* 108:1063-1075.